PROVINCE OF ALBERTA

RESEARCH COUNCIL OF ALBERTA

BULLETIN 9

SEDIMENTARY MAGNETITE DEPOSITS OF THE CROWSNEST PASS REGION, SOUTHWESTERN ALBERTA

by
G. B. Mellon

Edmonton
Printed by L. S. Wall, Queen's Printer for Alberta
1961

CONTENTS

ILLUSTRATIONS

TABLES

Sedimentary Magnetite Deposits of the Crowsnest Pass Region, Southwestern Alberta

ABSTRACT

Low-grade, titaniferous magnetite deposits of sedimentary origin are present at widely scattered localities in the folded Foothills belt of southwestern Alberta. The individual deposits are thin and lensing, forming a locally developed, iron-rich zone at the top of the basal sandstone member of the Upper Cretaceous Belly River formation.

The iron-rich rocks are composed of black, finely laminated, very fine-grained, magnetite-rich beds up to three feet thick, interbedded with dark green, fine-grained, calcareous sandstones composed of quartz, feldspar, fine-grained rock fragments, and clastic dolomite. The rocks are well cemented by authigenic chlorite and calcite. The lithologic and fossil assemblages associated with the magnetite-bearing sandstones suggest that they were concentrated as placer deposits along the margin of an ancient shoreline complex formed during the eastward regression of the late Cretaceous Colorado sea.

The average Fe_2O_3 content of 60 randomly selected samples from 17 localities is 29 per cent, distributed among magnetite, chlorite, and ilmenite. The average TiO_2 content of the samples is about 3.5 per cent, distributed among titaniferous magnetite, ilmenite, anatase, and leucoxene. The rocks are unsuitable for treatment by conventional beneficiation and smelting processes because of their high titanium and chlorite content, and fine grain size.

The richest deposits are located north of Burmis in the Crowsnest Pass, and near Dungarvan Creek, south of Pincher Creek. At both localities the rocks have been complexly faulted and folded, limiting the volume of ore that can be recovered by strip-mining. Reserves of potential iron ore grading between 25 and 30 per cent Fe are tentatively estimated at less than two million tons in the Burmis area, and less than six million tons in the Dungarvan Creek area.

INTRODUCTION

Scope of the Investigation

Low-grade, titaniferous magnetite deposits of sedimentary origin occur sporadically throughout the folded Foothills belt of southwestern Alberta in the general proximity of the Crowsnest Pass-Waterton Lakes National Park area. The deposits have been known to exist for at least 50 years, but the market for steel products in Western Canada has only recently expanded to the point where development of potential iron ore deposits in Alberta has become economically feasible. Thus, speculation has arisen in recent years over the possible utilization of the Crowsnest magnetite deposits in the operation of a steel industry in southern Alberta, particularly since they are close to the transportation facilities and coal reserves of the Crowsnest Pass area. The objective of this report is to describe those geologic and petrographic properties of the Crowsnest magnetite deposits which can be used as a basis in evaluating their economic potential.

To this end, a field survey of the deposits was made in the summer of 1959, in the course of which most of the known outcrops and borehole material were examined and sampled in detail. The stratigraphy, structure, and areal extent of the various occurrences are described, and maps of the most important deposits near Burmis and Dungarvan Creek have been prepared. The field data have been combined with the results of mineralogical and chemical analyses of randomly selected samples to provide an economic evaluation of the deposits, including tentative estimation of the iron ore reserves contained in the richer deposits.

In addition to the factors governing the economic potential of the deposits, the petrographic and chemical properties of the rocks have been described in some detail. The petrographic and chemical data have been obtained from microscopic, chemical, X-ray, and bulk density analyses of several hundred samples, and the interrelationships of the results obtained from these various analyses demonstrate the sampling and technique problems that may be expected in future investigations of this type. The petrographic and chemical data have also been integrated with the results of the field study to provide an account of the genesis of this rather unusual group of rocks.

Location and Access

Sedimentary magnetite deposits of late Cretaceous age crop out at widely scattered localities within the folded Rocky Mountains Foothills belt of southwestern Alberta, from the International Boundary north to Oldman River in township 10, a distance of approximately 60 miles. The geographic distribution of magnetite deposits is shown in figure 1, with respect to the general geologic features of southwestern Alberta, and the main population centres and transportation arteries of that part of the province.

The magnetite occurrences are called "the Crowsnest magnetite deposits" in this report from their general proximity to the Crowsnest Pass, which provides the main east-west transportation route between southwestern Alberta and adjacent British Columbia. For descriptive and sampling purposes the individual magnetite occurrences have been grouped according to their local geographic distribution: the Todd Creek occurrences in the northern part of the area (Locs. 10 to 15, Fig. 1); the Burmis occurrences (Loc. 9, Fig. 1); the Dungarvan Creek occurrences (Loc. 7, Fig. 1); and the southern occurrences (Locs. 1 to 6, and Loc. 8, Fig. 1), which include the deposits south of the Crowsnest Pass, excepting those at Dungarvan Creek. Another isolated magnetite occurrence is located near Willow Creek in Tp. 15, R. 3, W. 5th Mer., about 40 miles to the north of those near Todd Creek. It is probable that other magnetite-bearing rocks occur at or near the surface in the broad belt of folded Belly River strata that crops out along the strike of the Foothills between Oldman River

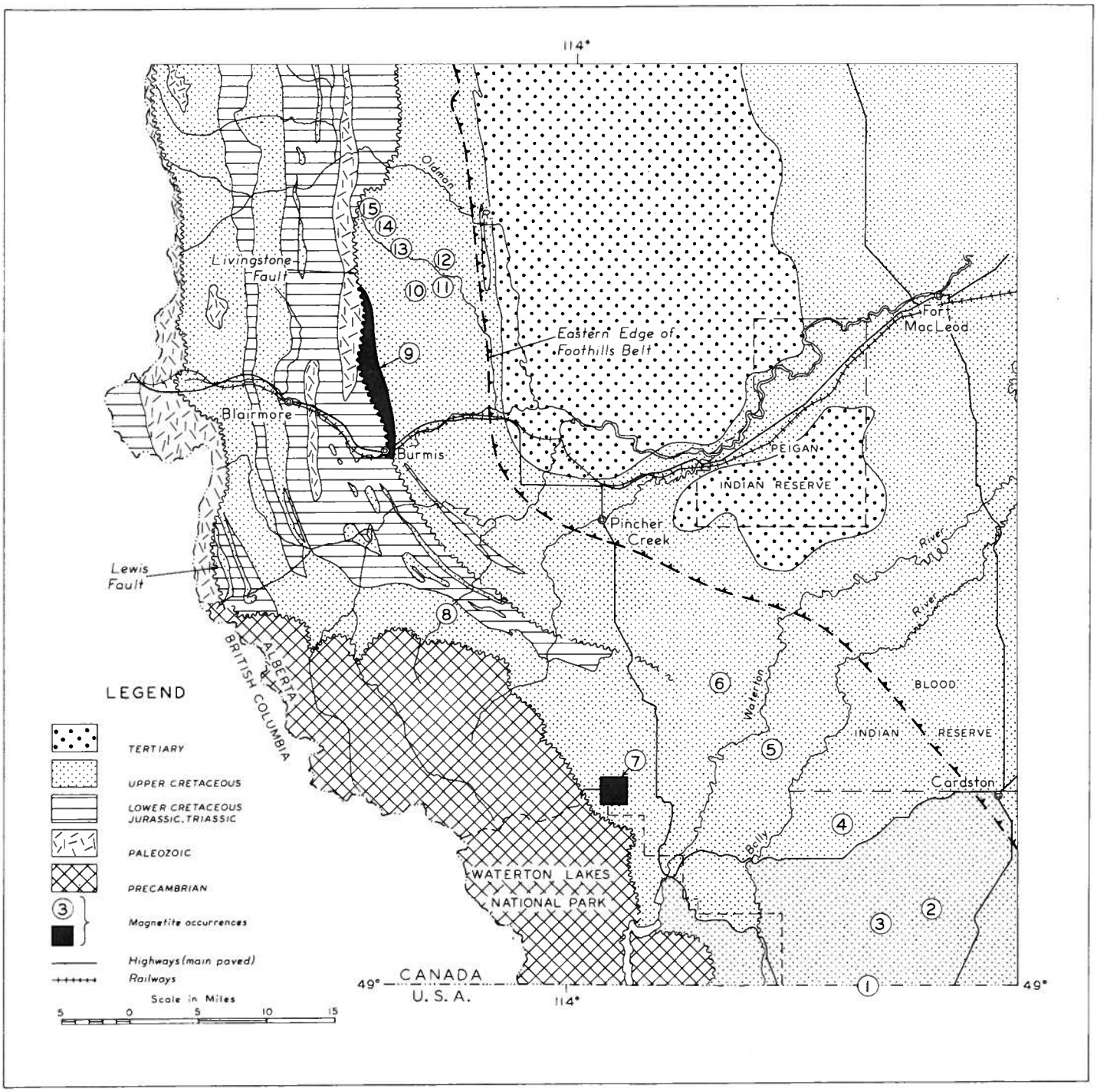

FIGURE 1. Index map of southwestern Alberta showing the locations of sedimentary magnetite deposits

and Willow Creek, but the results of the investigation of the more accessible deposits described here do not warrant a more detailed survey of this northern area at present.

All of the known magnetite occurrences, with the exception of the one near Willow Creek, are within 2 miles of main or secondary roads. However, the topographic relief in the Burmis and Todd Creek areas is relatively rugged, and access to the deposits north of the Crowsnest Pass is more difficult than to those in the southern part of the area.

The Crowsnest Pass region is also serviced by a main line of the Canadian Pacific Railway Company, which passes near the south end of the Burmis deposits. A branch line of the same railway company extends into the southeastern part of the area from Cardston, as indicated in figure 1. The Cardston branch line is about 15 miles east of the deposits at Dungarvan Creek, which contain the largest reserves of potential iron ore of any of the known magnetite deposits.

Previous Work

Very few geological data concerning the Crowsnest magnetite deposits have been published. The general geology of the occurrences north of Burmis was first described by Leach (1912), who was then mapping the general Blairmore area. Allan (1931) published a somewhat more detailed account of the stratigraphy and structure of the Burmis deposits, supplementing his report with various chemical analyses. Allan also prepared a brief unpublished report on the Dungarvan Creek magnetite deposits in 1941 at the request of the Minister of Lands and Mines for Alberta, in which he stated that the deposits were of no commercial importance at that time.

In 1956 and 1957 West Canadian Magnetic Ores Ltd. of Calgary carried out an extensive geological and magnetometer survey of those areas in the Foothills of southwestern Alberta which might possibly be underlain by sedimentary magnetite deposits. In addition, the company undertook a detailed drilling program in the Burmis and Dungarvan Creek areas to determine the structure and extent of potential ore-producing zones. Some of the results of this drilling program are incorporated in the present report.

Sedimentary magnetite deposits of late Cretaceous age have also been described from western Montana (Stebinger, 1912; Wimmler, 1946; De Munck, 1956). The American deposits are thin and lensing, of limited volume, and have a high titanium content. In these respects they are similar to the Crowsnest deposits, except that they occur at slightly different stratigraphic horizons from their Canadian analogues. Magnetite deposits have not been reported from the same stratigraphic units (Virgelle sandstone, Fox Hills sandstone) in southern Alberta.

Acknowledgments

The writer is indebted to the management of West Canadian Magnetic Ores Ltd., Calgary, Alberta, for permission to examine the numerous geological and geophysical maps, core samples, and chemical analyses resulting from the company's detailed survey of the Crowsnest magnetite deposits. Discussions and field trips with Mr. Martin Aschacker, mine superintendent for West Canadian Collieries, Limited, were particularly valuable in determining the locations of the numerous occurrences, a task which otherwise would have been impossible to complete within the time allotted for the survey.

Dr. D. J. Kidd, Research Council of Alberta geologist, provided information pertinent to the locations of the deposits, and G. P. Wysocki served capably as field assistant during the course of the survey.

GENERAL GEOLOGY

Physiography and Structure

Some of the general geologic features of the Rocky Mountains Foothills of southwestern Alberta are shown in figure 1. The eastern margin of the Foothills belt is marked by a gradual change from the gently dipping Upper Cretaceous and Tertiary strata of the Plains to the complexly folded and faulted Paleozoic and Mesozoic strata to the west. The western margin of the Foothills is defined by the range of Precambrian and Paleozoic rocks overlying the Lewis fault, so that the width of the folded Foothills belt varies from about 15 to 30 miles within the area covered by the map in figure 1.

The southern Foothills are underlain by a series of narrow, north- to northwest-trending zones of strata ranging in age from Mississippian to Paleocene. The rocks are complexly folded, and are cut by numerous closely spaced, subparallel, west-dipping thrust faults, the two most prominent of which are shown in figure 1. The Livingstone fault bounds the eastern flank of a south-plunging anticlinal structure composed of Mississippian, Jurassic, and Lower Cretaceous strata, which have been thrust over folded and faulted Upper Cretaceous rocks to the east. Similarly, Precambrian and Devonian strata have been thrust over Lower and Upper Cretaceous rocks along the west-dipping plane of the Lewis fault, which forms the western boundary of the Foothills.

The regional plunge of the folded strata between the Livingstone and Lewis faults is to the south, so that the Foothills belt south of Pincher Creek is underlain largely by a wide zone of faulted Upper Cretaceous strata, which abuts abruptly on the west against the Precambrian rocks of the Rocky Mountains.

The physiography of the southern Foothills is controlled by the lithology and structure of the underlying rocks. The south-plunging Livingstone Range is the most prominent topographic feature in the northern part of the area, where Paleozoic carbonate rocks cropping out along the axis of the structure achieve a maximum relief of about 3000 feet. Jurassic and Cretaceous rocks on either side of the Livingstone Range form narrow north-south trending sandstone ridges and shale valleys with variable topographic relief, the sandstone ridges rising up to 1500 feet above the surrounding terrain.

The topography of the Foothills becomes progressively more subdued south of the Crowsnest Pass, where alternating zones of faulted Wapiabi and Belly River strata underlie much of the area. In this region, the otherwise gently rolling terrain is broken up by a series of low northwest-trending ridges formed by west-dipping sandstone beds in the lower part of the

Belly River formation. Outcrops are scarce, apart from the sandstones exposed along the crests of the ridges, and much of the area is under cultivation.

Stratigraphy

A brief explanation of the stratigraphic framework of the Upper Cretaceous and Tertiary rocks of southern Alberta is in order here, primarily to indicate the relationship between the gross depositional environments of these rocks and the stratigraphic loci of the magnetite deposits of southern Alberta and Montana. The general Upper Cretaceous-Tertiary stratigraphic succession is schematized in figure 2 and is based largely upon the work of previous investigators, the details of which, however, are too voluminous to reiterate here. The relative formation thicknesses are approximately to scale within the Foothills part of the diagram, where the combined Upper Cretaceous-Tertiary sequence probably attained an estimated maximum thickness of 20,000 feet prior to post-Paleocene uplift and erosion, but the general thinning of the stratigraphic section toward the Plains is not shown. In addition, figure 2 shows the stratigraphic loci of known sedimentary magnetite occurrences in southern Alberta and Montana.

The lowest Upper Cretaceous strata in the Foothills of southwestern Alberta are the marine silty shales of the Blackstone formation, which lie unconformably on rocks of the Blairmore group and grade up into the quartzose sandstones of the Cardium formation. These latter have been interpreted as a sequence of marine, near-shore sandstone lenses indicating a minor eastward regression of the Colorado sea, as they grade laterally into silty shale near the eastern margin of the Foothills. The contact of the Cardium sandstones with the overlying Wapiabi formation is generally sharp, suggesting a sudden deeping of the Colorado sea at that time, with concomitant deposition of marine silty shales similar to those of the underlying Blackstone formation.

The Belly River formation constitutes a sequence of sandstones and vari-colored shales that interfingers to the south and east with the upper part of the Wapiabi (upper Colorado) shale, indicating a gradual withdrawal of the late Colorado sea in that direction, and the simultaneous building-up of a "continental" surface of sedimentation to the west. The marine Bearpaw shale and overlying sandstones and silty shales of the St. Mary River formation have the same stratigraphic-depositional interrelationship as the Colorado-Belly River sequence, the coarser detrital phases of the lower St. Mary River interfingering laterally with marine shales of the Bearpaw to the southeast. The upper part of the Bearpaw-St. Mary River sedimentary complex contains a high proportion of red "mottled" shale and is mapped separately as the Willow Creek formation in southwestern Alberta. These red-beds also contain a higher proportion of siltstone and shale than the underlying St. Mary River formation (Douglas, 1950) and indicate the widespread existence of a predominantly subaerial or truly

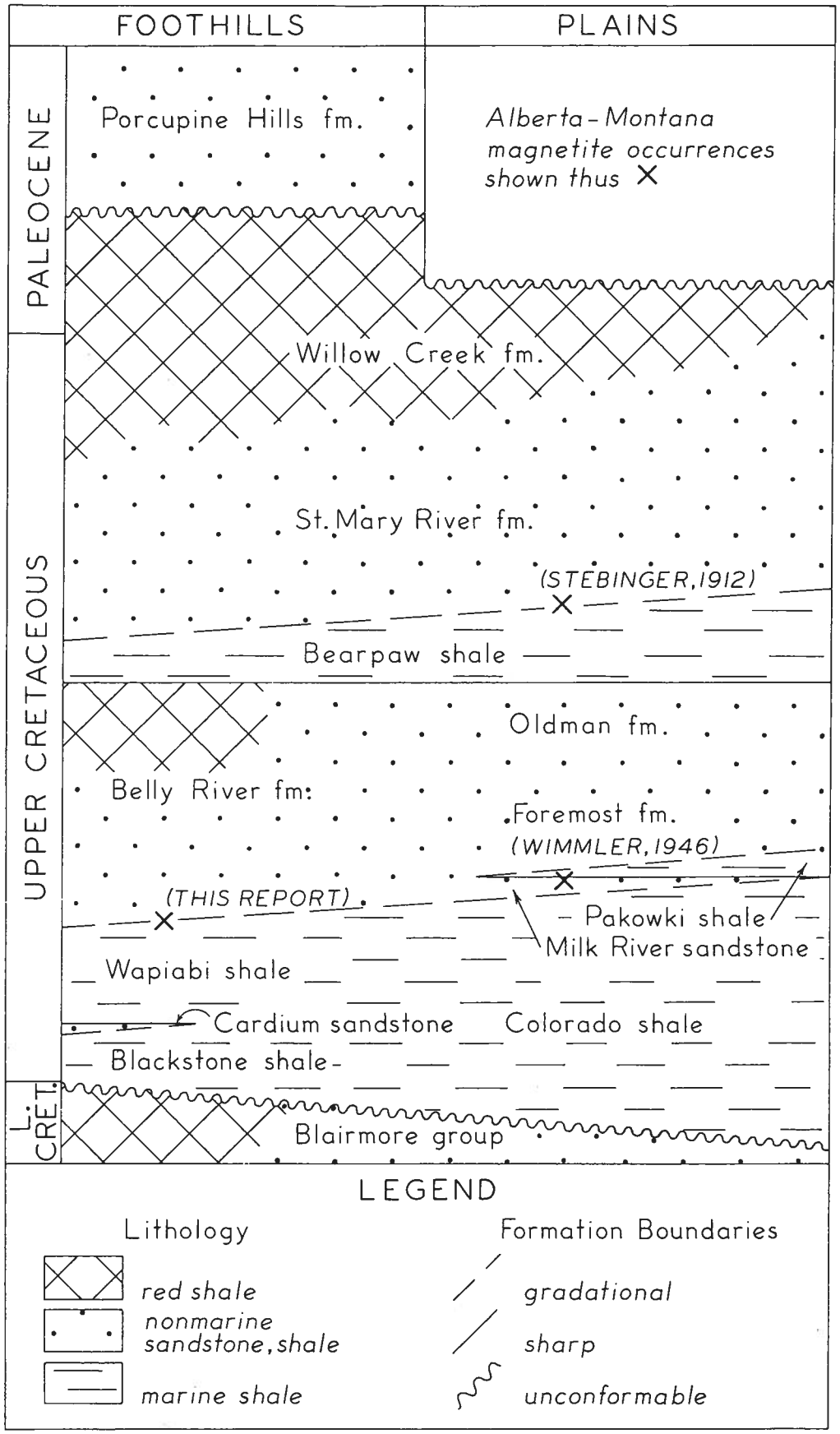

FIGURE 2. Cross section of the Upper Cretaceous and Tertiary strata of the southern Alberta Foothills and Plains

continental sedimentary facies in Willow Creek time, which was only incipiently developed in Belly River time in the Foothills south of the Crowsnest Pass.

The youngest sedimentary rocks of southwestern Alberta form a thick sequence of quartzose cherty sandstones and interbedded silty shales that crops out along the axis of a broad syncline margining the eastern edge of the folded Foothills belt (Fig. 1). The rocks are called the Porcupine Hills formation and are Paleocene in age. They appear to be of predominantly fluviatile origin, having been deposited as a coarse detrital infilling flanking the eastern margin of the then-rising Rocky Mountains, and lie unconformably on progressively older strata to the north (Douglas, op. cit.). The original thickness of the Porcupine Hills formation is not known as the upper boundary of the formation is an erosion surface, and, excluding the deposition of a relatively thin veneer of unconsolidated sediments composed of late Tertiary (?) sands and gravels and Pleistocene glacial deposits, the history of the Rocky Mountains and Plains of Alberta has been one of uplift and erosion since early Tertiary time.

The sedimentary magnetite deposits of southwestern Alberta occur within the Belly River formation, forming a local iron-rich zone at the top of the basal sandstone member, as shown in figure 3. Throughout the southern Foothills the basal sandstone member of the Belly River formation is underlain conformably by thin-bedded, dark grey, silty shale of the Wapiabi formation, which contains locally abundant concentrations of pelecypod and ammonite shells. The upper part of the Wapiabi formation is composed of interbedded dark grey, laminated, silty shale and grey, calcareous, silty sandstone in ripple-marked, cross-laminated beds a fraction of an inch to a few feet thick, the proportion and thickness of sandstone beds increasing towards the top of the unit. This sandy zone is called the "transition beds" (Webb and Hertlein, 1934) by field geologists, inferring a gradational change from the underlying shale to the overlying basal Belly River sandstone, although the lower boundary of the latter can be arbitrarily drawn within an interval of several feet. The "transition beds" are seldom well exposed, although a reliable thickness estimate was obtained from a road cut in Sec. 15, Tp. 8, R. 3, W. 5th Mer., north of the village of Burmis. Here, the zone is 75 to 80 feet thick, and examination of other exposures on Crowsnest River and Mill Creek indicates similar thicknesses there.

The basal member of the Belly River formation consists of pale grey weathering, cross-bedded, fine- to medium-grained, well sorted sandstone which forms numerous topographically prominent ridges throughout the southern Foothills region. The fresh rock is typically pale grey, calcareous, "salt-and-pepper" sandstone, which tends to split along certain bedding planes formed by the concentration of thin layers of biotite. From 10 to 20 per cent of the strata are composed of dark brown weathering, strongly calcareous sandstone lenses less than 3 feet thick, which are more resistant

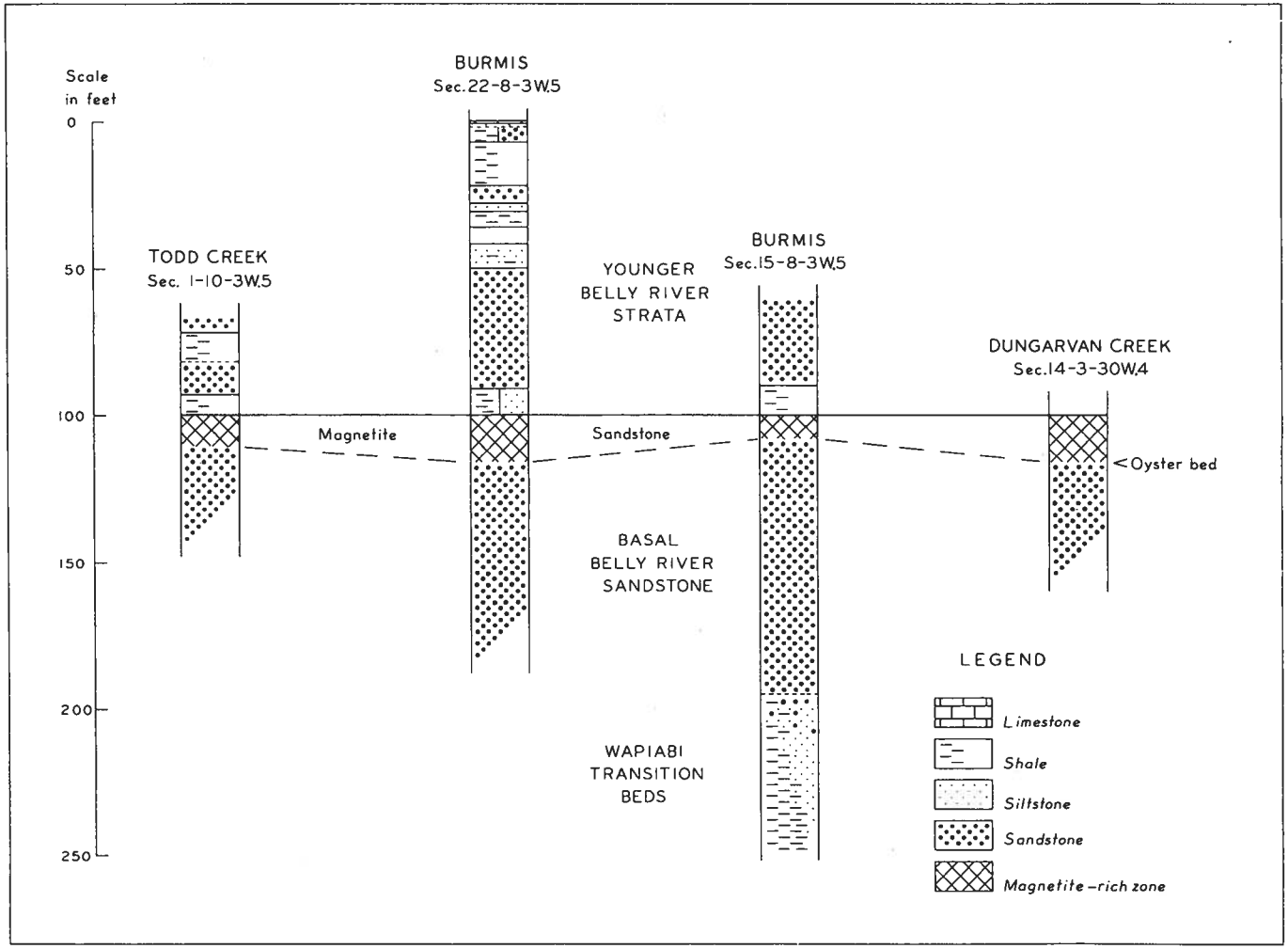

FIGURE 3. Columnar sections showing the stratigraphic locus of the Belly River magnetite-bearing sandstones

to weathering than the softer, pale grey sandstone zones among which they are intercalated. The unit is approximately 100 ± 25 feet thick, and has a sharp upper contact, in contrast to the lower gradational boundary with the "transition beds."

Younger Belly River strata immediately above the basal sandstone member consist of several thick homogeneous sandstone units interbedded with lesser amounts of siltstone and soft, pale greenish-grey, massive, silty shale quite unlike the typical dark grey laminated shale of the Wapiabi formation. These beds are exposed in a fresh road cut in Sec. 22, Tp. 8, R. 3, W. 5th Mer., north of Burmis (Fig. 3), and form the following stratigraphic succession:

Thickness (feet)	Top of section
	overlying beds covered
2.5	Hard, bluish-grey, silty, aphanitic limestone; grades below into
2.0	Pale greenish-grey, medium-grained, calcareous, micaceous sandstone with scattered green shale pebbles; grades below into
2.7	Soft, dark green, massive, silty shale
1.2	Pale greenish-grey siltstone and silty shale, grading below into greenish-grey, fine-grained, calcareous, micaceous sandstone
15.0	Slumped, poorly exposed, soft, olive-green, massive shale; dark green siltstone lens 10 ft. above base Pale grey, medium- to coarse-grained, calcareous, micaceous sandstone, with scattered pale green shaly partings and pebbles increasing towards the top
3.5	Pale grey, laminated, calcareous, micaceous siltstone, becoming hard, massive mudstone at base
5.0	Pale green, massive shale; silty in lower 12 inches
6.5	**covered**
8.5	Pale greenish-grey, slightly calcareous siltstone beds; separated by pale green, silty shale and pale grey, fine-grained sandstone lenses
40.0	Pale grey, medium-grained, calcareous, micaceous sandstone, becoming silty in upper 2 feet; grades below into
0.7	Medium green, fine-grained, micaceous sandstone; flattened shale pebble impressions on base
2.0	Green, massive shale, grading below into hard, dark green, slightly calcareous siltstone
3.7	Green, massive shale, grading below into hard, dark green siltstone, as above
3.0	Pale greyish-green shale, grading below into dark greenish-grey very fine-grained, calcareous, magnetic sandstone
4.0	Folded, dark green to black, magnetite-bearing sandstone; base concealed
105.8	**total thickness**

The upper 3000 to 4000 feet of Belly River strata are seldom well exposed except in some of the larger stream valleys and were not examined in detail. The middle and upper parts of the formation crop out discontinuously on Crowsnest River west of Lundbreck in Tp. 7, R. 2, W. 5th Mer. up to the contact with the overlying Bearpaw formation. The rocks consist largely of pale grey and green weathering shale and siltstone interbedded with thin, pale grey, fine-grained, micaceous sandstone beds. A similar sequence of strata is exposed along Mill Creek in Tp. 5, R. 2, W. 5th Mer., but none of the rocks above the basal sandstone member at these localities or elsewhere was observed to contain conspicuous placers of magnetite.

Lithology and Structure of the Magnetite Deposits

Throughout most of the southern Foothills region the basal Belly River member consists of pale grey "barren" sandstone from the base to the top, but at certain localities shown in figure 1 conspicuous beds of detrital magnetite are concentrated in the upper part of the unit (Fig. 3). These iron-rich rocks are typically hard, dark green to black, very fine-grained, laminated, calcareous sandstones composed in part of magnetite-rich beds less than an inch to 3 or 4 feet thick. The black magnetite-rich beds or zones are complexly interbedded with pale to dark bluish-green magnetite-poor sandstone beds composed of quartz, feldspar, carbonates, and chlorite. The characteristic greenish color of the iron-rich but magnetite-poor sandstones is due to the abundance of chlorite, which weathers to reddish-brown iron oxides, an effect which, upon casual inspection of outcrop sections, suggests that the iron-rich zone is relatively homogeneous.

The magnetite-bearing zone is from 5 to 25 feet thick, and the average thickness of twenty-six completely exposed sections (table 8) is about 11 feet, if the lower contact is placed at the change from dark brown weathering, green sandstone to underlying pale grey "barren" sandstone. This contact is arbitrary, as the color change upon which it is based is gradational over an interval of 2 or 3 feet. In the Dungarvan Creek area, a thin coquinoid layer less than 6 inches thick containing *Ostrea, Brachydontes,* other small pelecypods and gastropods, and conifer fragments occurs locally at or near the base of the zone (Figs. 3, 4). In the Todd Creek-Burmis area, the upper contact with a thin, pale greenish-grey shale unit is sharp where exposed (Fig. 3), but the strata immediately overlying the magnetite-bearing beds were not observed south of the Crowsnest Pass. According to Douglas (1951), the basal sandstone is "immediately overlain by fissile dark grey shales and thin coal seams or carbonaceous shale" in the Pincher Creek map-area.

The distribution of magnetite in the upper part of the basal sandstone member is extremely complex in detail. The gross stratification pattern of alternating magnetite-rich and magnetite-poor beds within four sampled outcrop sections is indicated in figure 4, where the rocks have been classified according to the percentage of magnetite by volume.[1] The class intervals are arbitrary, the upper 25 per cent volumetric boundary corresponding to approximately 40 per cent magnetite by weight. In fact, the rocks are laminated on a much finer scale than shown in figure 4, and the inferred thickness or homogeneity of individual beds within each of the four sections is, in part, a function of the size of the individual samples (from 1 to 2 inches thick) and the interval between samples.

Thus, most of the magnetite at sampling locality 292 is confined to a rich, relatively homogeneous interval about 3 feet thick intercalated among pale to medium green, chloritic sandstone containing only scattered

[1] Calculated from bulk density determinations using the regression equation on p. 66.

millimeter-thick magnetite laminae. The magnetite-rich bed is near the base of the iron-rich zone, where green chloritic sandstone grades below into pale grey "barren" sandstone. Magnetite is similarly distributed within the iron-rich zone at locality 368, where most of the mineral is concentrated in an interval 3 to 4 feet thick in the middle or upper part of the section (the top of the basal sandstone member is not exposed here).

The distribution of magnetite within the two thicker sections shown in figure 4 appears more complex. The magnetite-rich beds at locality 301 are relatively thin and spaced rather evenly throughout the section. At locality 310, magnetite-rich beds are confined to the upper two-thirds of the section, and it should be noted here that a closer sampling interval (6 inches) reveals a finer degree of stratification than that apparent in the other three sections.

The distribution of magnetite in other sampled sections is similar to that described above. Where the mineral is abundant it is concentrated in laminated beds less than an inch to 3 or 4 feet thick, alternating with green, chlorite-rich sandstone beds of similar thickness. Generally, the magnetite-rich sandstones are confined to the central part of the sampled section and are underlain and overlain by several feet of chlorite-rich but magnetite-poor sandstone which may be described as "iron-rich" only in comparison with the pale grey, micaceous sandstones that occur in the lower part of the Belly River formation in the southern Foothills.

The original size and shape of the various individual magnetite-bearing deposits is difficult to define in any particular case, largely because of lack of outcrops or borehole information. The deposits also have been folded and faulted with the subsequent removal of an unknown volume of rock by processes of erosion. The available data indicate that the deposits were laid down as lensing, sheet-like bodies, roughly ovoid in plan, attaining a maximum diameter of one-quarter to possibly two miles. The thickest, most abundant magnetite concentrations occur in the central parts of these lensing units, grading towards the periphery into low-grade, chloritic sandstone, and finally into grey, fine-grained, "barren" sandstone, typical of the greater bulk of the basal Belly River member. The areal extent of potential ore-producing zones is considerably less than the area encompassed by the peripheral zone of chlorite-rich but magnetite-poor sandstones, and the inherent lensing nature of the deposits cannot be overemphasized with respect to their possible economic development. The known extent and grade of the various individual occurrences is discussed in detail in the section on Economic Geology

Depositional Environment of the Magnetite Deposits

Speculation on the origin of ancient sedimentary rocks is based upon the premise that processes which have acted in the past to produce ancient rock assemblages are the same processes operating today, producing similar

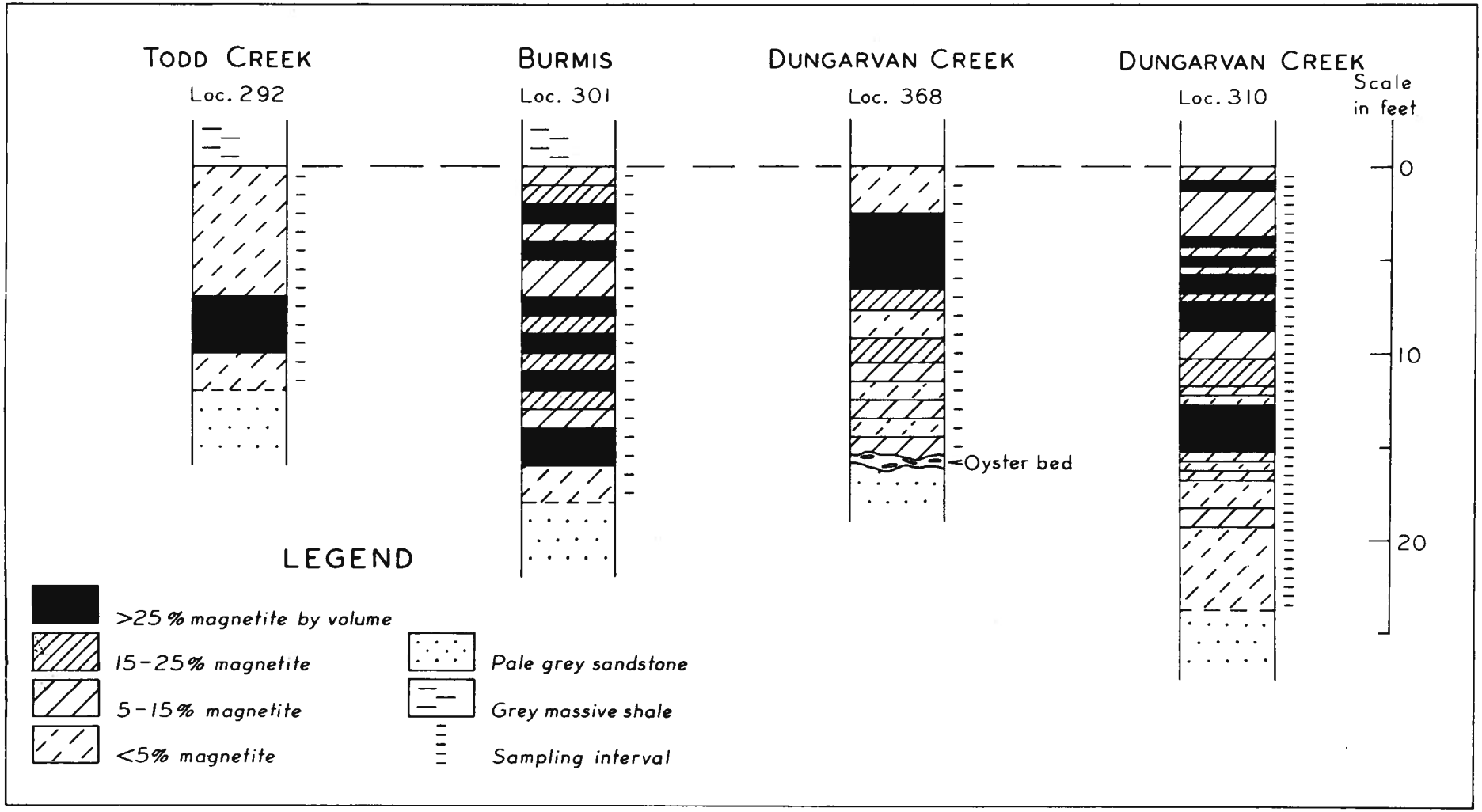

FIGURE 4. Columnar sections showing the distribution of magnetite in four sampled sections of the iron-rich zone

sedimentary assemblages characteristic of particular depositional environments. Previous investigators of sedimentary magnetite occurrences in Alberta and Montana have suggested that the sediments are placer deposits formed along beaches margining the late Cretaceous seas. This hypothesis is supported by the general observation that extensive concentrations of heavy minerals have been and are being deposited along Recent shoreline areas in various parts of the world today. Presumably those hydraulic conditions necessary for the large scale selective sorting and deposition of heavy minerals are more likely to be operative within the contexture of a shoreline environment than in a definitely marine or continental environment.

The assemblages of sediments, including noticeable concentrations of heavy minerals, which currently are being accumulated along two present-day shoreline areas are compared graphically with the gross lithologic units of the Wapiabi-Belly River regression complex[1] in figure 5. If it is assumed that the Recent deposits are parts of similar regression complexes, the geographic loci of the Recent sediments can be transposed into stratigraphic columns, each column showing a gradation from marine, off-shore deposits at the base to nonmarine, landward sediments at the top.

The first of the two complexes of Recent shoreline sediments schematized in this way in figure 5 is that described by Biederman (1958) from the New Jersey coast. At Barnegat Bay, New Jersey, there is a gradation from fine-grained, offshore sediments of the open sea into well sorted beach and dune sands, which are separated from the organic swamp deposits of the mainland by the silty muds of the lagoon. Because the prevailing wind direction is from the sea, the lagoon is a protected area in which relatively small waves concentrate the heavy minerals (largely ilmenite, zircon, and garnet) in beds of variable thicknesses along the upper part of the lagoonal beach. Thus, the heavy minerals are concentrated on the landward side of the beach-dune complex, or, in a stratigraphic sense, at the top of a sequence of well sorted sandy sediments analogous to the position of the magnetite beds at the top of the basal Belly River sandstone member.

The other sequence of Recent sediments illustrated in figure 5 is based upon Gardner's (1955) description of the sediments currently being deposited along the coast of southeastern Australia. There, heavy minerals (zircon, rutile, and ilmenite) are present in commercially exploitable quantities and are concentrated along the upper part of the ocean beach at the foot of the first of a series of parallel sand dunes (the foredune) during periods of stormy weather. Sediments on the leeward side of the foredune

[1] The term "regression complex" describes those sediments deposited during the gradual withdrawal of the late Colorado sea to the southeast in Belly River time. This includes at least the upper part of the Wapiabi shale and most of the Belly River sediments, although it is obvious from the relationship of the two formations (Fig. 2) that the nonmarine and shoreline environments represented by the Belly River sediments were advancing or transgressing over southwestern Alberta at the same time the late Colorado sea, in which the Wapiabi shales were deposited, was withdrawing.

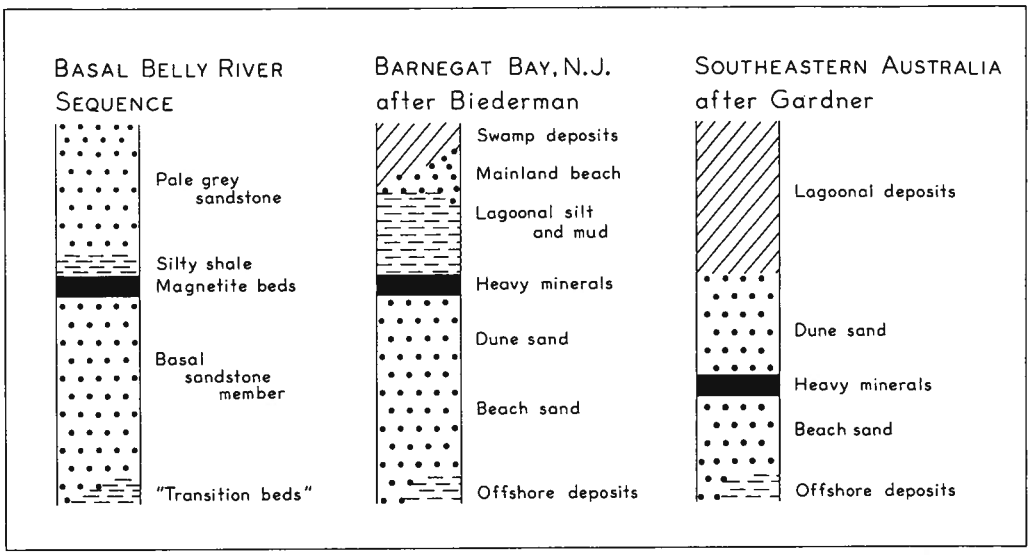

FIGURE 5. Comparison of the Wapiabi-Belly River regression complex with Recent shoreline sediments

towards the lagoon consist of one or more narrow sandy ridges (parallel dunes) overlying thin heavy mineral beds, and are obviously older foredunes which indicate successive stages in the seaward advance of the shoreline. The low sand ridges within the lagoonal area between the beach-dune area and the mainland proper are apparently older parallel dunes, although their origin is partly obscured by erosion and development of swamps. Thus, the sediments of the lagoon consist of an admixture of reworked dune sand and organic muck, although Gardner does not discuss their composition in detail. If the magnetite beds of the Belly River formation had been deposited in the same part of the shoreline complex as their Australian analogues, they would presumably occur in the middle of the basal sandstone member rather than at the top.

The distribution of fossils across the Wapiabi-Belly River contact gives additional support to the hypothesis that the magnetite beds were deposited along the margin of an ancient shoreline, in a manner similar to those now being deposited at Barnegat Bay. The various species of scaphoid ammonites and *Inoceramus* found in the upper part of the Wapiabi formation, although only rarely in the usually unfossiliferous "transition beds," distinctly indicate a marine environment in contrast to the fossil assemblage occurring at the base of the magnetite-bearing beds in the Dungarvan Creek area. The latter includes species of *Ostrea* and *Brachydontes*, both of which indicate an environment of relatively low salinity, possibly a lagoonal environment. Conifer fragments are associated with the *Ostrea* fauna, and dicotyledon leaf impressions occur in the thick sandstones overlying the basal member in the Burmis area, further emphasizing the increasingly nonmarine aspect of the fossil assemblages found in progressively younger strata.

Regardless of what inferences are made concerning the exact depositional environment of the Belly River magnetite deposits, the fact remains that they are thin lensing bodies of rock, which, if present, are found consistently at the same stratigraphic horizon. The local lensing nature of the deposits has little environmental significance in itself, because most discrete lithologic units within larger detrital sequences of strata have only very local lateral extent in any case. However, the thick homogeneous sandstones overlying the basal sandstone member are megascopically similar to the latter in composition and texture, except that the younger sandstones do not contain noticeable concentrations of heavy minerals. Furthermore, these sandstones contain scattered leaf impressions and are interbedded with pale green and grey, massive shale quite unlike the dark grey, fissile, silty shales of the "transition beds." Thus, whatever may have been the depositional environment of these beds, it was probably different from that of the basal sandstone member and the associated magnetite deposits. This fact in itself illustrates the essentially unidirectional (i.e. stratigraphically non-repetitive) character of the advancing Belly River shoreline complex in the Foothills region of southwestern Alberta.

Before leaving the subject of depositional environments, it should be noted that the sedimentary magnetite deposits of Montana, like those of southwestern Alberta, are confined to zones of strata which are transitional from rocks of marine to those of continental origin (Fig. 2). Stebinger (1912) describes titaniferous magnetite deposits which are present at the top of a thick sandstone member gradationally overlying the marine Bearpaw shale and containing (p. 330) "oysters and other brackish-water forms." This magnetite-bearing sandstone is stratigraphically analogous to the Blood Reserve sandstone of the southern Alberta Plains (Russell and Landes, 1940) and is probably an old shoreline deposit developed at the base of the St. Mary River continental complex during the eastward regression of the Bearpaw sea (Fig. 2). Other sedimentary magnetite deposits occur at the top of the Virgelle sandstone of northwestern Montana (Wimmler, 1946; Cobban, 1955). The Virgelle sandstone is stratigraphically analogous to the basal Belly River sandstone member of this report, and to the Milk River sandstone of the southern Alberta Plains (Slipper and Hunter, 1931; Meyboom, 1960). The nature of these occurrences, then, gives additional support to the general hypothesis that the basal Belly River magnetite deposits of southern Alberta are placer deposits formed by selective sorting processes along an ancient shoreline complex developed during the eastward regression of the late Colorado sea.

PETROGRAPHIC AND CHEMICAL PROPERTIES OF THE MAGNETITE-BEARING SANDSTONES

Introduction

General Statement

Among the various petrographic and chemical properties of the Belly River magnetite-bearing sandstones, those which are most closely concerned with the possible economic development of the deposits are the mineral composition, grain size, and iron and titanium content of the rocks. Regardless of the volume of rock involved, or its accessibility in terms of mining and transportation, if the petrographic and chemical properties of the rocks do not meet some predetermined standard, the deposits have little value as a source of iron ore within the framework of existing economic conditions. As few published data concerning these properties are available, considerable space is devoted here to a detailed account of the mineral and chemical composition, and grain size of the rocks. This information is not only necessary for determination of the grade of the deposits, but also indicates some of the difficulties that would be met in concentrating and smelting the ore.

Sampling and Analytical Procedures

A preliminary survey of the outcrop occurrences of the magnetite-bearing sandstones indicated that a large number of samples would have to be analyzed to determine accurately the average mineral and chemical composition of the various deposits, because of their scattered geographic distribution, and the local lensing distribution of magnetite-rich beds within the individual deposits (Fig. 4). In the course of the present investigation, all of the known magnetite-bearing outcrops were described and measured in detail, and 42 of the better exposed sections, including two cored sections, were sampled for petrographic and chemical analysis.

The choice of sampling sites was governed largely by the availability and completeness of outcrops, and the observed magnetite content of the iron-rich zone within each outcrop. The obviously low magnetite content of many outcrops and borehole sections did not warrant the collecting of large numbers of samples, although generally one suite of samples was collected from across the iron-rich zone at these localities to emphasize the low grade of the deposit. The locations, thicknesses, and grade of the sampled sections are given in table 8, and the geographic distribution of the sampled sections in the Burmis and Dungarvan Creek areas is shown in figures 18 and 19, all in the section on Economic Geology.

Even if the sampling sites are determined largely on the basis of outcrop availability, it is still necessary to define the sampled interval in stratigraphic terms. The upper stratigraphic boundary of the iron-rich zone with a thin, massive shale unit is sharp (although usually covered), whereas the lower stratigraphic boundary is gradational over an interval of several feet, as indicated by the change from hard, dark brown weathering sandstone to soft, pale grey weathering sandstone. It was decided to sample the

interval between the base and exposed top of the dark brown weathering sandstone, although there is some ambiguity in choosing the lower boundary, irrespective of the apparent distribution of magnetite-rich beds within this zone. The iron-rich zone was systematically sampled at equal stratigraphic intervals ranging from 6 inches to 2 feet, depending on the apparent magnetite content of the section. The first sample was taken near the base or the top of the iron-rich zone and the succeeding samples were taken at fixed distances from the first sample. Most samples are between one-half and two inches thick across the bedding. The average thickness of the 42 systematically sampled sections is approximately 11 feet, and the magnetite-rich beds are generally restricted to the central part of the sampled interval, as shown by the columnar sections in figure 4.

The selection of a number of discrete samples at fixed intervals is preferable to the conventional channel or "chip" sample across the entire sampled interval, because samples of the first type not only give an estimate of the mean value of the attribute being measured (such as iron or magnetite content), but also provide an estimate of the range or variation in values within the sampled section. The additional information contained in analyses of a series of discrete "spot" samples is particularly valuable in describing the stratigraphic distribution of magnetite within the various sampled sections listed in table 8.

The systematic sampling procedure outlined above has resulted in the collection of a large number of chlorite-rich samples with a low magnetite content, which has the effect of lowering the estimated average magnetite and iron content of many individual sampled sections below the generally accepted minimum values indicative of iron ore. On the other hand, if only the obvious magnetite-rich zones within each section were sampled, implying that only these beds should figure in the calculation of ore reserves, then it would have to be assumed that such zones could be selectively mined at any given locality and the interbedded chlorite-rich sandstones discarded. The complex distribution of magnetite-rich beds within the previously defined sampling interval indicates that such selective mining would be impractical on a large scale, although the lower few feet of the sampled section at most localities, immediately above the pale grey "barren" sandstones, rarely contain conspicuous magnetite lenses, and probably would be left behind in the course of mining the overlying magnetite-rich sandstones.

A total of 469 samples was collected from the 42 sampled sections of the iron-rich zone in the manner described above. The samples were subjected to the following sequence of analytical techniques.

The 469 samples were split and the bulk density of each sample was determined. The bulk densities of the samples selected for petrographic and chemical analyses were measured twice, and from the relationships among the petrographic, chemical, and bulk density data the average percentages of magnetite, iron, and titania in the 42 sampled sections were determined (table 8, in pocket).

Sixty of the 469 samples were selected for detailed petrographic and chemical analysis. Point counts of the percentages of mineral constituents (modal analyses) and grain size measurements were obtained from thin sections of all 60 samples (table 1, pp. 24 - 27). Five of the thin sections were stained for point counts of the proportions of calcite and dolomite (table 4, p. 36). Point counts of the proportions of magnetite, ilmenite, and hematite were obtained from polished sections of six magnetite-rich samples (table 2, p. 30).

The percentages of Fe_2O_3 and TiO_2 in the 60 modally analysed samples of table 1 were determined by X-ray fluorescent techniques (table 1, pp. 24 - 27). In addition, the percentages of nine oxides, including Fe_2O_3 and TiO_2, in 20 of the modally analysed samples were determined by conventional chemical techniques (table 6, p. 59).

Twelve of the 20 chemically analysed samples of table 6 were selected for further mineralogical analysis. Each sample was split into its light mineral, magnetic heavy mineral, and nonmagnetic heavy mineral fractions, respectively. The carbonate minerals were identified from X-ray diffraction powder patterns of the light mineral fractions of eight samples, and the composition of the magnetic opaque grains was determined from X-ray diffraction powder patterns of the magnetic heavy mineral fractions of eight samples. The relative frequencies of the nonopaque heavy minerals were determined from counts of grain mounts of the nonmagnetic heavy mineral fractions of all 12 samples (table 3, p. 33).

The various sample preparation and analytical techniques are discussed in more detail in the succeeding sections of the report, in conjunction with the results obtained from each type of analysis.

Mineral Composition

Sampling and Analytical Procedures

Sixty of the 469 samples collected from the various individual magnetite occurrences in the manner previously described were selected for detailed petrographic and chemical analysis. To detect possible compositional differences among the widely scattered deposits, the 60 samples were selected from 17 of the 42 sampled sections, distributed among the main geographic areas as follows:

three samples from each of four sections in the Todd Creek area;

three samples from each of six sections in the Burmis area;

six samples from each of three sections in the Dungarvan Creek area;

three samples from each of four sections between Mill Creek and the International Border (southern localities).

The 17 sections from which the samples were selected are among the more completely exposed of the 42 sampled sections and are spaced as widely as possible within each of the four areas mentioned above. As indicated by bulk density determinations of the average iron content of all 42 sampled sections (table 8, in pocket), the 17 sections are more iron-rich than average, but as only these rocks constitute potential iron ore in any case, the possible bias associated with the selection of the 17 sections is probably of little importance.

From 7 to 48 samples were collected initially from each of the 17 sections. Each set of samples was numbered in sequence, generally with respect to the base or the top of the iron-rich zone, and 3 or 6 samples were selected from each set by reference to random number tables. Thus, whereas the sampling procedure is arbitrary with respect to the choice of the 17 sections, it is random with respect to the selection of samples within each section, lending some validity to the argument that the petrographic and chemical properties of the 60 samples are representative of the much larger volume of rock tentatively defined as potential iron ore.

Estimated proportions of the basic mineral constituents of the magnetite-bearing sandstones (modal analyses) are based on point counts (Chayes, 1956) of the constituents in thin sections of the 60 samples selected in the manner decribed above. The thin sections were cut perpendicular to the apparent bedding of each sample, and are generally 2 cm. by 3 cm. in dimensions. The estimated mineral composition of each sample is based on counts of 200 points per thin section, arranged in ten equally spaced traverses (2 to 3mm. apart) of 20 points each (1 mm. apart). Because many of the samples are composed of a sequence of alternating, subparallel, magnetite-rich and magnetite-poor laminae, the traverses were made perpendicular to the visible lamination of the thin sections. This arrangement gives more stable mean estimates of the proportions of mineral constituents in each thin section, as the compositional differences among adjacent laminae are averaged out by traversing across them.

If, then, it is assumed that such a distribution of points eliminates the lamination effect of the samples (i.e. the thin sections are homogeneous), the expected precision (reproducibility) of the estimated mean proportions of mineral constituents in each thin section can be calculated, assuming that each constituent is binomially distributed within the area of a thin section. If such is the case, the standard deviation of the estimated mean proportion of each constituent is a function of the subsample size (20 points per traverse), the number of subsamples from which the mean is calculated (10 traverses per thin section), and the mean itself (Snedecor, 1956, p. 476). A general formula for calculating the standard deviation of the mean is:

$s_{\bar{x}} = \frac{s}{\sqrt{n}}$

$s_{\bar{x}}$ = the standard deviation of the mean

s = the standard deviation of n subsamples or measurements

n = the number of subsamples or measurements from which the mean, $\bar{x}$, is calculated.

If the results are expressed as percentages, the expected precision for different mean values, $\bar{x}$, can be defined in terms of the standard deviation of the mean, $s_{\bar{x}}$, as follows:

$\bar{x}$ (%)	$s_{\bar{x}}$ (%)
5	1.54
10	2.12
15	2.52
20	2.83
25	3.06
40	3.47

Two comments are worth making. The first is that whereas the absolute value of $s_{\bar{x}}$ increases with the mean percentage, the relative standard deviation of the mean, or coefficient of variation of the mean, $s_{\bar{x}} / \bar{x}$, decreases with increasing mean percentage of a particular constituent. Thus, the higher mean percentages give a relatively more stable estimate of the proportion of a particular constituent in a sample than the lower mean percentages. It is also worth noting from the equation above that to double the precision of the point count estimates of mineral percentages (i.e. to halve the standard deviation of the mean, $s_{\bar{x}}$) would require 40 traverses of 20 points each per thin section, a result which hardly merits the fourfold increase in expenditure of time.

Additional mineral composition data have been obtained from examination of polished sections, stained thin sections, grain mounts, and X-ray diffraction powder patterns of a number of selected samples. Each of these techniques is designed to distinguish among specific minerals not easily identified in thin sections, and their particular applications are discussed below.

Descriptions of Mineral Constituents

From a purely objective point of view the mineral composition of a rock should be described in terms of the relative proportions of mineral constituents per unit volume or weight. A more practical approach is required in classifying and estimating the proportions of constituents in the heterogeneous greywacke-type of sandstones typical of the Cretaceous rocks of Alberta. Much of the detritus in these rocks is inherently fine-grained, and the mineral composition and proportions of the various components

of this material cannot be determined in thin sections of conventional thickness at standard magnifications. For this reason, it is necessary to define operational classes of "mineral" constituents which are only partly correlative with the actual mineral constituents of the rock, but which, unlike the latter, can be easily distinguished and point-counted in thin sections. As long as the identification of these operational classes of constituents is consistent from sample to sample, and estimates of their relative proportions are accordingly precise, the possibility exists that the true mineral composition of this material can be more accurately determined by other analytical techniques, and the point-count estimates of the mineral composition of the rocks adjusted accordingly.

It is also preferable in classifying the mineral constituents of sedimentary rocks to distinguish among what Krynine (1948) has called the *textural elements* of sedimentary rocks. Thus, the mineral constituents of the magnetite sandstones can be described a a clastic framework of grains impregnated by authigenic cements. Grains are those discrete particles brought into the site of deposition from either a distant or a local source area, and form the primary detrital or clastic fabric of a sediment. Cements are those minerals precipitated in the initially fluid-filled interstices of a sediment subsequent to the deposition of the grains. Such minerals are authigenic or secondary and have a characteristic crystalline rather than a granular texture. The description of mineral constituents as grains or cements implies recognition of the twofold physicochemical origin of sedimentary rocks, and introduces genetic concepts into the classificatory scheme.

The various mineral constituents of the 60 modally analysed samples have been grouped for point-counting purposes into several operational classes, the composition and textures of which are discussed below. The proportions of mineral constituents in each sample are given in table 1, where the samples are arranged first according to their distribution within four main areas, and then in sampled sections within each area. Each sample number (e.g. 290-04) refers to the location of the sampled section (290) and the particular sample from that section (-04). The locations of the individual sampled sections are given in table 8 in the section on Economic Geology.

Quartz, Quartzite Fragments, and Chert. Quartz (SiO_2) is the most abundant detrital constituent in the 60 modally analysed samples of table 1. It occurs most commonly as single or discrete grains with an average maximum diameter observed in thin sections of about 0.2 mm. The grains are clear and colorless, with complete extinction, and are generally free of inclusions. Authigenic quartz overgrowths are absent or only incipiently developed and have been included in the estimated proportions of detrital quartz in table 1.

Most of the grains have an irregular shape and are markedly angular (Figs. 22, 23, 24), even in the absence of authigenic overgrowths. However,

numerous grains are partly bounded by smooth, straight edges which indicate the presence of primary crystal faces (Figs. 23, 25), and a few grains show regular hexagonal outlines. These euhedral or subhedral grains are of probable volcanic, pyroclastic origin.

Quartz is present less commonly as aggregate grains in the form of metaquartzite fragments and chert, the estimated proportions of which are shown separately from those of single quartz grains in table 1. The mineral is also a common component of many finely crystalline volcanic and silty rock fragments, which have been counted as a separate class.

Feldspars. Estimates of feldspar proportions in table 1 refer to the distribution of single grains, although feldspars are also minor components of finely crystalline volcanic rock fragments. Feldspars are colorless, but, unlike quartz, are usually slightly cloudy in transmitted light owing to the presence of small amounts of disseminated impurities, such as sericite, chlorite, or kaolinitic (?) "dust." In many samples some of the feldspar grains have been partly replaced by authigenic calcite, and in a few samples by authigenic chlorite.

The average maximum diameter of feldspar grains observed in thin sections is about 0.2 mm., the same as quartz. The grains are generally subrectangular in shape, being bounded by one or more straight edges which parallel crystal faces or cleavage directions. The corners of most grains are moderately rounded and the grains are distinctly less angular in appearance than most quartz grains.

It is difficult to distinguish among the various feldspar species in thin sections. Between 25 and 30 per cent of the feldspar grains show characteristic albite twinning indicative of plagioclase ($NaAlSi_3O_8$ - $CaAl_2Si_2O_8$), but the remaining grains are homogeneous. The ratio of the average percentages of Na_2O and K_2O in 19 chemically analysed samples (table 6, p. 59) is 2.96, suggesting that most of the untwinned feldspar is also plagioclase. Some of the K_2O is also derived from biotite, further emphasizing the sodic nature of the feldspars. This interpretation of the chemical analyses is supported by the relative frequencies of stained and unstained feldspar grains observed in four thin sections of "barren" sandstones from above and below the magnetite-bearing sandstones. From 75 to 85 percent of the single feldspar grains are unstained[1] and are presumably plagioclase, whereas the remaining 15 to 25 per cent of the feldspar grains are stained, and are presumably sanidine or orthoclase ($KAlSi_3O_8$). The compositional range of the plagioclase has not been determined.

Biotite. Biotite [$K(Mg,Fe,Al)_3(Si,Al)_4O_{10}(OH)_2$] is the only common coarse-grained micaceous mineral in the 60 modally analysed samples. Because of its platy habit, it is observed in thin sections cut perpendicular

[1] The staining technique is based on the reaction of potash-rich feldspar with sodium cobaltinitrite (Chayes, 1952).

Table 1A. Percentages of Mineral Constituents, Fe_2O_3, and TiO_2; Grain Size; and Bulk Densities of Sixty Belly River Iron-rich Sandstones

TODD CREEK

Sample	QUARTZ	QUARTZITE CHERT	FELDSPAR	BIOTITE	ROCK FRAGMENTS	MAGNETITE	ACCESSORY MINERALS	CARBONATES			AUTHIGENIC CHLORITE	MISCELLANEOUS	TOTAL	Fe_2O_3[1]	TiO_2[1]	GRAIN SIZE[2] phi units	BULK DENSITY[3]
								Clastic	Authigenic	Total							
278-01	18.5	3.5	3.5	—	18.5	2.0	2.0	*25.0*	—	25.0	23.5	3.5	**100.0**	13.13	1.51	2.70	2.795
278-04	12.5	1.0	—	0.5	10.0	29.0	7.5	*13.0*	*0.5*	13.5	21.5	4.5	**100.0**	38.35	7.08	2.92	3.323
278-05	25.5	3.5	—	0.5	14.5	0.5	—	*17.5*	*4.5*	22.0	33.0	0.5	**100.0**	19.14	1.85	2.59	2.911
290-04	19.5	1.0	0.5	—	14.5	10.0	1.5	*15.0*	—	15.0	34.0	4.0	**100.0**	36.36	3.75	2.80	3.028
290-08	20.5	2.0	—	—	10.5	5.5	2.5	*26.0*	*7.0*	33.0	23.5	2.5	**100.0**	19.82	2.52	2.36	2.966
290-12	19.5	5.0	2.5	0.5	12.0	2.0	1.0	*27.0*	—	27.0	27.5	3.0	**100.0**	12.60	0.99	2.23	2.765
295-03	21.5	2.0	—	1.0	16.0	4.0	0.5	*25.0*	—	25.0	26.0	4.0	**100.0**	25.48	2.39	2.33	2.942
295-10	20.0	2.0	10.5	1.0	17.5	4.5	2.0	*15.0*	*0.5*	15.5	21.5	5.5	**100.0**	17.78	2.50	2.49	2.816
295-13	17.0	4.0	16.0	1.5	10.0	2.5	—	*21.0*	*19.5*	40.5	5.5	3.0	**100.0**	9.59	1.58	2.57	2.827
297-03	31.5	4.5	15.0	1.0	11.5	—	—	*12.5*	*12.0*	24.5	9.0	3.0	**100.0**	4.84	0.78	2.16	2.691
297-07	1.5	0.5	—	—	1.5	31.0	5.5	—	—	—	53.5[4]	6.5	**100.0**	71.23	9.66	3.32	3.430
297-09	21.5	3.0	—	—	19.0	0.5	—	*18.5*	*4.5*	23.0	32.0	1.0	**100.0**	17.32	1.42	2.62	2.747
Locality mean	19.08	2.67	4.00	0.50	12.96	7.63	1.88	*17.96*	*4.04*	22.00	25.88	3.42	**100.02**	23.81	3.00	2.59	2.937

(1) Determined by X-ray fluorescent techniques.
(2) Average phi grain size of 20 grains per sample.
(3) Average of two replicate analyses per sample.
(4) Includes weathered chloritic-limonitic matrix of detrital origin.

Table 1B. Percentages of Mineral Constituents, Fe_2O_3, and TiO_2; Grain Size; and Bulk Densities of Sixty Belly River Iron-rich Sandstones

BURMIS

Sample	QUARTZ	QUARTZITE CHERT	FELDSPAR	BIOTITE	ROCK FRAGMENTS	MAGNETITE	ACCESSORY MINERALS	CARBONATES			AUTHIGENIC CHLORITE	MISCELLANEOUS	TOTAL	Fe_2O_3	TiO_2	GRAIN SIZE phi units	BULK DENSITY
								Clastic	Authigenic	Total							
301-01	25.0	3.0	12.5	0.5	8.5	4.0	0.5	*15.5*	—	15.5	29.0	1.5	**100.0**	13.96	2.05	2.64	2.761
301-14	4.5	—	—	—	2.0	53.0	8.0	—	—	—	24.5	8.0	**100.0**	74.41	7.79	3.14	3.759
301-18	26.0	0.5	12.0	0.5	14.0	13.0	1.5	*5.5*	*3.5*	9.0	19.0	4.5	**100.0**	28.31	3.37	2.75	2.983
386-03	16.0	1.0	—	—	10.5	11.0	3.0	*24.0*	*4.0*	28.0	25.5	5.0	**100.0**	26.63	3.15	2.56	3.107
386-09	10.5	—	—	0.5	9.0	18.0	3.5	*24.0*	*4.5*	28.5	23.5	6.5	**100.0**	41.12	5.35	2.70	3.468
386-17	20.5	3.0	10.5	0.5	15.5	5.5	1.5	*16.0*	*1.5*	17.5	18.5	7.0	**100.0**	17.81	3.62	2.35	2.920
338-06	25.5	3.0	7.0	—	15.0	0.5	—	*17.5*	*9.5*	27.0	20.0	2.0	**100.0**	13.54	1.06	2.44	2.801
338-14	15.0	2.5	1.5	1.5	12.5	5.0	1.0	*28.5*	*7.0*	35.5	22.5	3.0	**100.0**	16.45	2.03	2.55	2.951
338-17	16.5	1.5	6.5	0.5	9.5	13.5	4.0	*17.5*	*0.5*	18.0	22.0	8.0	**100.0**	28.89	4.42	2.94	3.095
342-02	33.0	3.5	8.0	1.0	16.0	3.0	0.5	*11.5*	—	11.5	22.0	1.5	**100.0**	17.24	1.74	2.29	2.817
342-05	4.5	1.0	—	—	0.5	59.0	3.0	—	—	—	27.0	5.0	**100.0**	68.67	9.99	3.05	3.828
342-09	16.0	3.5	—	—	15.0	10.5	3.0	*24.0*	*0.5*	24.5	22.5	5.0	**100.0**	35.86	4.83	2.79	3.197
348-02	19.5	1.5	14.0	—	15.0	—	—	*28.5*	*15.5*	44.0	3.5	2.5	**100.0**	5.83	0.89	2.33	2.749
348-05	1.5	—	—	—	0.5	61.5	6.0	—	—	—	19.5	11.0	**100.0**	81.35	8.39	3.11	3.997
348-07	29.5	2.0	12.5	1.5	13.5	—	—	*18.5*	*7.5*	26.0	11.5(5)	3.5	**100.0**	5.31	1.23	2.32	2.676
385-01	15.5	1.0	—	—	11.5	13.0	8.0	*18.0*	*1.5*	19.5	24.5	7.0	**100.0**	28.97	4.49	2.75	3.128
385-07	7.5	0.5	—	—	8.5	34.0	1.0	*19.0*	*5.5*	24.5	21.0	3.0	**100.0**	45.81	5.35	2.96	3.512
385-14	24.0	4.5	19.0	0.5	13.0	—	—	*19.0*	*2.5*	21.5	15.0(5)	2.5	**100.0**	6.18	1.18	2.70	2.700
Locality mean	17.25	1.78	5.75	0.39	10.56	16.92	2.47	*15.94*	*3.53*	19.47	20.60	4.81	**100.00**	30.91	3.94	2.69	3.136

(5) Includes authigenic kaolinite.

Table 1C. Percentages of Mineral Constituents, Fe_2O_3, and TiO_2; Grain Size; and Bulk Densities of Sixty Belly River Iron-rich Sandstones

DUNGARVAN CREEK

Sample	QUARTZ	QUARTZITE CHERT	FELDSPAR	BIOTITE	ROCK FRAGMENTS	MAGNETITE	ACCESSORY MINERALS	CARBONATES			AUTHIGENIC CHLORITE	MISCELLANEOUS	TOTAL	Fe_2O_3	TiO_2	GRAIN SIZE phi units	BULK DENSITY
								Clastic	Authigenic	Total							
308-01	1.5	—	—	—	—	62.0	1.0	*2.5*	*1.0*	3.5	19.5	12.5	**100.0**	71.12	8.98	3.57	3.898
308-04	3.0	0.5	—	—	1.5	57.5	2.0	—	—	—	29.0	6.5	**100.0**	73.11	9.12	3.44	3.912
308-07	6.5	1.0	—	1.0	1.5	36.5	1.0	*15.5*	—	15.5	32.5	4.5	**100.0**	46.33	5.24	2.89	3.376
309-03	25.5	1.5	16.0	—	11.5	0.5	—	*25.0*	*7.0*	32.0	11.5	1.5	**100.0**	3.45	1.00	2.27	2.693
309-04	22.5	1.5	10.5	0.5	11.0	—	0.5	*33.5*	*19.0*	52.5	1.0	—	**100.0**	7.08	0.61	2.23	2.743
309-09	17.0	1.5	13.0	1.0	12.5	—	0.5	*30.0*	*11.0*	41.0	11.5	2.0	**100.0**	8.80	1.45	2.33	2.829
310-04	19.5	3.0	17.0	1.5	14.0	4.5	2.0	*18.0*	*6.0*	24.0	13.0	1.5	**100.0**	9.94	1.72	2.24	2.748
310-09	20.0	4.0	14.0	1.5	11.5	5.5	1.0	*22.5*	*3.5*	26.0	15.0	1.5	**100.0**	12.91	2.00	2.26	2.819
310-19	12.5	2.0	—	0.5	12.0	22.0	4.5	*11.0*	—	11.0	28.0	7.5	**100.0**	49.37	5.94	2.88	3.464
310-24	21.0	3.5	6.5	0.5	13.0	3.0	—	*22.0*	*6.0*	28.0	23.0	1.5	**100.0**	19.51	1.17	2.13	2.849
310-33	9.0	4.0	—	0.5	8.5	29.5	7.5	*12.0*	—	12.0	27.5	1.5	**100.0**	59.11	7.03	3.28	3.477
310-36	—	—	—	—	—	62.5	10.0	—	—	—	24.5	3.0	**100.0**	78.17	8.87	3.24	4.060
368-01	21.5	3.0	8.0	1.0	16.0	8.0	2.0	*21.0*	*10.0*	31.0	7.5	2.0	**100.0**	13.67	2.14	2.61	2.868
368-05	16.0	1.5	7.5	—	8.5	5.0	0.5	*32.5*	*26.0*	58.5	1.0	1.5	**100.0**	8.46	1.37	2.57	2.882
368-08	20.5	2.5	8.5	0.5	8.5	—	—	*27.5*	*1.0*	28.5	28.5	2.5	**100.0**	11.65	0.70	2.62	2.728
368-10	0.5	—	—	—	0.5	61.5	3.0	—	—	—	28.5	6.0	**100.0**	78.43	9.93	3.24	4.267
368-12	1.5	—	—	—	—	67.0	1.0	—	—	—	30.0	0.5	**100.0**	84.05	8.23	3.25	4.325
368-15	14.5	4.0	16.5	—	20.0	1.0	—	*13.5*	—	13.5	25.5	5.0	**100.0**	16.16	1.78	2.41	2.761
Locality mean	12.92	1.86	6.53	0.47	8.36	23.67	2.03	*15.92*	*5.03*	20.94	19.83	3.39	**100.01**	36.18	4.29	2.75	3.261

Belly River Iron-rich Sandstones

SOUTHERN LOCALITIES

Sample	QUARTZ	QUARTZITE CHERT	FELDSPAR	BIOTITE	ROCK FRAGMENTS	MAGNETITE	ACCESSORY MINERALS	CARBONATES			AUTHIGENIC CHLORITE	MISCELLANEOUS	TOTAL	Fe_2O_3	TiO_2	GRAIN SIZE phi units	BULK DENSITY
								Clastic	Authigenic	Total							
364-02	16.5	0.5	2.5	0.5	9.5	6.0	0.5	*33.5*	—	33.5	21.0	9.5	**100.0**	12.92	1.71	2.53	2.875
364-06	9.0	2.0	—	0.5	5.5	10.5	4.5	*42.0*	*0.5*	42.5	21.5	4.0	**100.0**	23.06	3.66	2.67	3.059
364-10	21.5	3.5	3.5	0.5	15.0	3.5	3.5	*18.5*	—	18.5	28.5	2.0	**100.0**	15.48	1.21	2.66	2.858
371-03	19.0	0.5	7.0	2.0	7.0	2.0	—	*38.0*	*1.0*	39.0	20.5	3.0	**100.0**	9.90	1.46	2.72	2.785
372-03	19.0	3.0	9.0	0.5	6.0	6.5	3.0	*26.5*	*1.0*	27.5	24.5	1.0	**100.0**	18.37	2.12	2.64	2.880
373-05	1.5	—	—	—	0.5	60.5	1.5	—	—	—	29.0	7.0	**100.0**	86.28	8.35	3.13	4.341
374-02	27.5	2.0	23.5	0.5	15.0	0.5	0.5	*10.5*	*3.5*	14.0	16.0	0.5	**100.0**	12.11	1.40	2.25	2.659
374-05	21.0	1.5	11.0	—	4.0	6.5	1.0	*23.5*	*17.5*	41.0	11.0	3.0	**100.0**	14.09	2.02	2.55	2.939
374-07	29.0	3.0	9.5	0.5	7.5	3.0	1.5	*21.5*	*1.0*	22.5	21.5	2.0	**100.0**	14.37	1.72	2.57	2.839
378-03	27.5	6.5	13.0	0.5	14.5	1.5	0.5	*10.0*	—	10.0	24.0	2.0	**100.0**	18.79	2.90	2.00	2.825
378-10	16.0	—	—	1.5	12.5	3.5	0.5	*28.0*	*22.0*	50.0	13.5	2.5	**100.0**	18.40	1.63	2.40	2.930
378-12	34.5	2.5	—	1.0	19.0	0.5	—	*11.0*	—	11.0	30.5	1.0	**100.0**	23.22	1.26	2.21	2.634
Locality mean	20.17	2.09	6.58	0.66	9.67	8.71	1.41	*21.92*	*3.88*	25.79	21.79	3.13	**100.01**	22.25	2.45	2.53	2.968
$\bar{x}$ (6)	16.90	2.04	5.80	0.49	10.20	15.45	2.01	17.53	4.15	21.68	21.66	3.77	**100.00**	29.34	3.56	2.66	3.100
s (7)	8.86	1.52	6.48	0.52	5.60	21.06	2.39	10.49	6.24	14.33	8.95	2.68					
$s_{\bar{x}}$ (8)	1.14	0.20	0.84	0.07	0.72	2.72	0.31	1.35	0.81	1.85	1.15	0.35					
c_v (9)	0.52	0.75	1.12	1.06	0.55	1.36	1.19	0.60	1.50	0.66	0.41	0.71					

(6) Grand mean of sixty samples from four localities (tables 1A, 1B, 1C, 1D).
(7) Standard deviation.
(8) Standard deviation of the mean.
(9) Coefficient of variation.

to the bedding as lath-like, reddish-brown, pleochroic grains, commonly distorted by compaction of the surrounding, more rigid grains. The mineral is present sparingly in the magnetite-rich sandstones, but is locally abundant in the underlying and overlying pale grey "barren" sandstones, forming fissile, biotite-rich beds up to 6 inches thick.

Rock Fragments. Rock fragments are discrete mineral aggregates of variable composition, texture, and origin. Such a heterogeneous collection of detrital constituents invariably leads to difficulties in performing quantitative modal analyses (Griffiths, 1960b), because, although rock fragments can be point-counted as a single class for the sake of convenience, the mineral components of many fragments are too fine-grained or intimately intergrown to be sorted out or even identified in thin sections. In many sedimentary rocks the softer rock fragments tend to rupture under pressure produced by compaction processes, forming a fine-grained, "argillaceous" paste that literally has flowed into the surrounding interstices bounded by more rigid grains, and is commonly indistinguishable from certain fine-grained authigenic silicate cements. This "matrix effect" is quantitatively unimportant in most of the samples listed in table 1, although there is some difficulty in distinguishing between authigenic chlorite cement and crushed chloritic rock fragments in several samples.

Some rock fragments are characterized by their predominant or gross mineral composition, such as chert (aggregates of equidimensional quartz crystals), micaceous fragments (illite-sericite aggregates), or chloritic fragments. The gross mineral composition can be combined with typical textures and structures to indicate the origin of the fragments by the use of such terms as "fossiliferous" or "sedimentary" chert, "phyllite," "volcanic fragment," etc. Classification of rock fragments according to the nature of the parent or source rocks, however, is often ambiguous, and there is usually a sizeable proportion of fragments in most sedimentary rocks, the origin of which is obscure.

In performing modal analyses of the iron-rich sandstones listed in table 1, quartzite fragments and chert, essentially monominerallic aggregates, were counted as a separate class. An attempt was made to classify the remaining fine-grained rock fragments into volcanic and nonvolcanic groups on the basis of their composition and texture, and at the same time to estimate the proportions of their individual component minerals. The net results of this double count are not consistent from sample to sample, and the nonsiliceous rock fragments have been left as a single class in table 1. Nevertheless, because these rock fragments make up a sizeable proportion of many samples, a brief summary of their composition and inferred origin is in order.

The average mineral composition of the rock fragments in the 60 samples of table 1, irrespective of their origin, is approximately 40 per cent chlorite, 10 per cent quartz, 5 per cent fine-grained micas, 5 per cent

feldspar, and 40 per cent unresolved, finely crystalline matter. The latter consists of intimately intergrown chlorite, quartz, feldspar, and cryptocrystalline opaque matter, such as leucoxene and limonite.

At least 40 per cent of the fragments are of probable volcanic origin. Many of the remaining 60 per cent may also be of volcanic origin, particularly certain fine-grained, homogeneous, chloritic ovoids that are abundant in some samples. Other common types of rock fragments include chloritic-micaceous siltstone fragments, and chloritic chert or felsite. Micromicaceous slate and phyllite fragments are rare, as are dark brown or grey, cryptocrystalline "argillite" fragments typical of some of the Cretaceous sandstones of the Foothills. These data, although qualitative, are of considerable help in interpreting the composition of the source rocks which have been broken down and reconstituted to form the Belly River iron-rich sandstones.

Magnetite. The mineral constituent described as "magnetite" in table 1 includes all of the black opaque grains point-counted in thin sections of the 60 modally analysed samples, as it is not possible to distinguish between such minerals as magnetite (Fe_3O_4) and ilmenite ($FeTiO_3$) in thin sections, even with the help of reflected light. The strongly magnetic character of the samples in general indicates that a large proportion of the black opaque grains are magnetite, but the relatively high titanium content of the rocks (table 1) showed the need for a more detailed examination of the mineral composition of the opaque fraction of the samples.

To this end, standard polished sections of six magnetite-rich samples were examined in reflected light, and 50 opaque grains were randomly selected from each sample and classified. The resulting grain frequencies are shown in table 2.

Most of the grains identified as magnetite are homogeneous metallic grains with a slightly pinkish color in reflected light and are isotropic. Many of the grain boundaries are primary crystal faces, although the corners have been well rounded. Small inclusions are more common than observed in thin sections and appear to be largely zircon, quartz, and possibly apatite.

In four samples from outcrop sections, many of the magnetite grains show partial replacement by silvery-white hematite, which occurs as small, irregular patches about the grain boundaries, coalescing in some cases to form a grain composed of a hematite rim and a magnetite core. Hematite also partly replaces or is intergrown with magnetite in the form of large irregular patches, fine dendritic mosaics, or as exsolution lamellae. Hematite-magnetite intergrowths are more common than inferred by the data in table 2, as only magnetite grains composed of more than 10 per cent hematite have been counted separately. Replacement of magnetite by hematite is rare in samples 385-07 and 297-07. The former is from an unweathered cored section, but the latter sample is from a weathered outcrop section, and all the mineral constituents but quartz and magnetite have

Table 2. Frequencies of Opaque Minerals in Polished Sections of Six Belly River Magnetite-rich Sandstones

Sample	Magnetite		Magnetite-ilmenite	Ilmenite		Hematite	Total
	unaltered	partly altered to hematite		homogeneous	with hematite intergrowths		
297-07	40	5	—	1(?)	1	3	50
308-01	27	11	3	7	—	2	50
342-05	38	2	3	1(?)	2	4	50
365-10	33	8	—	8	—	1	50
373-05	33	7	5	2	2	1	50
385-07(1)	34	2	6	8	—	—	50
Total frequency	205	35	17	27	5	11	300
Average percentage	68.3	11.7	5.7	9.0	1.7	3.7	100.1

Locations of samples are given in table 8. Modal analyses are given in table 1.

(1) Core sample

altered to a cryptocrystalline limonitic matrix. Thus, although textural criteria indicate that magnetite is altering in situ to hematite as a consequence of surficial oxidation in the other four outcrop samples, the absence of this phenomenon in sample 297-07 is puzzling.

Grains classified as ilmenite in table 2 are almost identical in morphology, color, and reflectivity value to magnetite, but are anisotropic with pale brown to bluish-grey polarization colors. They are less susceptible to replacement by hematite, although a few grains are composed of both minerals, with hematite the more abundant component. Similarly, scattered composite grains composed of variable proportions of magnetite and ilmenite were observed. The texture of these grains is variable, one mineral appearing as irregular patches in the other, or as subparallel exsolution lamellae. However, the two minerals are generally mutually exclusive in their occurrence, discrete grains being composed of either magnetite or ilmenite.

The frequencies in table 2 indicate that the ratio of magnetite to ilmenite (the latter including ilmenite-magnetite grains) is about 5 to 1, but this frequency ratio is not consistent among the six samples. Ilmenite is rare or possibly absent in samples 297-07 and 342-05, although chemical analyses (table 1) show that the Fe_2O_3/TiO_2 ratios of these two samples are as high as those of the others. It is possible that ilmenite was originally present in the two samples, but has altered largely to the leucoxene-like aggregates observed in thin sections, or to anatase, which forms the largest part of the nonmagnetic heavy mineral fraction.

Because of the relatively poor optical and textural criteria for differentiating between magnetite and ilmenite, and the variable distribution of ilmenite in the samples listed in table 2, the composition of the magnetic heavy mineral fractions from eight magnetite-rich samples was determined from X-ray diffraction powder patterns. The magnetic and nonmagnetic heavy mineral fractions of each sample were separated using a Franz Isodynamic Separator at high amperages, so that ilmenite, if present as discrete grains or as intergrowths with magnetite, would be included in the magnetic fraction.

The powder patterns indicate that magnetite is the most abundant component in the magnetic fractions of all eight samples. Much lesser amounts of ilmenite are indicated in the magnetic fractions of four samples (308-01, 342-05, 368-10, 373-05), but the mineral was not detected in the magnetic fractions of the other four samples (295-10, 297-07, 364-06, 386-03). Thus, although the powder patterns confirm the presence of ilmenite in some samples, the amount appears to vary from sample to sample.

Although optical and X-ray diffraction data do not provide a precise estimate of the average amount of ilmenite in the rocks, the indication is that the amount is low. The proportion of other identifiable titanium-bearing minerals (anatase, rutile, leucoxene) is equally low or uncertain, and the high titanium content of the rocks remains partly unexplained in mineralogical terms. In this light, it is probable that a significant proportion of the titanium occurs in solid solution in the magnetite. The hypothesis is supported by the results of mineral dressing tests (table 10, p. 72), which show that less than two-thirds of the titanium can be removed from finely crushed samples by magnetic separation techniques. The hypothesis is also tentatively supported by the results of detailed measurements of X-ray diffraction powder patterns of the magnetic heavy mineral fractions of three samples. The patterns were measured under the direction of L. B. Halferdahl, Research Council of Alberta, whose report is given below.

> The cell edges of magnetite in three samples were determined by means of X-ray powder diffraction, the reflections (440) and (333) being used. Quartz was the internal standard. Patterns were recorded on a North American Philips diffractometer using filtered iron radiation (wavelength = 1.9373 Å). The mean cell edges, $\overline{a}$, calculated from six patterns for each of the two reflections from the three samples, are given below.

Sample	$\overline{a}$ (Å)	Broadening (Å)
368-10	8.387 ± 0.003	± 0.011
342-05	8.393 ± 0.002	± 0.009
373-05	8.391 ± 0.002	± 0.010

The magnetite peaks are broader than the quartz peaks. Estimates of the effect of this broadening on the cell edges are shown under the column marked "broadening." The estimates were derived by comparing the width of the magnetite peaks with those of quartz peaks of equal height.

The mean values for the samples do not differ greatly; they are slightly below that of pure magnetite, the cell edge of which is 8.3963 ± 0.0005 Å at 18°C. (Basta, 1957). In view of the mode of occurrence of the samples, the broadening of the magnetite peaks is attributed to variation in composition from grain to grain within each sample. Basta (*ibid.*) concluded, however, that the composition of magnetite cannot be determined from measurements of its cell edge only, as substitutions of Mn^{2+} or Ti^{4+} will increase the cell edge, whereas other common substitutions, as well as partial oxidation, will decrease the cell edge. In spite of these objections, if one (1) ignores substitutions other than Ti^{4+}; (2) chooses the maximum cell edge as 8.404 Å as given by the measurements above (including the broadening); and (3) applies Vegard's Law to the solid solution relationship between magnetite and ulvospinel ($\bar{a} = 8.495$ Å, Vincent, *et al.*, 1957), the amount of Fe_2TiO_2 in solid solution in the magnetite of the three samples is 8.1 mol per cent, or 1.7 weight per cent titanium.

Accessory Heavy Minerals. These minerals constitute the nonopaque heavy mineral fraction of the magnetite-bearing sandstones, forming 2 per cent of the mineral constituents of the 60 samples in table 1. However, they are more easily identified and their relative proportions assessed when they are separated from the light mineral and magnetic mineral fractions of the bulk rock by heavy liquid and electromagnetic techniques. The resulting grain concentrates contain both the nonmagnetic opaque and transparent mineral fractions, the specific gravities of which exceed 2.95 for the samples listed in table 3.

The nonmagnetic heavy mineral fraction was separated from each of 12 samples, and the resulting loose grain concentrates were mounted in Canada balsam on glass slides. Twenty-five nonopaque grains from each sample were randomly selected and identified and at the same time a count was made of the relative frequency of the opaque grains in each sample. The results are summarized in table 3, which shows the relative proportions of nonopaque heavy minerals based on counts of 25 grains per sample, and the corresponding frequencies of nonmagnetic opaque grains in each sample.

Approximately one-quarter of the nonopaque heavy mineral grains in table 3 are zircon ($ZrSiO_4$). Most of these grains are clear and colorless, or

Table 3. Frequencies of Heavy Minerals in Nonmagnetic Heavy Mineral Concentrates from Twelve Belly River Iron-rich Sandstones

Sample	NONOPAQUE						OPAQUE			
	Zircon	Anatase	Tourmaline	Garnet	Others	TOTAL	Black	White	Red	TOTAL
290-14	5	18	—	—	2	25	5	3	1	9
295-10	5	20	—	—	—	25	8	5	—	13
297-07	1	23	—	—	1	25	4	1	—	5
308-01	20	4	—	—	1	25	18	—	—	18
310-04	4	12	4	2	3	25	31	16	—	47
342-05	9	13	1	1	1	25	5	—	1	6
348-02	4	20	1	—	—	25	12	27	—	39
364-06	9	15	—	1	—	25	8	24	—	32
368-10	5	18	—	1	1	25	7	1	—	8
373-05	11	11	—	1	2	25	6	—	—	6
374-02	2	22	—	1	—	25	3	2	7	12
386-03	4	17	—	4	—	25	22	—	2	24
Total frequency	79	193	6	11	11	300	129	79	11	219
Average percentage	26.3	64.3	2.0	3.7	3.7	100.0	58.9	36.1	5.0	100.0

Locations of samples are given in table 8. Modal analyses are given in table 1.

less commonly deep pink, with the high birefringence and indices of refraction typical of zircon. Most of the grains are euhedral or subhedral (Fig. 20), although the crystal faces may be slightly rounded. A few very well-rounded, ovoid grains were also observed in each sample.

Anatase (TiO_2) is the most abundant nonopaque heavy mineral, forming approximately two-thirds of the nonopaque grains in table 3. Anatase is pale to deep yellow, has high birefringence and refractive indices, and most grains exhibit incomplete extinction and anomalous interference colors. Much of the anatase in grain mounts is present as aggregate grains composed of several small, nearly opaque crystals, brownish-yellow in reflected light, which appear to grade through a series of partly altered aggregates into white cryptocrystalline leucoxene classified in table 3 as white opaque grains.

Most of the anatase is of detrital origin. As observed in thin sections, euhedral or subhedral anatase crystals are commonly intergrown with black opaque grains (magnetite or ilmenite), chloritic fragments, or well rounded calcite grains. Because of their high specific gravity, these grains are concentrated in the magnetite-rich laminae of many samples, but break up into their component mineral or crystal units when the rock is disaggregated. For this reason, most of the discrete anatase grains or aggregates observed in grain mounts are conspicuously smaller than corresponding zircon grains (Fig. 20).

A few grains of angular varicolored tourmaline and pale pink to colorless garnet were observed in most of the grain mounts, although their presence in several samples is not indicated in table 3. Other nonopaque heavy minerals include rare, reddish-brown rutile grains, and colorless anisotropic grains of unknown mineral composition. None of these constituents is quantitatively important, and they are therefore not described in detail.

The nonmagnetic opaque grains have been classified on the basis of color, and the frequencies of the three resulting groups are given in table 3. Sixty per cent of the opaque grains are composed of a black metallic mineral, probably ilmenite. Many of these grains are partly altered to white leucoxene or red iron oxides. Most of the other opaque grains are white, matted, leucoxene aggregates, many of which appear to have been derived from alteration of fine-grained anatase. The remaining opaque grains are composed of red or brown iron oxides.

Carbonates. Carbonate minerals as a group are easily identified in thin sections by their optical and physical properties, but identification of specific carbonate minerals requires the use of supplementary analytical techniques. In sedimentary rocks carbonates can also be classified according to their mode of origin, based on certain textural criteria (Krynine, 1948). This classification scheme has been followed in estimating the percentages of carbonates shown in table 1, where they have been divided into *clastic* and *authigenic* carbonates.

Clastic carbonates occur as single discrete grains which have been brought into the site of deposition from some pre-existing source terrain in the same manner as quartz, feldspar, magnetite, and fine-grained rock fragments. Most of the grains are composed entirely of carbonates, but their internal structure—i.e., the number, size, and shape of the component carbonate crystals that make up the individual grains—is variable, depending on whether the carbonate is calcite or dolomite. In contrast to quartz and feldspar, clastic carbonate grains are relatively well rounded, with an average maximum diameter observed in thin sections of approximately 0.175 mm.

Authigenic (or secondary) carbonate occurs as irregularly shaped patches of interstitial cement, emplaced subsequent to the deposition of the grains. Authigenic carbonate is clear and colorless and has crystallized as relatively large, optically continuous units, each crystal filling a cluster of adjacent pores (Fig. 23), some partly replacing enclosed feldspar grains and volcanic rock fragments. Thin section observations fail to indicate an obvious relationship between the distribution of authigenic and clastic carbonates.

The distribution of clastic and authigenic carbonates is not necessarily correlative with the occurrence of specific carbonate minerals. These were identified from X-ray diffraction powder patterns of the light mineral fractions of eight of the samples listed in table 1. The percentages of total carbonates in the eight samples range from 14 to 44 per cent, and the corresponding magnetite percentages range from 1 to 11 per cent.

X-ray diffraction powder patterns confirm the presence of calcite ($CaCO_3$) and dolomite [$CaMg(CO_3)_2$] in all samples; other carbonates, including siderite ($FeCO_3$), were not detected. The ratio of the intensities of the calcite (104) reflection and the dolomite (112) reflection varies between 0.15 and 1.15 (as determined from the relative heights of the two diffraction peaks), indicating a relatively large variation in the relative proportions of the two minerals in the eight samples. In this respect, there is a partial correlation between the intensity ratio of the two diffraction peaks and the relative proportions of clastic and authigenic carbonates in the eight samples, the relative intensity of the calcite peak increasing with the amount of authigenic carbonate.

The relationship between carbonate textural elements and composition was investigated further by staining thin sections of five carbonate-bearing samples with Alizarin Red-S, according to the procedure described by Friedman (1959). Fifty carbonate points were randomly selected in each thin section and classified with respect to mineral composition, grain structure, and mode of origin (table 4).

The data in table 4 show that authigenic carbonate is invariably calcite, whereas the clastic carbonates of table 1 are composed of either calcite or dolomite, the two minerals rarely forming component parts of the same grain. Clastic calcite was observed as large single crystals or as grains composed of two or three large anhedral crystals. Many of these grains have a subrectangular shape and appear to be pseudomorphic after feldspar. This interpretation is supported by the partial replacement of numerous feldspar grains and volcanic rock fragments by patches of calcite which are in optical continuity with adjacent patches of authigenic calcite. Calcite also occurs in combination with heavy minerals, commonly as well rounded composite grains composed of a single calcite crystal enclosing small anatase crystals.

Table 4. Frequencies of Carbonate Types in Thin Sections of Five Samples from Iron-rich and "Barren" Basal Belly River Sandstones

Sample	CLASTIC							AUTHIGENIC	TOTAL
	Calcite			Dolomite			Calcite-dolomite(3)	Calcite	
	single crystals	crystal aggregates	composite(1) grains	single crystals	crystal aggregates	composite(2) grains			
278-05	6	2	1	15	15	2	—	9	50
309-03	—	—	2	14	26	5	1(?)	2	50
372-03	2	1	6	14	21	6	—	—	50
386-03	12	4	5	8	11	4	1	5	50
387-22(4)	1	—	3	11	20	8	—	7	50
Total	21	7	17	62	93	25	2	23	250

Locations of samples are given in table 8. Modal analyses are given in table 1 and table 5 (sample 387-22).

(1) Grains composed of calcite and feldspar or calcite and rock fragments.
(2) Grains composed of dolomite and quartz.
(3) Grains composed of both calcite and dolomite.
(4) "Barren" basal sandstone from cored section, Burmis.

Clastic dolomite is distributed throughout all but the most magnetite-rich samples as well rounded, predominantly monominerallic grains. Many grains are composed of a single large dolomite crystal, whereas others are composed of very fine-grained, translucent crystal aggregates. Regardless of crystal size, the mineral invariably tends to express its rhombic crystal habit, in marked contrast to the anhedral habit of clastic and authigenic calcite. About 15 per cent of the dolomite grains contain scattered quartz silt grains or, less commonly, large, well rounded quartz grains. Dolomite is also present as small rhombic inclusions in chert fragments. Dolomite was not observed as a replacement of feldspar or volcanic rock fragments, nor as an authigenic cement, although some of the clastic fragments in a few samples appear to have been subjected to local recrystallization.

Authigenic Chlorite. Chlorite $[(Mg,Fe,Al)_3(Al,Si)SiO_5(OH)_4]$ is the most abundant mineral constituent in the samples listed in table 1 and is responsible for the characteristic green color of the iron-rich sandstones at the top of the basal Belly River member. Authigenic chlorite, point-counted as a separate mineral constituent because of its inferred origin, forms an average 22 per cent of the mineral constituents of the 60 modally analysed samples. Detrital chlorite, point-counted as a component of fine-grained rock fragments, makes up an additional 4 to 6 per cent of the total volume of the 60 samples, so that the total amount of chlorite in the rocks of table 1 averages between 25 and 30 per cent.

Thus, of the total proportion of the chlorite in the rocks, about 80 per cent is present as an authigenic cement, forming a thin, fibrous coating of variable thickness about the walls of the detrital grains. The more magnetite-rich samples are completely cemented by authigenic chlorite (Figs. 21 and 22), whereas the less magnetite-rich samples are generally cemented by both authigenic chlorite and calcite in variable proportions (Fig. 23). Both authigenic and detrital chlorite are pale green and isotropic in thin sections from unweathered borehole samples, but are bluish-to yellowish-green in thin sections from most outcrop samples. In more completely weathered samples chlorite has altered along with many of the other constituents of the rocks (but not magnetite) to reddish-brown iron oxides (e.g. sample 297-07, table 1).

X-ray diffraction powder patterns of the light mineral fractions of eight of the samples in table 1 confirm the presence of chlorite. The percentage of iron in the rocks above that inferred to be present in magnetite or ilmenite (p. 61 - 63) suggests that most of the chlorite is iron-rich, but the mineral is too fine-grained and too intimately mixed with the other constituents of the rocks to allow confirmation of its composition by chemical or optical techniques.

Kaolinite. Kaolinite $[Si_2Al_2O_5(OH)_4]$ is present in trace amounts in only two of the 60 samples listed in table 1 (samples 348-07, 385-14), but is

relatively common in the pale grey "barren" sandstones underlying the iron-rich zone at the top of the basal Belly River member.

Most of the kaolinite is of definite authigenic origin, having been precipitated from solution among the pores of the rock subsequent to the deposition of the clastic grains. It is commonly associated with authigenic quartz (Fig. 11) and is observed in thin sections as clusters of small, colorless, equidimensional, isotropic plates, or as a coating of very thin, colorless fibres growing out from the pore walls, in a manner similar to that of authigenic chlorite. The fibrous variety is distinctly anisotropic, with white to pale yellow first order interference colors. There appears to be a gradation between the morphological and optical properties of the isotropic platy variety and the anisotropic fibrous variety. Well developed kaolinite peaks are present in X-ray diffraction powder patterns of the oriented clay fractions from five unweathered samples of "barren" basal sandstone selected from a cored section in the Burmis area. The average mineral composition of the five samples is given in table 5 (p. 49).

Miscellaneous Mineral Constituents. This group of mineral constituents is composed largely of fine-grained, opaque aggregates of uncertain mineral composition. Whitish cryptocrystalline leucoxene makes up about 60 per cent of this group, commonly occuring as thin patchy films about the margins of detrital grains, or as indistinct patches in authigenic chlorite cement. As such, the substance appears to be authigenic or secondary, although it is more common in some samples than in others. Leucoxene also is present as discrete detrital aggregates, as intergrowths with magnetite or ilmenite grains, and as small inclusions in volcanic rock fragments.

Reddish brown hematite or limonite aggregates form about 20 per cent of the miscellaneous group, and are most common in weathered outcrop samples. Most of this material has resulted from the alteration of chloritic rock fragments or cement, as few of the magnetite grains show signs of alteration, even in the more highly weathered samples (e.g. sample 297-07, table 1).

Other miscellaneous constituents include rare sporitoid (?) bodies, pyrite, and unidentified matter, none of which, however, forms more than a fraction of one per cent of any particular sample.

Distribution and Interrelationships of the Mineral Constituents

The percentages of mineral constituents in each of the 60 modally analysed samples of iron-rich Belly River sandstones are given in table 1. The percentages can be averaged for each of 17 sampled sections, then for each of four general localities (Todd Creek, Burmis, Dungarvan Creek, and the southern localities; cf. Fig. 1), and finally for all 60 samples. The sampled section means (not shown) are based upon modal analyses of three or six samples per section, and their degree of precision is accordingly low.

More precise estimates of the magnetite content of individual sampled sections determined from bulk density analyses are given in table 8 in the section on Economic Geology.

If, however, the 60 samples in table 1 are considered as randomly selected samples representative of a single population, then the over-all or grand mean estimates of each of the mineral constituents in table 1 are relatively precise. These means are shown near the end of table 1D with their corresponding standard deviations (s, a measure of the spread or dispersion of the 60 individual sample estimates about the mean), and coefficients of variation (c_v, a measure of the relative standard deviation about the mean). The degree of precision associated with each mean value is estimated by the standard deviation of the mean ($s_{\bar{x}}$), the calculation and interpretation of which have been discussed previously (p. 21).

The average mineral composition of the rocks is useful information in itself, but does not describe how the mineral constituents are distributed throughout the sampled population, nor does it indicate the spatial interrelationships among the various constituents. Some idea of the distribution of the more important mineral constituents can be gained by grouping the sample percentages into frequency histograms, shown in figures 6 and 7. The composition data of sample 297-07 have been omitted from some of the frequency histograms and succeeding scatter diagrams, as most of the original mineral constituents of the rock have been weathered to a limonitic matrix.

The sample frequency distribution of magnetite (including ilmenite) percentages (Fig. 6) illustrates the excellent sorting of the detrital constituents into magnetite-poor and magnetite-rich layers: 44 samples contain less than 15 per cent magnetite, 9 samples contain more than 50 per cent magnetite, but only 7 samples lie between these extreme values. This bimodality or sorting effect would be emphasized even more strongly were it not for the fact that the estimated magnetite percentages in table 1 are in many cases the averages of two or more magnetite-poor and magnetite-rich laminae within the same thin section. If these laminae were modally analysed as separate units, the resulting magnetite percentages would presumably generate a U-shaped frequency distribution composed only of extreme values.[1]

The frequency distributions of accessory minerals and feldspar (Fig. 6), like that of magnetite, are highly skewed, with a large number of samples containing low percentages of these two constituents. Unlike the frequency distribution of magnetite, those of accessory minerals and feldspar are not obviously bimodal, although the distribution of feldspar is erratic in the higher percentage class intervals, whereas the accessory heavy mineral percentages decrease uniformly away from the modal frequency.

[1] Griffiths (1960a) has suggested a mathematical model that may describe the frequency distribution of heavy minerals in sandstones.

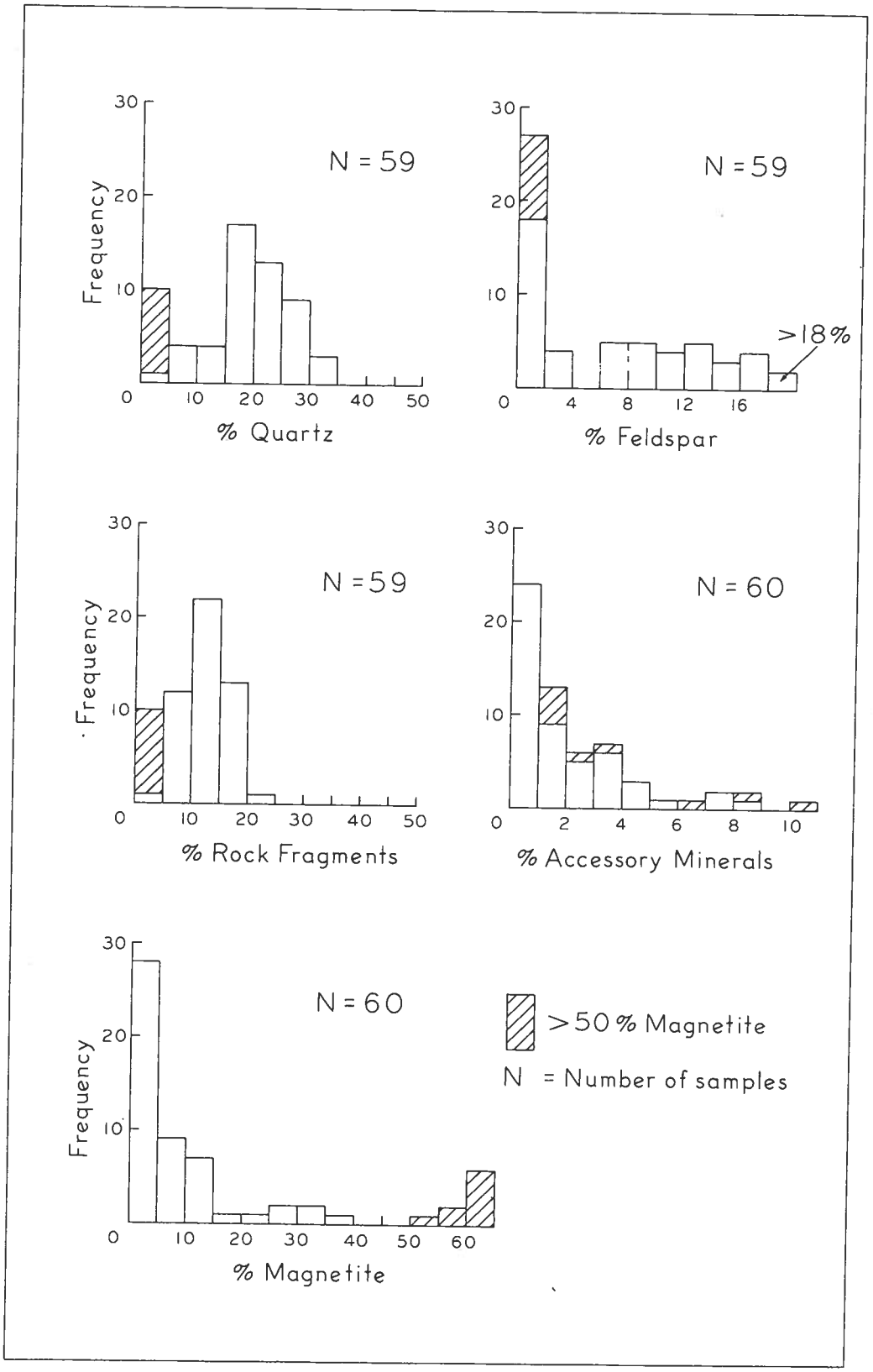

FIGURE 6. Histograms showing the frequency distributions of quartz, feldspar, rock fragments, accessory minerals, and magnetite percentages in 60 Belly River iron-rich sandstones

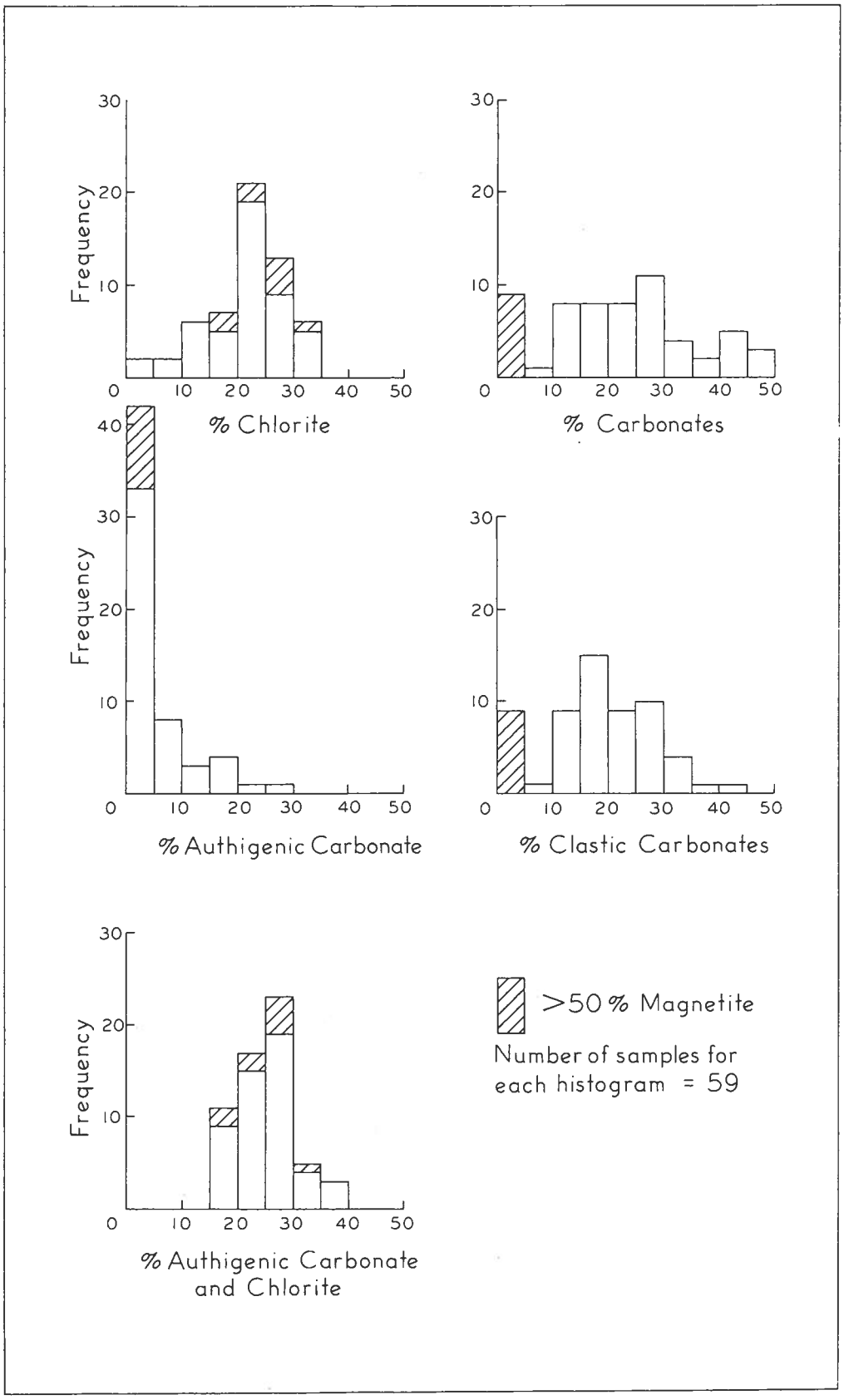

FIGURE 7. Histograms showing the frequency distributions of carbonate and authigenic chlorite percentages in 59 Belly River iron-rich sandstones

The frequency distributions of quartz and fine-grained rock fragments (Fig. 6) are unimodal, excluding the nine samples containing more than 50 per cent magnetite (shown as barred areas in the histograms), with frequencies gradually decreasing on either side of the modal class. The frequency distribution of clastic carbonates (Fig. 7) is more variable than those of quartz and rock fragments, but as clastic carbonates are composed of two minerals (calcite and dolomite) of different origins, it is surprising that the frequency distribution of their combined proportions is not more dispersed.

Histograms illustrating the frequency distributions of authigenic chlorite and authigenic calcite are shown in figure 7. Both histograms are unimodal, but the distribution of chlorite is skewed towards the lower percentages, whereas that of calcite is skewed towards the higher percentages. If the proportions of authigenic chlorite and calcite in each of the 59 samples are combined, the resulting frequency distribution (Fig. 7) of the combined percentages is unimodal, and superficially resembles a binomial distribution. The histogram, in effect, indicates the frequency distribution of the proportions of initially void (or fluid-filled) interstitial spaces among the detrital grains in which the authigenic cements have crystallized. This proportion is a function of the properties of the clastic "framework" grains, and is largely independent of the mineral composition of the cements themselves (Krynine, 1951, Mellon, 1959).

Some of the information obtained from visual comparisons of the frequency histograms can be summarized by comparing the coefficients of variation of the mineral constituents, given in table 1D. Comparison of the standard deviations of the mean percentages of the mineral constituents is misleading, as the standard deviations of data expressed as proportions or percentages are usually related to their means; that is, as the mean increases so does the standard deviation. Use of the coefficient of variation partly circumvents this difficulty, because it is a measure of the relative standard deviation of a set of data, calculated from the expression (Snedecor, 1956, p. 62):

$$c_v = \frac{s}{\bar{x}}$$

c_v = the coefficient of variation

s = the standard deviation

$\bar{x}$ = the mean.

Thus, the coefficients of variation of quartz, clastic carbonates, rock fragments, and authigenic chlorite are small (0.41 to 0.60) in comparison with those of magnetite, accessory heavy minerals, feldspar, and authigenic calcite (1.06 to 1.50). The coefficients of variation of magnetite and calcite are largest, indicating that the sample frequency distributions of the two constituents are similar, although their origins are entirely different.

The interrelationships of some of the modal constituents in table 1 are shown graphically in figures 8, 9, and 10. Figures 8 and 9 show plots of the magnetite percentages against those of three detrital constituents, total carbonates, and authigenic chlorite. The percentages of both quartz and rock fragments exhibit a marked inverse relationship with those of magnetite: the distribution of points is approximately linear, with the scatter of points increasing as the magnetite percentage decreases. The relationship between feldspar and magnetite is also inverse, but more hyperbolic than linear: feldspar is absent in all samples containing more than 15 per cent magnetite, but is erratically distributed in samples containing less magnetite.

The combined proportions of clastic and authigenic carbonates vary inversely with the proportion of magnetite (Fig. 9), but the scatter of points is high, indicating a relatively low correlation between the percentages of the two constituents. This is not surprising in view of the heterogeneous composition and origin of the carbonates. In fact, when the percentages of clastic carbonates (calcite and dolomite) and authigenic calcite are plotted separately against the magnetite percentages, the proportions of both constituents vary inversely with that of magnetite.

The relationship between the proportions of authigenic chlorite and magnetite (Fig. 9) is analogous to that of feldspar and magnetite: the proportion of chlorite in samples containing more than 15 per cent magnetite is relatively constant, but is highly variable in samples containing a low percentage of magnetite. Figure 10 shows plots of clastic and authigenic carbonate percentages versus chlorite percentages. There is no obvious relationship between the proportions of clastic carbonate and authigenic chlorite, nor between the proportions of clastic carbonate and authigenic calcite (not illustrated). However, because authigenic calcite and chlorite are the only authigenic minerals in the rocks, excluding a small amount of authigenic quartz, and have competed to fill the same pore spaces that were present subsequent to the deposition of the detrital grains, there is a well defined inverse correlation between the proportions of the two constituents (Fig. 10). The relationship is linear and a straight line drawn through the scatter of points intersects both the ordinate and abscissa of the graph between the 25 and 35 per cent class intervals. This suggests that the average proportion of initial pore space is constant regardless of the relative proportions of authigenic chlorite and calcite in each of the 59 samples.

Discussion of Results

The composition, distribution, and interrelationships of the mineral constituents of the magnetite-bearing sandstones have been described in some detail. The economic implications of the results are self-explanatory: the most important is that the average magnetite content of the deposits, considering them as a whole, is low, indicating that many of the iron-rich

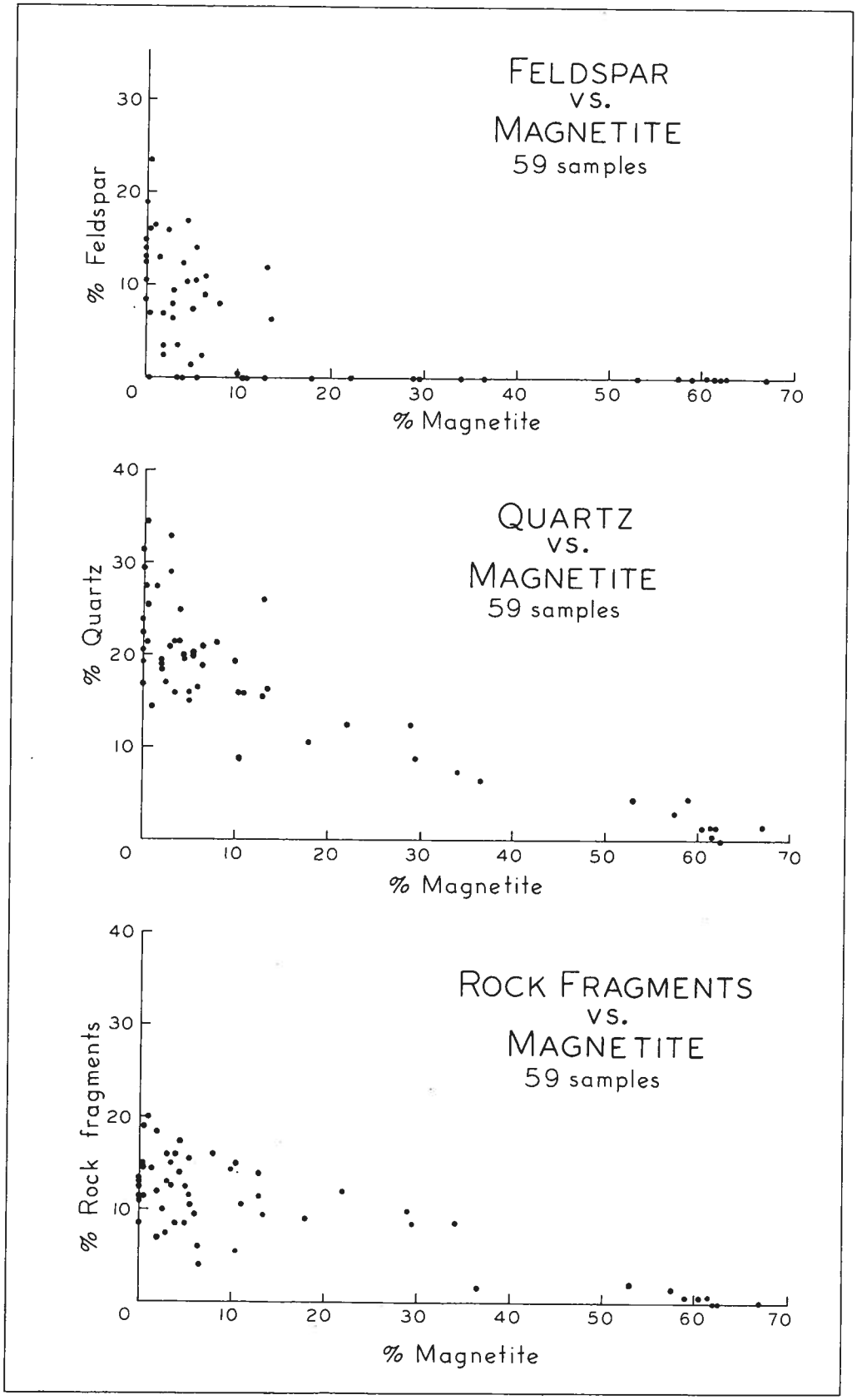

FIGURE 8. Scatter diagrams: feldspar vs. magnetite percentages; quartz vs. magnetite percentages; and rock fragments vs. magnetite percentages, in 59 Belly River iron-rich sandstones

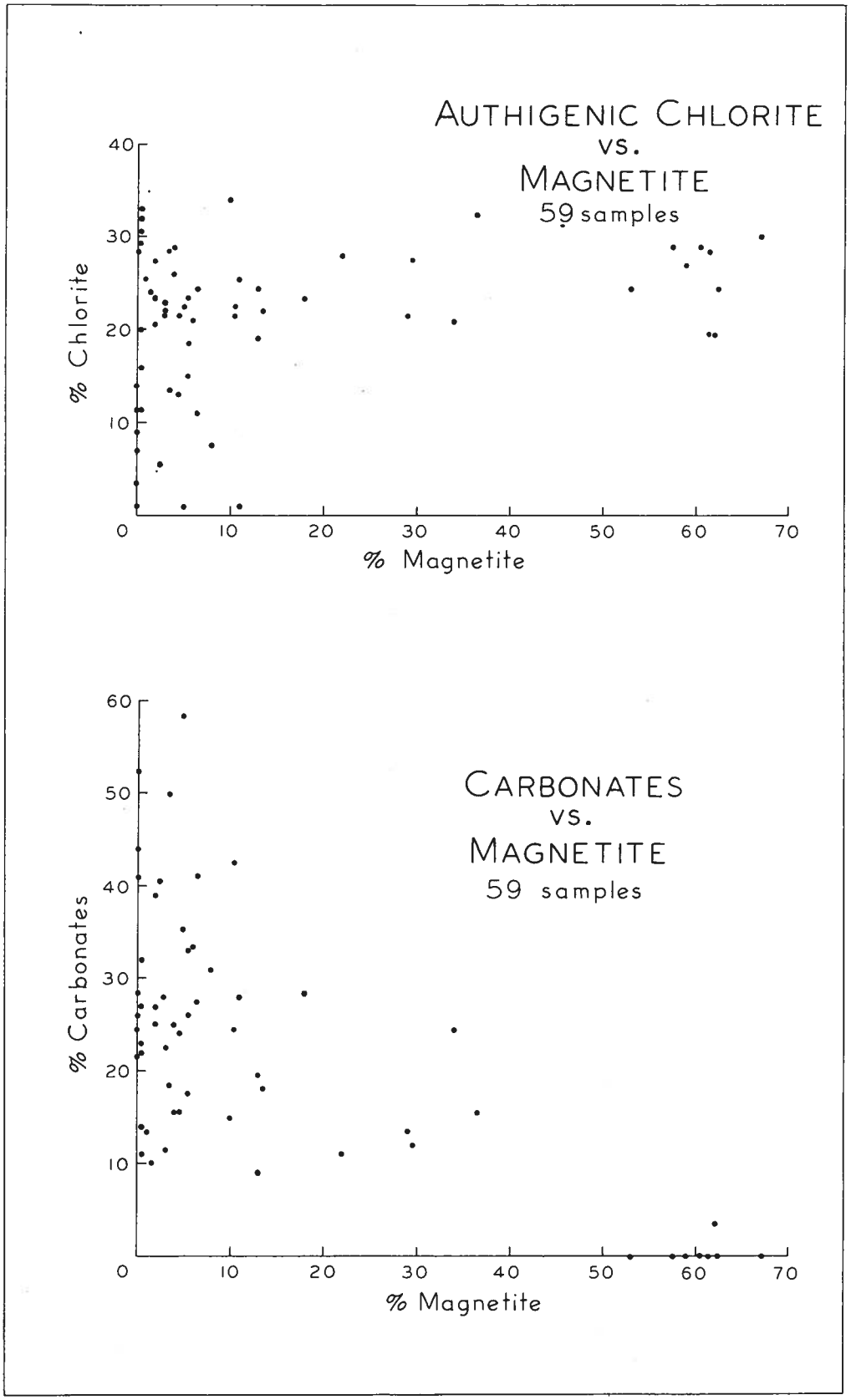

FIGURE 9. Scatter diagrams: authigenic chlorite vs. magnetite percentages; carbonates vs. magnetite percentages, in 59 Belly River iron-rich sandstones

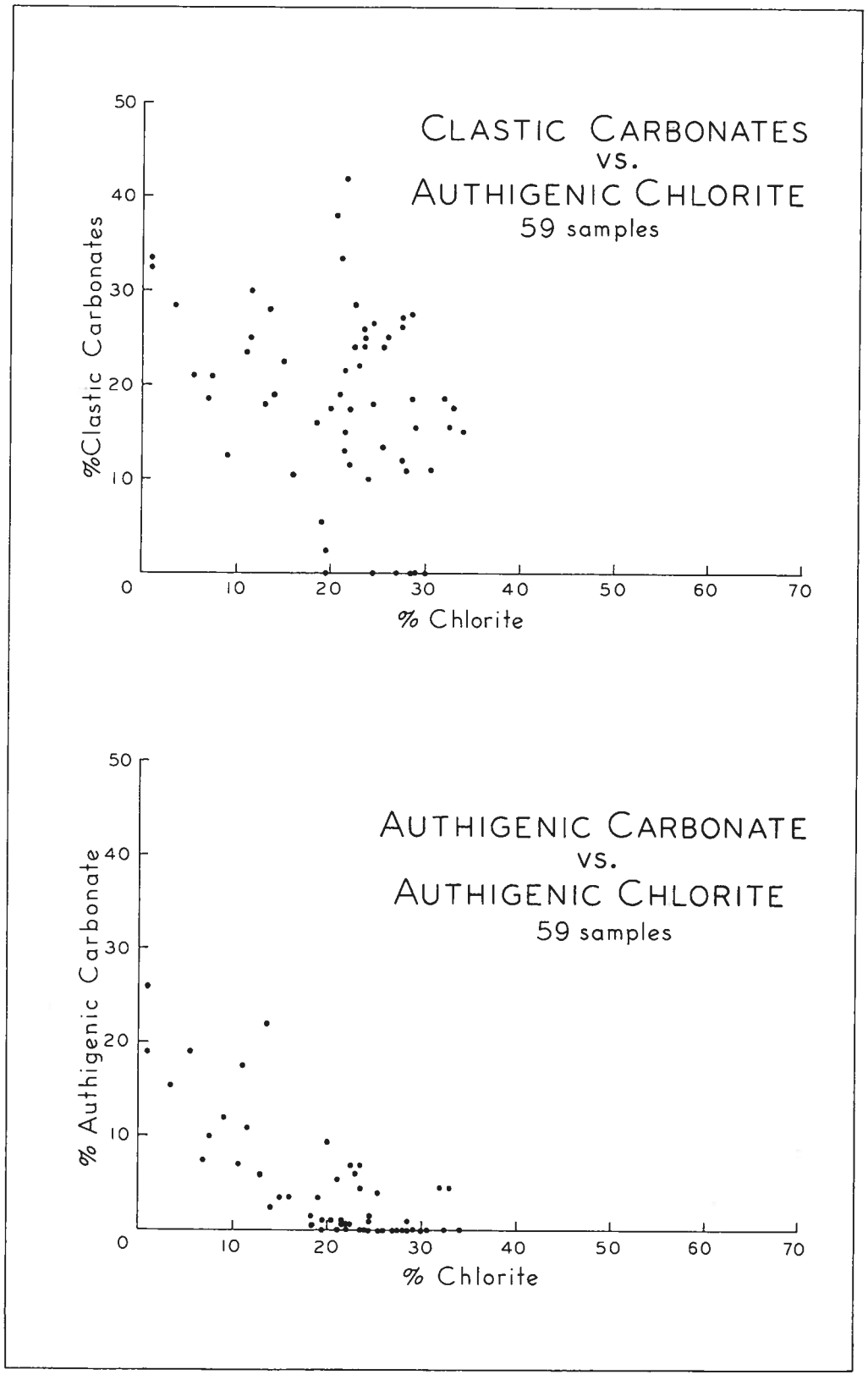

FIGURE 10. Scatter diagrams: clastic carbonates vs. authigenic chlorite percentages; authigenic carbonate vs. authigenic chlorite percentages, in 59 Belly River iron-rich sandstones

deposits at the top of the basal Belly River member cannot be considered as potential iron ore. However, the possibility exists that some of the deposits may contain locally concentrated magnetite-bearing zones thick enough and rich enough to warrant further consideration from an economic point of view: field examination of the various occurrences shows that some have a noticeably larger magnetite content than others, although in a qualitative or compositional sense the mineral constituents of the widely scattered deposits are identical.

Apart from the economic implications of the mineral composition data, which are discussed at length elsewhere, such data contribute much to an understanding of the genesis or origin of the magnetite-bearing sandstones. This is best illustrated by interpreting the data in terms of the three major factors which govern the mineral composition and texture of any sedimentary rock: the composition of the source material, which controls the initial composition of the detritus; processes of selective sorting, which stratify the bulk detritus into a sequence of beds of different composition and texture; and authigenic processes, which are concerned with post-depositional lithification changes in the unconsolidated sediment.

Like the mineral constituents of most sedimentary rocks, those of the magnetite-bearing sandstones can be divided into detrital and authigenic components. The detrital constituents have been derived from some pre-existing source terrain either composed in large part of volcanic rocks, or of a series of active volcanoes ejecting pyroclastic debris into the depositional basin to the east. The feldspar, biotite, and much of the quartz and fine-grained rock fragments are of obvious volcanic origin, and, from its association with these constituents, most of the magnetite is also probably of volcanic origin. The euhedral or angular boundaries of many of the discrete quartz, feldspar, and magnetite grains suggest that the detritus has been subjected to a minimum degree of mechanical abrasion, and it is possible that much of it is of pyroclastic origin, having been blown into the site of deposition rather than derived from the erosion of pre-existing volcanic rocks. The pyroclastic origin is favored to some extent by the "acidic" composition of the volcanic detritus, if it is assumed that most of the feldspar is soda-rich plagioclase.

Detritus of nonvolcanic origin includes clastic dolomite grains, fine-grained silty rock fragments, quartzite fragments, and chert. The euhedral, coarsely crystalline, quartz-bearing fabric of the clastic dolomite grains is typical of many Proterozoic or early Palaeozoic "secondary" dolomites which are distributed throughout the Rocky Mountain regions of the continent in association with other carbonate rocks and orthoquartzites. Some of the well rounded quartz grains and dolomite-bearing chert grains have also probably originated through the breaking-down and redeposition of this type of carbonate terrain.

Rock types other than volcanic or quartzose-dolomitic have probably contributed a lesser proportion of detritus to the iron-rich Belly River rocks, but the criteria for determining the origin of these constituents are ambiguous. Irrespective of the composition and configuration of the source terrain, the fact remains that the magnetite-bearing sandstones have an unusual, heterogeneous mineral composition.

If it is assumed that the detrital fraction of the magnetite-bearing sandstones was transported to the site of deposition as a more or less homogeneous sediment, the bulk detritus has since been selectively sorted into a complex sequence of magnetite-poor and magnetite-rich laminae or beds ranging from a fraction of an inch to 2 or 3 feet thick. The nature of these sorting processes, like the exact composition and configuration of the source terrain, is a subject for speculation, but their effect is readily observed at the megascopic or outcrop level (Fig. 4), and at the microscopic or thin section level, as evidenced by the sample frequency distributions of the detrital constituents (Figs. 6 and 7).

The sorting or placering of the detrital constituents of the magnetite-bearing sandstones is simply a local phase of a much larger phenomenon that transcends the stratigraphic boundary of the Wapiabi-Belly River regression complex. This is best illustrated by examining the distribution of detrital constituents within the basal Belly River member as a whole. To facilitate the comparison, modal analyses of four "barren" Belly River sandstones from above and below the iron-rich sandstones of the basal member are given in table 5.

The detrital fraction of the pale grey "barren" sandstones is composed of quartz, feldspar (largely plagioclase), fine-grained rock fragments (predominantly volcanic), with lesser amounts of chert, detrital dolomite, and biotite (Fig. 25). The last-named mineral is concentrated throughout the "barren" sandstones in sporadic zones up to 6 inches thick, which are analogous to the magnetite-rich lenses in the iron-rich sandstones. Both the magnetite-rich and biotite-rich beds are, in a sense, "placer" deposits which have been sorted from the bulk of the quartzose-feldspathic-dolomitic detritus by analogous physical processes. In fact, the basal Belly River member can be construed as a gradational sequence of rock types which can be arranged according to the inferred reaction of the constituent minerals to current velocities: the magnetite-rich sandstones of the iron-rich phase ⟿ clastic dolomite-rich sandstones of the iron-rich phase ⟿ quartz-feldspar-rich sandstones of the "barren" phase ⟿ biotite-rich sandstones of the "barren" phase ⟿ siltstones and shales of the Wapiabi "transition beds." At one end of the scale the heavy, equidimensional magnetite grains have been selectively sorted from the other detritus under the influence of the strongest current velocities, whereas at the other end of the scale the light, platy biotite grains and clay minerals have been segregated by relatively weak current velocities.

Table 5. Percentages of Mineral Constituents in Four Sandstone Samples from the Lower Part of the Belly River Formation, Southern Alberta Foothills

Sample	QUARTZ	QUARTZITE CHERT	FELDSPAR	BIOTITE	ROCK FRAGMENTS	MAGNETITE	ACCESSORY MINERALS	CARBONATES			AUTHIGENIC SILICATES[5]	MISCELLANEOUS	TOTAL
								Clastic	Authigenic	Total			
289[1]	35.5	7.5	20.0	0.5	24.0	—	—	*1.0*	*4.5*	5.5	6.0	1.0	**100.0**
337[2]	19.0	1.5	20.0	2.5	15.5	—	—	*11.0*	*6.0*	17.0	21.0	3.5	**100.0**
360[3]	26.5	17.5	8.5	2.5	25.5	—	—	*3.5*	*14.5*	18.0	—	1.5	**100.0**
387[4]	22.8	6.4	20.0	5.2	25.6	—	—	*6.0*	*2.2*	8.2	8.6	3.2	**100.0**
Mean	26.0	8.2	17.1	2.7	22.7	—	—	*5.4*	*6.8*	12.2	8.9	2.3	**100.0**

(1) Spot sample from sandstone overlying the iron-rich zone, Burmis.

(2) Spot sample from "barren" basal sandstone, Burmis.

(3) Spot sample from sandstone about 200 ft. above the iron-rich zone, Mill Creek.

(4) Average of five samples from a cored section through the "barren" basal sandstone, Burmis.

(5) Largely authigenic kaolinite.

The final step in the formation of the magnetite-bearing sandstones has been the crystallization of authigenic chlorite and calcite among the initially fluid-filled pores of the detrital constituents. The spatial relationships of the two minerals observed in thin sections shows that authigenic chlorite, the most abundant cementing mineral, was the first to form, completely filling the interstitial spaces of some samples, including those containing the most magnetite (Figs. 21, 22). However, in many of the magnetite-poor rocks both authigenic chlorite and calcite have jointly filled the available pore space in the manner shown in figure 23. In a few samples (Fig. 24) calcite is the only important cementing mineral, in which case carbonate-bearing solutions were apparently introduced into the wet sediment before authigenic chlorite could develop.

In the light of these observations the volumetric relationship between chlorite and magnetite (Fig. 9) can be explained in terms of a third factor: the distribution of authigenic calcite. The relatively constant proportion of chlorite in the magnetite-rich samples is explained by the fact that a relatively constant proportion of pore spaces has been completely filled by authigenic chlorite. In the other samples, both chlorite and calcite have competed to fill the same pore space, resulting in widely fluctuating proportions of the two minerals from sample to sample. Thus, while the total proportion of cement-filled spaces is similar in the magnetite-rich and magnetite-poor samples, the percentage of authigenic chlorite is extremely variable in the latter.

Similarly, the erratic distribution of feldspar in magnetite-poor samples (Fig. 8) is a result of the patchy distribution of authigenic calcite. The results of staining tests (table 4, p. 36) show that many detrital feldspar grains have been partly or completely replaced by calcite, even in rocks where the visible pore spaces have been largely cemented by chlorite. In such rocks, late-forming, carbonate-bearing solutions have apparently infiltrated along cleavage fractures in feldspar, completely replacing it in some samples. As a result, the distribution of feldspar is only partly correlative with the distribution of magnetite, in contrast to the well-defined inverse relationship between quartz or rock fragment percentages and magnetite percentages. A corollary to these observations is the fact that much of the calcite included with the clastic carbonate percentages of table 1 is really of authigenic origin. This type of calcite may be termed metasomatic as it has replaced previously existing mineral constituents, although it appears to have been emplaced in the rock at the same time as the pore-filling variety.

The gradational change in the bulk composition of the detrital components of the iron-rich sandstones to the underlying "barren" sandstones is correlative with a change in the composition of the associated authigenic minerals. The abundant chlorite cement of the magnetite-rich zone gradually decreases in amount over an interval of several feet, its place being taken by authigenic quartz and kaolinite. This change in the authigenic silicates

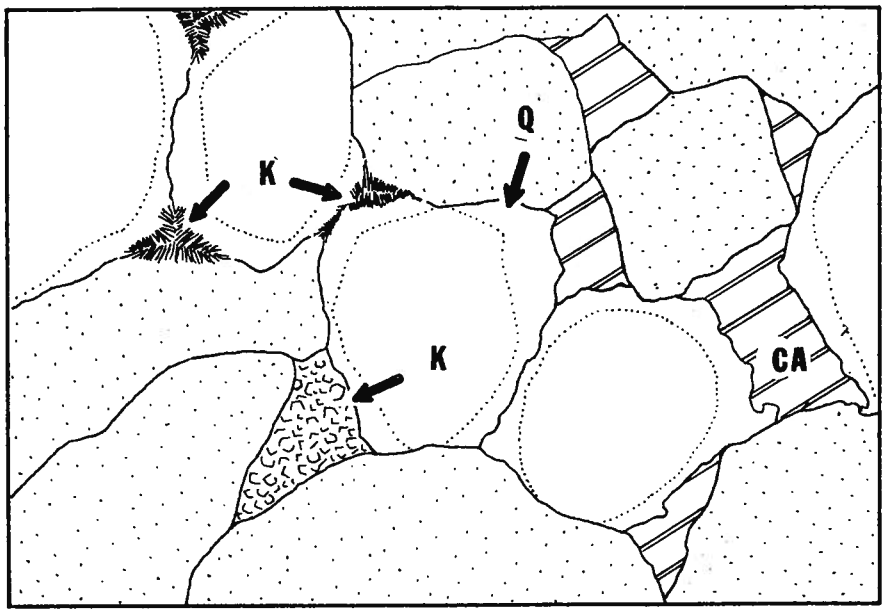

FIGURE 11. Typical authigenic fabric of "barren" basal Belly River sandstone. Quartz grains are clear; other grains (feldspars, rock fragments, micas) are stippled. Authigenic cements are quartz as overgrowths (Q) on detrital quartz grains; kaolinite (K) as platy or fibrous interstitial patches; and calcite (CA, barred areas) as large optically continuous patches filling clusters of adjacent pores

corresponds to a change in the color of the sandstones from dark green to pale grey. Samples 348-07 and 385-14 in table 1 are from this transitional zone and are partly cemented by both chlorite and kaolinite.

The typical authigenic fabric of the "barren" sandstones is shown in figure 11. Authigenic quartz is abundant as irregularly shaped, optically continuous overgrowths on detrital quartz grains, making it difficult to distinguish the original boundaries of the grains. The remaining intergranular space is filled by either kaolinite and/or calcite distributed in characteristic patchy fashion within the area of a single thin section.

In contrast to the stratigraphic changes in the composition of the authigenic silicate minerals, authigenic calcite is distributed similarly throughout the iron-rich and "barren" phases of the basal Belly River member. Figures 11 and 23 illustrate in principle the distribution of authigenic calcite within individual thin sections, where a cluster of adjacent pores is occupied by a single large calcite crystal. Many quartz overgrowths are in contact with authigenic calcite, but kaolinite-impregnated areas, although commonly adjacent to detrital dolomite grains, are seldom observed in contact with authigenic calcite. As a result, the intergranular spaces within each thin section can be divided into discrete quartz-kaolinite and quartz-calcite cemented areas of variable size.

In summary, the composition and distribution of authigenic silicates in the basal Belly River sandstone can be correlated with concomitant changes in the bulk composition of the detrital mineral constituents,

whereas those factors controlling the distribution of authigenic calcite are apparently independent of the gross mineral or chemical composition of the rocks. These same conclusions apply to rocks of the Lower Cretaceous Blairmore group of the Alberta Foothills (Mellon, 1959).

Grain Size

Sampling and Analytical Procedures

The grain size of the more important detrital constituents in each of the 60 modally analysed samples of Belly River iron-rich sandstones (table 1) has been determined, and the results are presented here in summary form. The measurements were obtained from thin sections because the rocks are hard and well cemented and cannot be disaggregated without crushing many of the component grains. Sieve analyses of such crushed samples largely reflect the nature of the disaggregation technique and not the original size of the discrete particles that make up the clastic framework of the rock.

Twenty grains from each of 60 thin sections were selected at random, and the maximum observed dimension of each grain was measured to the nearest 0.003 mm. with a micrometer eyepiece. Twelve hundred grains consisting of quartz, feldspar, clastic carbonate, and magnetite grains were measured; quartzite fragments, chert, and micas are too scarce to warrant special attention, and fine-grained rock fragments are commonly crushed or distorted by compaction of the surrounding rigid grains, making determination of their original maximum dimensions in thin sections difficult.

Results

The grain size measurements have been grouped into frequency histograms in figure 12 according to their mineral composition. The original measurements in millimeters have been transformed to phi units, a logarithmic scale to the base 2 devised by Krumbein (1934) to make markedly skewed millimeter grain size frequency distributions approximate log normal distributions. This logarithmic transformation also permits direct comparison of the standard deviations of grain size frequency distributions, which would otherwise vary with the frequency distribution means. The relationship between the millimeter and phi scales is shown at the bottom of figure 12.

The reason that the number of grain size measurements for each of the four mineral constituents is different is that the 20 grains measured in each of 60 samples were selected without preference to their mineral composition. Most of the magnetite grain size measurements are from the magnetite-rich samples, whereas most of the grain size measurements of the other three constituents are from magnetite-poor samples. As a result,

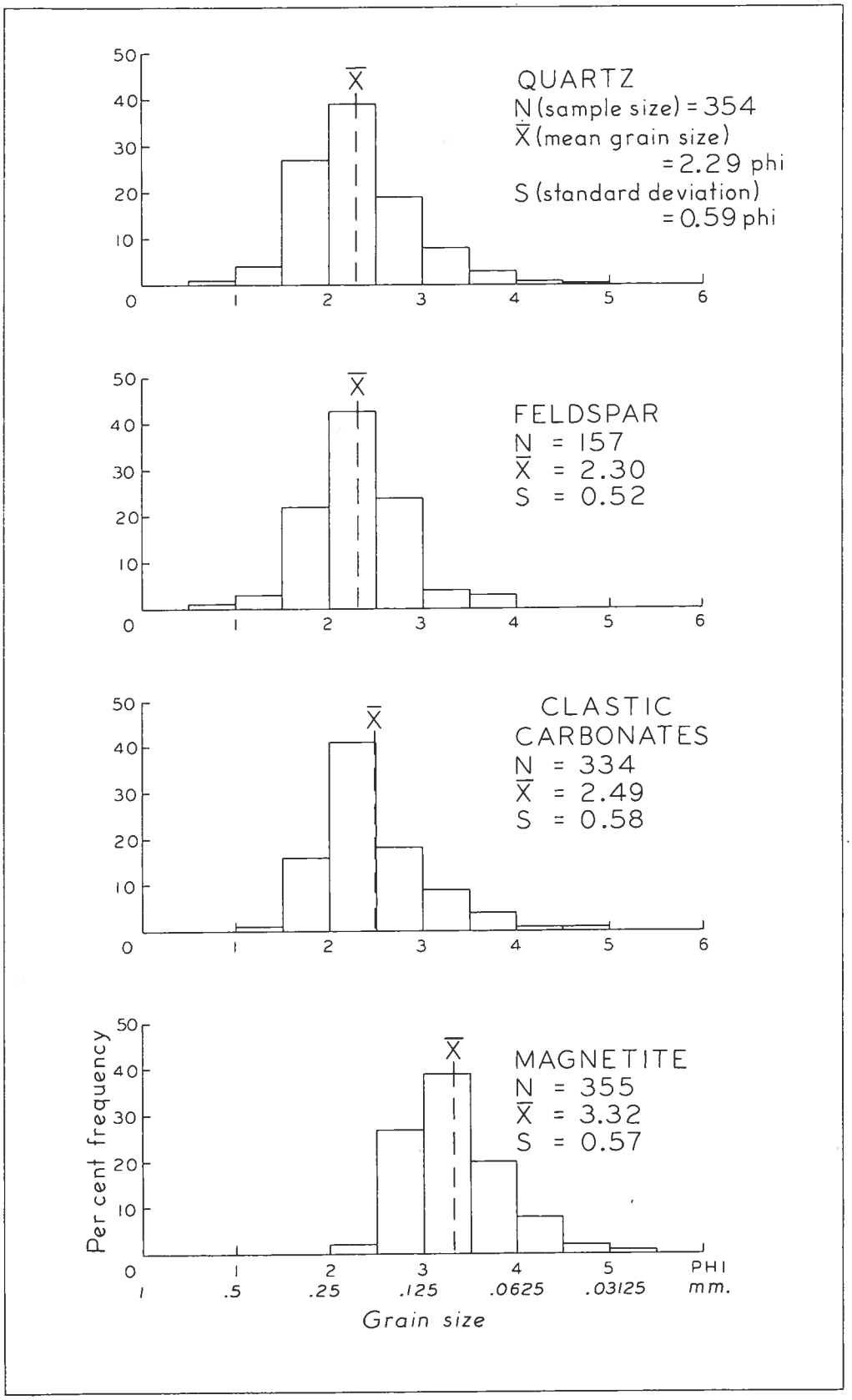

FIGURE 12. Histograms showing grain size frequency distributions of quartz, feldspar, clastic carbonates, and magnetite in 60 Belly River iron-rich sandstones

the grain frequencies of the histograms in figure 12 are roughly proportional to the relative abundance of the four minerals in the 60 samples of table 1. To facilitate visual comparison of the histograms, the frequencies have been converted to percentage frequencies.

The size frequency distributions of the four mineral constituents are all unimodal with a similar range of values about the modal frequency. More critical comparison of the histograms (although no formal statistical tests of significance have been applied to the differences discussed here) shows that the size distribution of quartz, clastic carbonates, and magnetite have the same standard deviation and are moderately skewed towards the finer grain sizes. However, there are no feldspar grains in the silt-size class intervals (less than 4 phi units), with the result that the distribution of feldspar is approximately symmetrical and has a smaller standard deviation than those of the other three constituents.

The summary statistics that accompany the frequency histograms indicate that quartz and feldspar have the same mean grain size, the modal frequency of both constituents lying in the upper part of the fine-grained sand interval (2.0 - 2.5 phi or 0.25 - 0.18 mm.). Detrital carbonate is slightly finer-grained than quartz or feldspar, and magnetite is conspicuously finer-grained than the other three constituents, the difference between quartz mean grain size and magnetite mean grain size corresponding to approximately one class interval (one phi unit) on the Wentworth grade scale. The modal frequency of magnetite is in the upper part of the very fine-grained sand class interval (3.0 - 3.5 phi or 0.125 - 0.088 mm.).

Discussion of Results

The skewness of the quartz, carbonate, and magnetite size frequency distributions is probably an inherent effect of the thin section measurement technique, which underestimates the true maximum dimension of the grains (Krumbein and Pettijohn, 1938, p. 129 *et seq.*). But if this is the case, it would be expected that the symmetrical feldspar size frequency distribution also would be skewed towards the finer grain sizes. It is possible that this lack of skewness has been caused by selective calcite replacement of the feldspar grains in certain size - class intervals, but because information is lacking as to which of the measured clastic carbonate grains are dolomite or calcite (largely replaced feldspar), this hypothesis remains speculative.

The differences among the mean grain sizes of the four constituents can be related to the specific gravities of the minerals, assuming shape factors to be constant. That is, under a constant set of hydraulic conditions quartz grains of a particular grain size will be deposited with magnetite grains of a smaller grain size because of the difference between the specific gravities of the two minerals. Rittenhouse (1943) has determined the "hydraulically equivalent" sizes of a number of heavy minerals with respect

to quartz grain size, expressing the results in terms of the Wentworth grade scale. According to Rittenhouse's calculations, the difference between the mean grain size of magnetite (or ilmenite) should be one Wentworth grade size (one phi unit) less than the mean grain size of quartz deposited under the same hydraulic conditions. This is the observed difference between the mean grain sizes of the two minerals in the Belly River magnetite-bearing sandstones. Similarly, the difference between the grain sizes of quartz and clastic carbonates can be explained in terms of hydraulic equivalence, clastic carbonates being the finer-grained and heavier of the two constituents. The difference would probably be even greater were it not for the fact that clastic carbonates are a mixture of clastic dolomite grains and calcite-replaced feldspar grains. The mean grain size of the latter is probably greater than that of clastic dolomite, the net effect of combining the size frequency distributions of the two constituents being to overestimate the average grain size of truly clastic carbonates.

Chemical Composition

Sampling and Analytical Procedures

The general chemical composition of the Belly River iron-rich sandstones has been determined by conventional analytical techniques from a small, randomly selected number of samples. In addition, the percentages of iron and titanium have been determined from X-ray fluorescent and bulk density analyses of a much larger number of samples, as the commercial value of the deposits depends primarily upon the amounts of these two elements. The discussion here is concerned with the results of conventional chemical and X-ray fluorescent analyses, and the relationships between the mineral and chemical composition data.

The percentages of the oxides of nine elements in 20 of the 60 modally analysed samples listed in table 1 were determined by conventional wet analytical techniques (table 6). The samples were chosen by randomly selecting one sample from each group of three modally analysed samples representing one of 14 sampled sections, and two samples from each group of six samples representing one of the three sampled Dungarvan Creek sections. The 20[1] samples, therefore, constitute a stratified subsample of the larger population of 60 samples and provide a relatively unbiased estimate of the average chemical composition of the magnetite-bearing sandstones as a whole.

To obtain more precise estimates of the iron and titanium content of the rocks than that afforded by the 20 conventional chemical analyses, the weight-percentages of the two elements in all 60 samples of table 1 were determined by X-ray fluorescent techniques. The samples were prepared by

[1] One of the 20 analyses was later rejected because of the gross discrepancy between the conventional and X-ray fluorescent determinations of the amounts of iron and titanium.

grinding crushed rock fragments to a fine powder, adding a constant amount of a binding agent (boric acid) to each sample, and pelletizing the resulting mixture in a hydraulic press. The intensities of the fluorescent X-radiation emitted by the two elements in each pelletized sample were measured twice and averaged to give a more precise intensity reading.

A conventional way of determining the percentages of a particular element in a group of "unknown" samples by X-ray fluorescent techniques is to prepare a set of artificial standards containing known proportions of the element, and to determine the intensities of the fluorescent X-radiation emitted by the standards. The resulting relationship between the proportions of the element and the corresponding fluorescent X-radiation intensities can then be used to determine unknown proportions of the element in natural samples from corresponding fluorescent X-radiation intensities.

Several sets of artificial standards were prepared by combining known weight-percentages of iron and titanium in the form of chemically pure salts or the metal itself with appropriate proportions of quartz, calcium carbonate, and boric acid. The intensities of the fluorescent X-radiation emitted by various proportions of iron and titanium were determined from both the artificial standards and the 19 chemcially analysed samples in table 6, and from each set of samples a relationship between the radiation intensities emitted by the two elements and the respective weight-percentages of their oxides was derived. The calibration curves are shown in figure 13.

The relationship between weight per cent TiO_2 and fluorescent X-radiation intensity for the 19 chemically analysed samples in table 6 is given by the linear regression equation:[1]

$Y = 0.1407 + 0.0858\,X$

$Y =$ per cent TiO_2 by weight

$X =$ the intensity of fluorescent TiK_α radiation in counts per second.

The regression between the two variables in a set of artificial standards containing known proportions of chemically pure TiO_2 is also linear, but becomes increasingly less accurate as the TiO_2 percentage increases. The standard curve overestimates the proportion of TiO_2 by approximately 2 per cent for an observed intensity of 100 counts per second, which is well beyond the maximum error accepted in most analytical work.

The relationship between weight per cent Fe_2O_3 and fluorescent X-radiation intensity for the 19 samples in table 6 is given by the multiple regression equation:

$Y = 2.0196 + 0.107X + 0.0032X^2$

$Y =$ per cent Fe_2O_3 by weight

$X =$ the intensity of fluorescent FeK_β radiation in counts per second.

[1] Calculated by the least squares principle illustrated in most standard statisical textbooks.

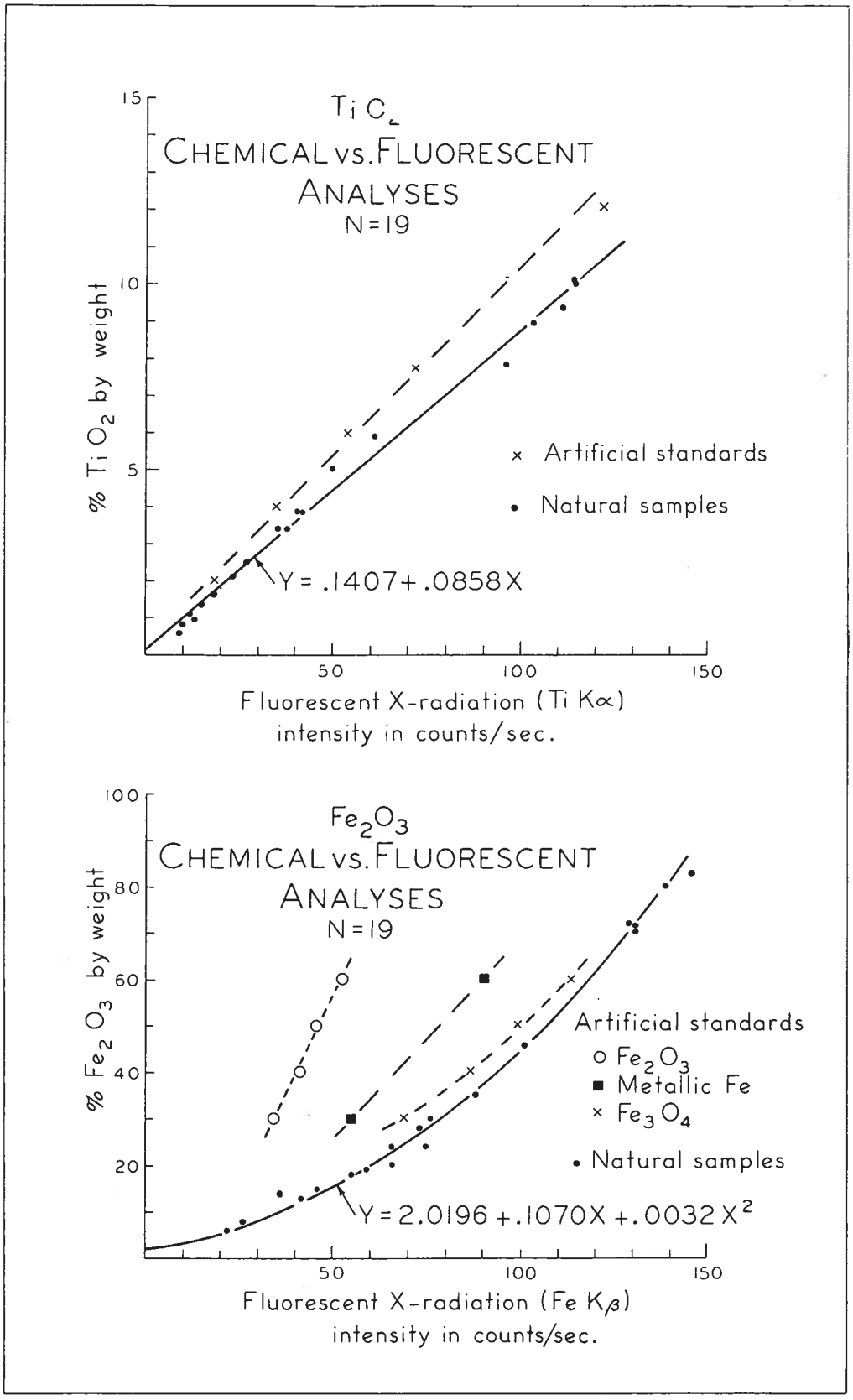

FIGURE 13. Scatter diagrams: chemical vs. X-ray fluorescent analyses of TiO_2; chemical vs. X-ray fluorescent analyses of Fe_2O_3, in artificial standards and 19 Belly River iron-rich sandstones

The regression is curvilinear with the intensity/weight-percentage ratio decreasing with increasing percentages of Fe_2O_3. Curves generated by artificial standards containing equivalent weight percentages of iron in three different chemical combinations all overestimate the proportion of Fe_2O_3 in the natural samples, the two curves based on chemically pure Fe_2O_3 and metallic Fe being grossly inaccurate. Thus, while the *precision* of the relationship between iron content and corresponding X-radiation intensities (measured in terms of the scatter of individual points about the regression curve) is lower than that of the curves generated by artificial standards, the *accuracy* of the latter (in terms of deviations from the true percentage of iron in the natural samples) is much too low to permit their use.

The factors responsible for the large variation among the intensities of the X-radiation emitted by the same weight-percentages of an element occurring in different chemical or mineralogical states are too complex to describe here. An excellent discussion of these factors (absorption effects) and of some sample preparation techniques designed to improve the accuracy of the analytical results is given by Claisse (1960). In the examples described here, the use of chemical analyses of natural samples has circumvented the various absorption effects inherent in the technique, and the relative lack of precision of the regression curves of the natural samples can be just as well attributed to variation caused by splitting the samples. That is, the sample fractions which were analysed by fluorescent X-ray techniques (table 1) contain slightly different proportions of iron and titanium than the corresponding sample fractions which were analysed by conventional chemical techniques (table 6). However, this lack of precision in the regression curves of the natural samples is extremely small compared to the ranges in the percentages of the two oxides in the samples: the correlation coefficient (r) for the TiO_2 regression data is 0.99, and the multiple correlation coefficient (R) for the Fe_2O_3 regression data is 0.98, indicating that nearly all of the variation in the intensities of fluorescent X-radiation can be explained by corresponding variation in the weight percentages of the two oxides.

Results

The chemical composition of 19 Belly River iron-rich sandstones, as determined by conventional analytical techniques, is given in table 6. The chemical composition of the samples corresponds approximately to that which would be expected from their mineral composition; ferric oxide and silica are the most abundant chemical constituents, but the titania content is unusually high. The sulfur content of the samples was not determined, but previous chemical analyses of samples from the Burmis and Dungarvan Creek areas (Allan, 1931) indicate that the element is present only in trace amounts. The manganese, zirconium, and vanadium content of three magnetite-rich samples from Burmis and Dungarvan Creek has been determined by the Mineral Processing Division, Department of Mines and

Table 6. Chemical Analyses of Nineteen Belly River Iron-rich Sandstones

Sample	SiO_2	TiO_2	Al_2O_3	Fe_2O_3	MgO	CaO	Na_2O	K_2O	L.O.I.(1)	P_2O_5	Total
290-04	39.42	3.77	6.53	35.35	3.47	3.88	0.10	0.13	6.95	0.21	99.81
295-10	44.32	2.40	11.62	17.88	6.29	4.74	1.48	0.31	9.89	0.20	99.13
297-07	7.60	9.33	3.88	71.71	1.23	1.35	0.03	0.17	3.47	0.37	99.14
301-18	51.06	3.41	8.29	23.82	4.66	1.60	1.49	0.26	4.77	0.24	99.60
308-01	11.03	8.94	2.16	69.82	2.66	1.94	—	—	2.24	0.33	99.24
309-03	50.31	0.83	8.38	7.67	5.65	9.61	1.74	0.83	13.58	0.12	99.12
310-04	38.72	1.64	7.77	13.51	14.32	5.29	1.32	0.63	16.07	0.23	99.50
310-24	44.84	1.10	8.23	19.03	7.90	4.72	0.98	0.25	11.30	0.10	98.45
338-17	35.28	5.04	8.05	29.69	6.78	4.47	0.61	0.13	9.20	0.34	99.59
342-05	9.19	9.98	3.86	71.91	1.19	1.13	0.07	0.12	0.65	0.51	98.61
348-02	42.63	0.62	6.86	6.04	19.39	3.58	1.42	0.33	19.08	0.08	100.03
364-06	22.46	3.85	8.94	23.66	13.19	8.55	0.35	0.21	18.54	0.25	100.00
368-01	38.46	2.15	11.73	14.53	11.57	4.83	1.56	0.51	12.66	0.15	98.15
368-10	4.88	10.13	1.39	79.58	1.01	0.95	0.12	0.08	—	0.48	98.62
373-05	3.83	7.80	2.37	83.01	1.41	0.92	0.09	0.10	—	0.45	99.98
374-02	60.33	1.32	9.90	12.87	3.45	2.37	2.46	0.36	5.58	0.14	98.78
378-12	54.32	0.95	8.46	20.09	5.06	4.19	0.08	0.17	8.46	0.18	101.96
385-07	15.12	5.91	4.53	45.55	11.55	3.50	0.05	—	11.81	0.39	98.41
386-03	32.49	3.44	6.00	27.92	11.08	4.35	0.13	0.09	13.22	0.23	98.95
Mean	31.91	4.35	6.79	35.45	6.94	3.79	0.74	0.25	8.81	0.26	99.31

Locations of samples are given in table 8. Modal analyses are given in table 1. Analyses by H. Wagenbauer, Research Council of Alberta.

(1) Loss on ignition (largely H_2O, CO_2).

Technical Surveys, Ottawa (Report MD-3187, 1957). The Mn content of the three samples is 0.28, 0.32, and 0.21 per cent, respectively; the ZrO_2 content is 0.10, 0.24, and 0.12 per cent, respectively; the V_2O_5 content is 0.29, 0.38, and 0.28 per cent, respectively.

X-ray fluorescent determinations of the percentages of Fe_2O_3 and TiO_2 in the 60 modally analysed samples are given in table 1, and the sample frequency distributions of the two oxides are shown in figure 14. The mean Fe_2O_3 content of the samples is 29.34 per cent, and the mean TiO_2 content is 3.56 per cent, which are somewhat less than the mean weight percentages of the two oxides in the 19 chemically analysed samples of table 6. As the samples in table 6 constitute a randomly selected subsample of the 60 modally analysed samples, some variation between the average proportions of chemical constituents of the two groups of samples is to be expected, the estimated Fe_2O_3 and TiO_2 content of the larger group of

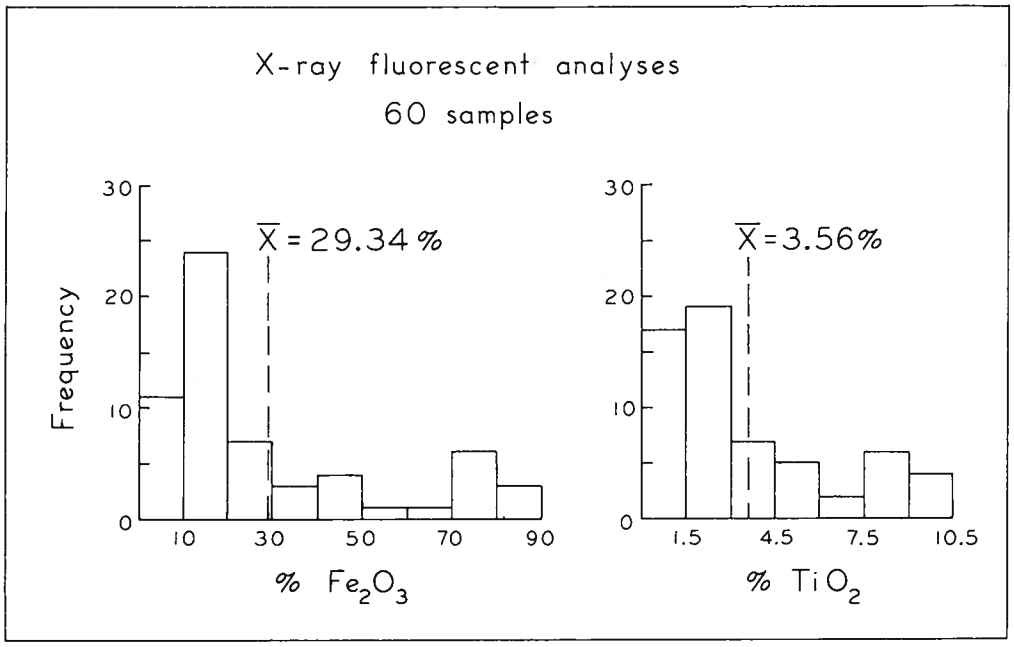

FIGURE 14. Histograms showing the frequency distributions of Fe_2O_3 and TiO_2 percentages in 60 Belly River iron-rich sandstones

samples being the more precise. The Fe_2O_3/TiO_2 ratio of the samples in table 1 is 8.24, and that of the samples in table 6 is 8.14.

The relationship between the percentages of the two oxides in the 60 samples of table 1 is shown in figure 15. There is a well defined linear relationship between the two variables, the TiO_2 content of the samples increasing at a constant rate with respect to the Fe_2O_3 content. The relationship is defined by the regression equation:

$Y = 8.82\,X - 2.07$

Y = per cent Fe_2O_3 by weight

X = per cent TiO_2 by weight.

Conversely, if the percentage of TiO_2 is to be predicted from the corresponding Fe_2O_3 percentage, the regression equation can be written:

$Y = .23 + .11\,X$

Y = per cent TiO_2 by weight

X = per cent Fe_2O_3 by weight.

The correlation coefficient (r) of the two variables is 0.96, indicating that 92 per cent of the variation in one variable can be predicted from concomitant variation in the other variable.

The relationship between weight per cent Fe_2O_3 and volume per cent magnetite (black opaque grains) in the 60 samples of table 1 is also shown in figure 15. The curve generated by plots of the two variables is linear and is described by the regression equation:

$Y = 12.17 + 1.11\,X$

Y = per cent Fe_2O_3 by weight

X = per cent magnetite by volume.

The correlation coefficient (r) of the two variables is 0.96, although some of the individual sample plots deviate by an appreciable amount from the regression curve. This lack of precision is due to the sample-splitting effect previously discussed: the point-count estimates of magnetite percentages were determined from thin sections cut from larger samples, whereas the Fe_2O_3 percentages were determined by X-ray fluorescence from a different portion of the same sample. For example, a thin section may have included a magnetite-rich band several millimeters thick which was missing from the sample fraction used for X-ray fluorescent analysis. Variation in analytical results due to differences among splits of the same sample is particularly difficult to control in analyzing small samples of strongly laminated rocks such as the Belly River magnetite-bearing sandstones.

Discussion of Results

The distribution of the chemical constituents of the iron-rich sandstones among the major minerals of the rocks is shown below. The minerals are arranged from left to right according to their importance as contributors to the total amount of each of the nine oxides and the loss-on-ignition:

SiO_2: quartz, chlorite, feldspars, micas;
TiO_2: titaniferous magnetite, ilmenite, anatase, leucoxene;
Al_2O_3: chlorite, feldspars, micas;
Fe_2O_3: magnetite, chlorite, ilmenite;
MgO: dolomite, chlorite;
CaO: calcite, dolomite, plagioclase;
Na_2O: plagioclase;
K_2O: orthoclase, micas;
L.O.I. (CO_2, H_2O): carbonates, chlorite, micas;
P_2O_5: origin unknown.

The most important economic property of the magnetite-bearing sandstones is the percentage of iron which can be profitably extracted from the raw ore. Chemical analyses alone give the percentage of total iron in the rocks, but do not allocate it among the three quantitatively important minerals. However, if it is assumed that only the iron in magnetite (and possibly ilmenite) can be recovered by conventional smelting techniques, then the grade of the rocks depends upon the amount of iron in magnetite, and not the total amount of iron.

The proportion of iron in the rocks occurring as magnetite is indicated by the regression equation on p. 61, which describes the relationship between the percentages of magnetite (i.e. dark opaque grains, which probably include from 10 to 20 per cent ilmenite) and Fe_2O_3. The equation

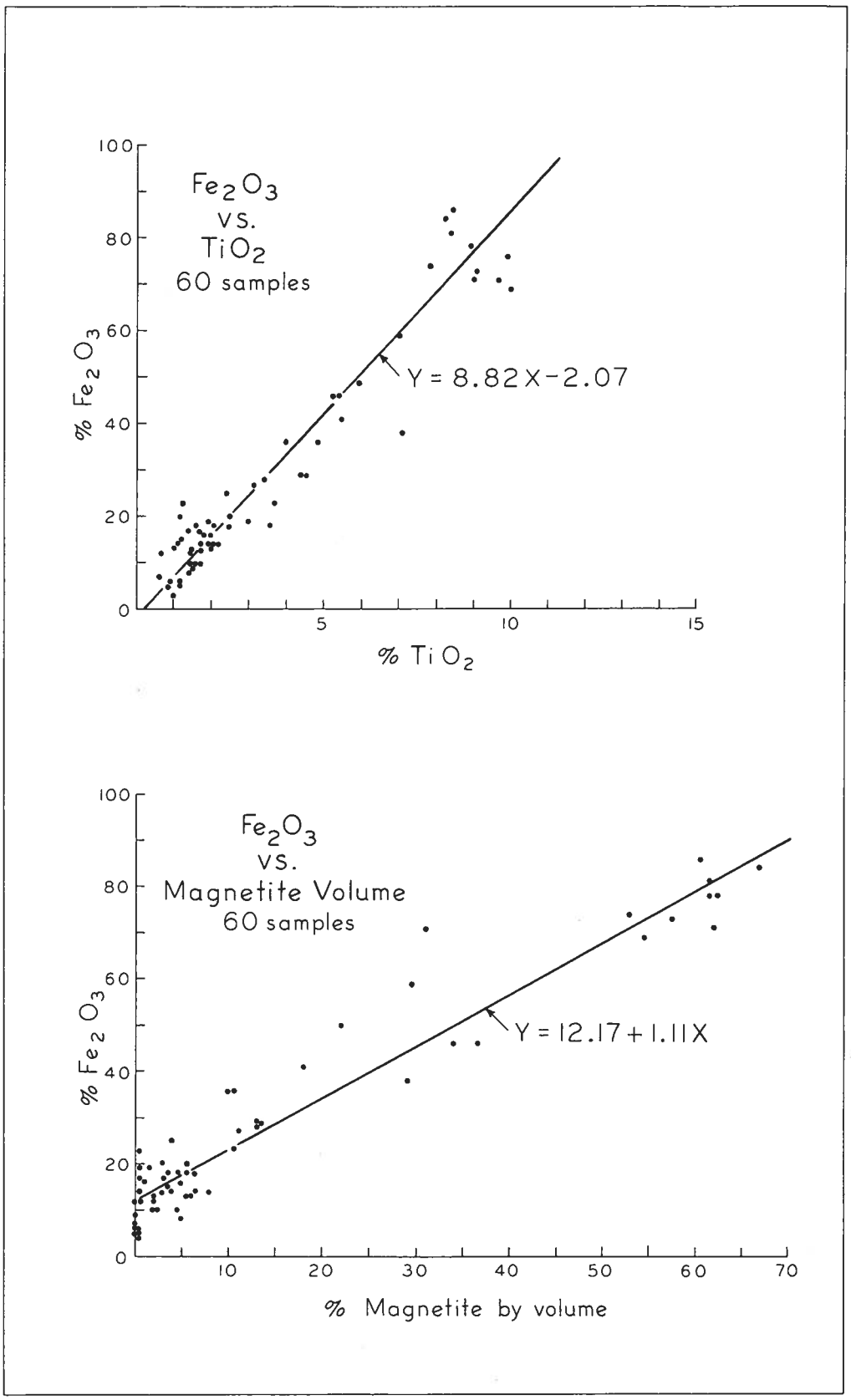

FIGURE 15. Scatter diagrams: Fe_2O_3 vs. TiO_2 percentages; Fe_2O_3 vs. magnetite percentages, in 60 Belly River iron-rich sandstones

shows that when the magnetite content (X) of the rocks is zero (as it nearly is in many of the dark green, chloritic sandstones interbedded with the magnetite-rich sandstones), the average Fe_2O_3 content is still 12.17 per cent by weight. This gives some idea of the amount of iron present in the rocks in minerals other than magnetite and ilmenite—largely chlorite (or limonite in weathered samples). If this amount is constant for rocks containing a given volume of magnetite, the percentage of the total Fe_2O_3 in the 60 samples of table 1 (29.34 per cent) present in chlorite or limonite is $12.17/29.34 \times 100 = 41$ per cent by weight. If the deposits were selectively mined to obtain a raw ore averaging 25 per cent magnetite (including ilmenite) by volume, the total Fe_2O_3 content of the rocks, estimated from the regression equation above, would be $12.17 + (1.11)(25.00) = 39.92$ per cent. Of this total, $12.17/39.2 \times 100 = 30$ per cent of the Fe_2O_3 is present in chlorite or limonite, indicating that the estimated iron content of potential reserves determined from chemical analyses would have to be scaled down by a factor of 25 to 35 per cent.

The other major compositional factor concerning the economic potential of the iron-rich sandstones is their high titanium content. Titanium is present in ilmenite, titaniferous magnetite, anatase, and leucoxene, although the quantitative mineralogical distribution of the element is uncertain: the accuracy of the point-count estimates of the various titanium-bearing minerals (tables 1, 2, 3) is probably low, and the composition of titaniferous magnetite and leucoxene is uncertain.

The high correlation between the iron and titanium content of the rocks (Fig. 15) does not necessarily infer that the two elements are components of the same minerals, such as titaniferous magnetite or ilmenite. Both anatase and ilmenite have high specific gravities and are concentrated in the magnetite-rich zones of the rocks along with zircon and other heavy minerals. However, it is interesting to note that the regression curve of Fe_2O_3 on TiO_2 almost passes through the origin of the graph, indicating that the iron-titanium ratio is nearly constant throughout the range of values involved. As discussed above, samples containing little or no magnetite or ilmenite still contain about 12 per cent Fe_2O_3 by weight. These samples also contain an average 1.57 per cent TiO_2 by weight, as determined from the regression equation on p. 60. Much of the iron content of these magnetite-poor rocks has been ascribed to the presence of authigenic chlorite, and it is possible that their titanium content is explained by the presence of interstitial films and patches of leucoxene which may also be of authigenic origin.

The Cretaceous sedimentary magnetite deposits of Montana are also rich in titanium. The average Fe/TiO_2 ratio of a composite sample of ore from the Choteau deposit, which is found at about the same stratigraphic horizon as the Belly River deposits of southwestern Alberta, is 6.07 (Wimmler, 1946). The Fe/TiO_2 ratio of four channel samples of magnetite-rich sandstones from the base of the St. Mary River formation on the Blackfeet

Indian Reservation is 4.12 (Stebinger, 1912). The ratio of the average percentages of Fe and TiO_2 in the 60 samples of table 1 (20.52 and 3.56 per cent, respectively) is 5.76, which compares favorably with that of the Choteau rocks, but is somewhat greater than that of the younger Blackfeet Reservation rocks.

ECONOMIC GEOLOGY

Grade of the Deposits

Analytical Procedure

The grade of the Belly River magnetite deposits has been determined from analysis of 469 samples from 42 sampled sections of the iron-rich zone, collected in the manner previously described (p. 17 - 19). To determine the mineral and chemical composition of such a large number of samples by conventional analytical techniques would be both expensive and time-consuming, and, considering other factors concerned with the commercial value of the deposits, hardly justified. For this reason the average magnetite, iron, and titanium contents of the deposits have been determined from bulk density analyses, using regression equations derived from the relationships among the data in table 1. The rocks are well suited to such an analytical procedure: they are composed of highly variable proportions of minerals ranging in specific gravity from about 2.6 (feldspars) to 5.1 (magnetite), and exhibit a correspondingly large range of bulk densities which can be correlated with concomitant variation in their petrographic and chemical properties.

The bulk density of each of the 469 samples was determined by the following procedure. A thin slab weighing from 15 to 60 grams was cut from each sample, crushed into fragments ranging from one-quarter to one-half inch in diameter, and weighed to the nearest 0.01 grams. The volume of the crushed sample was determined by measuring the volume of water displaced by the fragments in a glass tube graduated in milliliters, and the bulk density of the sample calculated by dividing the weight by the volume. Most of the samples exhibited little evidence of porosity, so that the bulk densities of the samples provide an accurate estimate of the average specific gravity of their constituent minerals.

The precision of the technique (or analytical error) has been determined from replicate bulk density analyses of the 60 modally analysed samples in table 1. Each of the 60 bulk density analyses shown there is an average of two duplicate analyses performed on the same crushed sample according to the procedure outlined above. The average difference of 60 pairs of duplicate analyses is 0.031 gm./cc., which in terms of the magnetite and Fe_2O_3 content of the samples is 1.37 per cent and 1.58 per cent, respectively, as calculated from the regression coefficients of the equations on p. 66. Relative to other sources of variation among the regression data, the amount of variation caused by the analytical error of the bulk density determinations is very small.

The average bulk density of each of the 60 modally and chemically analysed samples is given in table 1. The average bulk density of the 60 samples is 3.10 gm./cc., with individual values ranging between 2.63 and 4.33 gm./cc.

The relationships between the magnetite and Fe_2O_3 percentages and the bulk densities of the 60 samples in table 1 are illustrated by the scatter diagrams in figure 16. The regression of per cent magnetite on bulk density is linear and is described by the equation:

$Y = 44.31\,X - 121.94$

Y = per cent magnetite by volume

X = bulk density in gm./cc.

The correlation coefficient (r) of the two variables is 0.97.

The regression of per cent Fe_2O_3 on bulk density is also linear and is described by the equation:

$Y = 50.95\,X - 128.62$

Y = per cent Fe_2O_3 by weight

X = bulk density in gm./cc.

The correlation coefficient (r) of the two variables is 0.97.

As would be expected, some of the points in each of the scatter diagrams show an appreciable deviation from the regression curve. As the rocks are not visibly porous, most of the variation in the samples not explained by the regression equations can be attributed to the "sample splitting" effect, previously discussed (p. 58). However, the deviations of individual sample estimates of the magnetite or Fe_2O_3 percentages from those predicted by the regression equations is of little practical importance, as the equations have been used to calculate the *average* magnetite and Fe_2O_3 percentages in *groups* of samples from their mean bulk densities (table 8). In such calculations, the deviations between the observed (point-counted or chemically analysed) and calculated (from bulk densities) magnetite or Fe_2O_3 percentages tend to average out.

Some idea of the precision of the average magnetite and Fe_2O_3 percentages of groups of samples calculated from the mean bulk density of each group can be obtained by comparing the observed mean magnetite and Fe_2O_3 percentages of groups of samples randomly selected from table 1 and the corresponding percentages of the two constituents calculated from the mean bulk density of each group, using the regression equations above. This has been done for nine groups of 10 samples each, selected with the aid of random number tables from the 60 samples in table 1. The results are given in table 7. As the observed magnetite and Fe_2O_3 percentages were used in deriving the regression equations from which the predicted percentages were calculated, the observed differences between the two sets of data in table 7 are somewhat less than would be expected if they had been determined from groups of "independent" samples, i.e. analyses of samples other than those in table 1.

Results

Data describing the locations, thicknesses, and average composition of 40 sampled outcrop and 2 sampled borehole sections of the iron-rich zone are given in table 8 (in pocket). The sampled sections are arranged

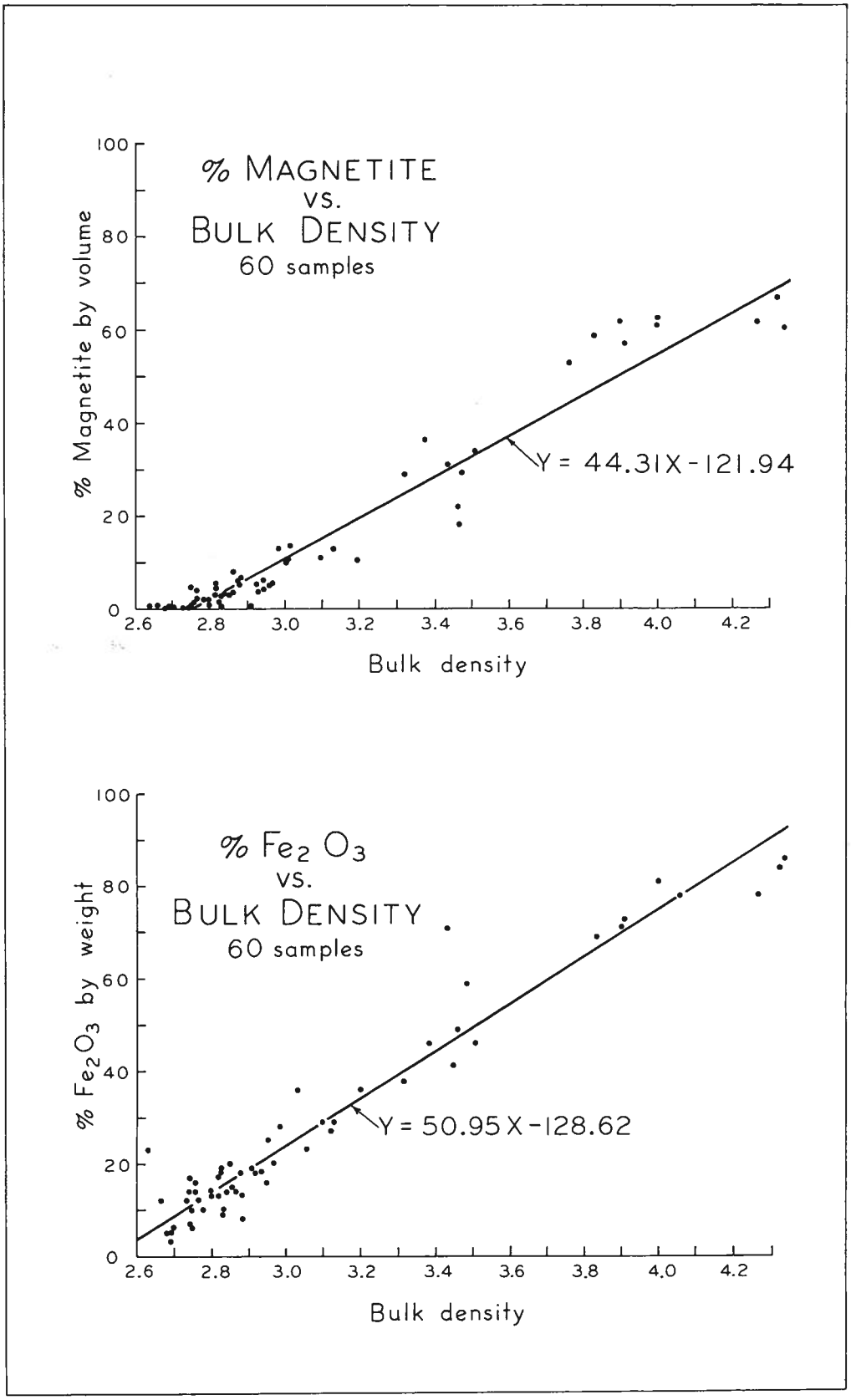

FIGURE 16. Scatter diagrams: magnetite percentage vs. bulk density; Fe_2O_3 percentage vs. bulk density, in 60 Belly River iron-rich sandstones

Table 7. Comparison of Observed Magnetite and Fe_2O_3 Percentages of Randomly Selected Groups of Samples with Corresponding Percentages Calculated from Bulk Densities

Group	% Magnetite		% Fe_2O_3		Average bulk density
	observed(1)	calculated(2)	observed(1)	calculated(2)	
1	4.55	*6.11*	17.83	*18.63*	2.89
2	4.35	*4.79*	18.38	*17.10*	2.86
3	5.70	*6.56*	18.67	*19.14*	2.90
4	11.75	*12.76*	26.27	*26.27*	3.04
5	11.55	*10.10*	24.45	*23.21*	2.98
6	10.20	*9.22*	20.08	*22.19*	2.96
7	13.90	*13.21*	24.13	*26.78*	3.05
8	9.40	*10.99*	22.87	*24.23*	3.00
9	21.05	*20.29*	36.38	*34.93*	3.21

(1) Average values of groups of 10 samples randomly selected from table 1, determined by point-count and X-ray fluorescence techniques.
(2) Calculated from average bulk density using the regression equations on p. 66.

according to their geographic proximity and their structural setting. For example, sections 275, 277, and 278 are located within the same contiguous iron-rich zone which crops out sporadically along the flank of a small anticline in Secs. 25 and 26, Tp. 9, R. 3, W. 5th Mer.

The type of exposure, the stratigraphic interval sampled, the thickness of each sampled section, and the number of samples collected from each section are shown in table 8. The samples were collected at systematic intervals from the exposed top or base of each section, except at three localities (277, 349, 308) where they were collected from talus.

The mean percentage of magnetite by volume and the mean percentage of Fe_2O_3 by weight of each sampled section have been calculated from the mean bulk density of each set of samples, using the regression equations on p. 66. The standard deviation of the mean magnetite content of each section has been calculated from the bulk density determinations of the individual samples from each section, converted to magnetite percentages using the regression equation on p. 66. It should be noted that, in general, the standard deviation increases with the mean magnetite percentages of the sampled sections, thus reflecting the strongly laminated or banded structure of the more magnetite-rich deposits.

The mean percentages of TiO_2 by weight have been calculated from the corresponding mean Fe_2O_3 percentages of table 8, using the regression equation on p. 60. The mean Fe percentages have also been calculated from

the corresponding Fe_2O_3 percentages, so that, ultimately, all of the composition data in table 8 have been determined from bulk density analyses.

The magnetite content of the 469 samples from the 42 sampled sections is illustrated by the frequency histograms of figure 17. The samples have been grouped according to their distribution among the Todd Creek, Burmis, Dungarvan Creek, and southern areas (table 8). The magnetite percentages have been calculated from bulk density determinations, using the regression equation on p. 66, and the percentages of samples containing more than 25 per cent magnetite by volume are shown for each histogram.

If it is assumed that "potential iron ore" must contain at least 25 per cent magnetite by volume (approximately 40 per cent Fe_2O_3 or 28 per cent Fe by weight), then it is obvious from figure 17 that the great majority of samples do not meet this requirement. The samples from Burmis and Dungarvan Creek are more magnetite-rich than the others, but even in these areas it is evident that much of the volume of rock tentatively defined for sampling purposes as "potential iron ore" is of very low grade.

Table 9. Average Percentages of Iron in Belly River Iron-rich Sandstones from Four Localities in Southwestern Alberta

Locality	% Fe			Total footage of sampled sections
	Average of chemically analysed samples Table 1	Average of sampled sections Table 8	Weighted average of sampled sections Table 8	
Todd Creek	16.7	14.5	13.4(1)	66.5(1)
Burmis	18.9	19.3	19.9(2)	223.0(2)
Dungarvan Creek	25.3	25.0	24.5	68.5
Southern localities	15.6	13.4	12.0	42.5

(1) Excluding section 277.
(2) Excluding section 349.

These observations are confirmed by the average Fe percentages of the individual sampled sections in table 8. The data are summarized in table 9 for each of the four groups of samples shown in figure 17. The mean Fe percentages of the first two columns have been determined from the 60 chemically analysed samples of table 1 and from the mean Fe percentages of the sampled sections in table 8. Differences between the two sets of percentages indicate the random sampling error involved in selecting two sets of samples from the same population. The third set of percentages has been determined from the mean Fe percentages of the sampled sections weighted according to the thicknesses of the sections and estimates the average Fe content per foot of sampled section for each of the four groups of samples.

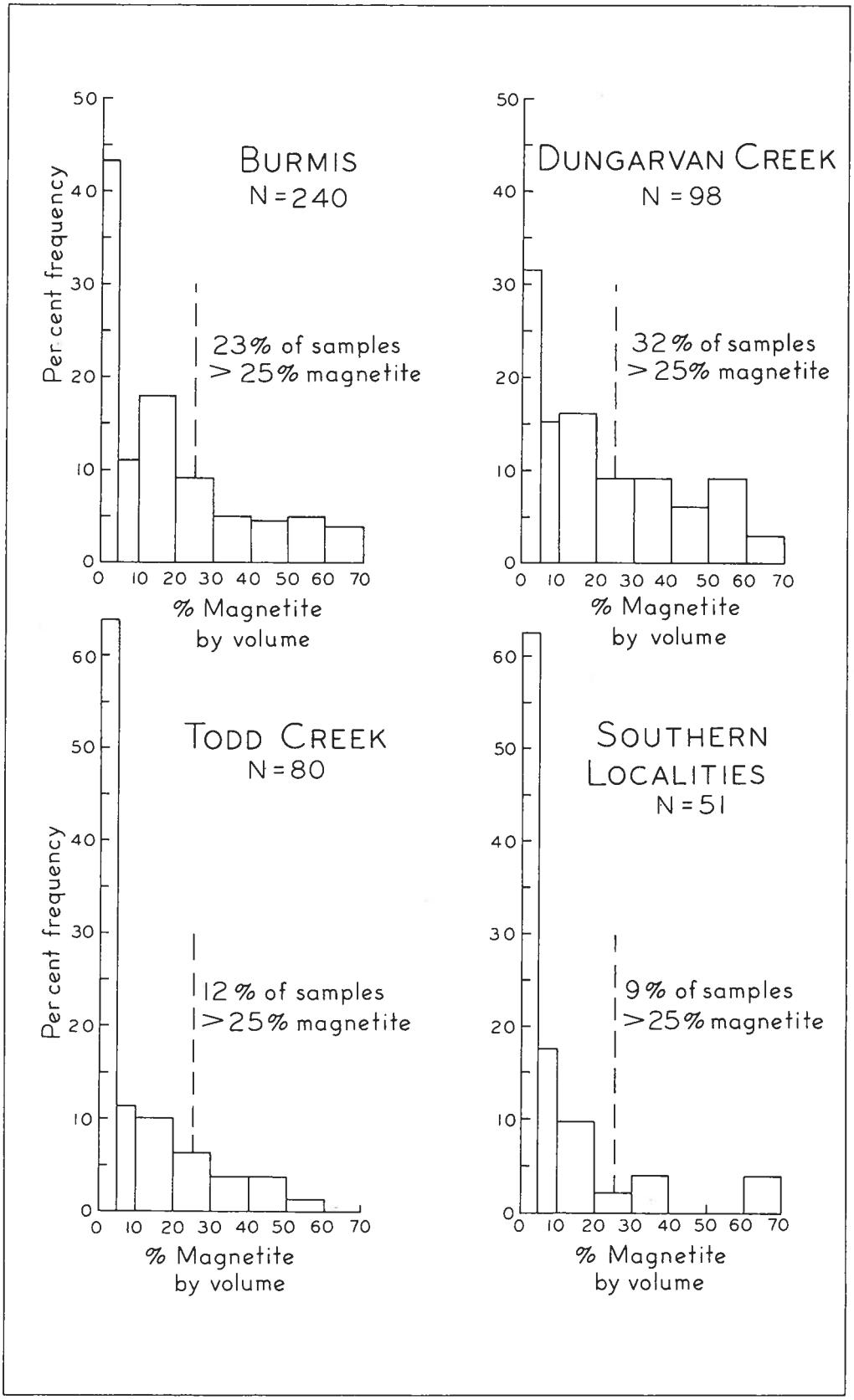

FIGURE 17. Histograms showing the frequency distribution of magnetite percentages in 469 Belly River iron-rich sandstones

Beneficiation of the Magnetite-bearing Sandstones

Some of the problems that would be met in extracting an acceptable furnace product from the Belly River magnetite-bearing sandstones are suggested by the petrographic and chemical properties of the rocks. Those properties most directly concerned are:

(1) the fine grain size,
(2) the high TiO_2 content, and
(3) the high chlorite content,

which, in combination, indicate that the rocks are unsuitable for mineral dressing and smelting by conventional techniques.

The rocks are very fine-grained, the average grain size of magnetite as observed in thin sections being about 0.100 mm. (Fig. 12), which is somewhat less than the true mean grain size. The true grain size can be estimated approximately by multiplying the mean thin-section grain-size of magnetite by 1.32 (Krumbein and Pettijohn, 1938, p. 130), giving a corrected mean grain size of 0.132 mm. This means that the rocks would have to be crushed to approximately 100 to 150 mesh in order to separate most of the magnetite from the gangue minerals (assuming that the rocks would not break across the grains) for concentration by some beneficiation process. In view of the toughness and well cemented nature of the magnetite-bearing sandstones, crushing the rocks to such a fine size would probably be a costly procedure.

The high titanium content of the Belly River iron-rich sandstones is in line with the titanium content found in many low grade igneous and sedimentary magnetite deposits (Roe, 1957, p. 62 *et seq.*). The average TiO_2 content of the 60 samples in table 1 is 3.56 per cent, giving an Fe/TiO_2 ratio of 5.76 (p. 64), which remains nearly constant with increasing iron content of the rocks. Because of the difficulty in smelting titanium-rich ores in conventional blast furnaces, and because the demand for titanium-rich pig iron is low, it is of interest to know whether the TiO_2 content of the raw ore can be reduced by some mineral dressing process prior to smelting.

Various magnetic and heavy media concentration tests of Belly River magnetite-bearing sandstones have been carried out by the Mineral Processing Division, Department of Mines and Technical Surveys, Ottawa (Reports MD-995, 1941; MD-507-OD, 1951; MD-3034, 1954; MD 913-OD, 1957; MD-3187, 1957). The results of two such tests run on a sample of magnetite-rich sandstone from the Burmis area are given in table 10. Both tests involve the separation of sample fractions ground to minus 100 mesh into magnetic and nonmagnetic fractions.

The initial feed in the first test contained 7.19 per cent TiO_2 and was separated into two components under the influence of a permanent magnetic field. The nonmagnetic tailings contain 63 per cent of the total TiO_2 content of the initial sample. The initial feed in the second test was separated into three components under the influence of a variable magnetic

Table 10. Results of Magnetic Concentration Tests of a Sample of Belly River Magnetite-rich Sandstone Ground to Minus 100 Mesh

(Data from tests run by Mineral Processing Division, Department of Mines and Technical Surveys, Report MD-3034.)

Test 1

Sample	% Total sample	% Fe	% TiO_2	Fe/TiO_2
Concentrate	59.20	62.14	4.45	13.9
Tailings	40.80	25.98	11.17	2.3
Total feed	100.00	47.39	7.19	6.1

Test 2

Sample	% Total sample	% Fe	% TiO_2	Fe/TiO_2
Concentrate	51.31	62.40	4.08	15.3
Middlings	12.34	57.27	11.30	5.1
Tailings	36.35	28.23	10.40	2.7
Total feed	100.00	49.35	7.27	6.8

field. The nonmagnetic tailings contain 52 per cent of the total TiO_2 content of the initial sample. If the samples were crushed largely into their constituent mineral grains, it appears that from 50 to 65 per cent of the titanium is present in weakly magnetic or nonmagnetic minerals, and the remaining 35 to 50 per cent is either physically or chemically associated with the magnetic fraction of the rock. Needless to say, the resulting Fe/TiO_2 ratios of the magnetic concentrates is still too high for an acceptable blast furnace feed.[1]

Magnetic concentration tests of other samples from Burmis and Dungarvan Creek crushed to various size fractions give essentially the same results as those outlined above. Heavy media (sink-float) techniques are considerably less effective in concentrating the iron and reducing the titanium content of the rocks than magnetic techniques. Similar magnetic and heavy media concentration tests of samples from the titaniferous magnetite deposits near Choteau, Montana (Wimmler, 1946) failed to reduce the titanium content of the resulting iron-rich concentrate below 5 per cent.

[1] Conceivably, the smelting difficulties posed by the high titanium content of the Crowsnest magnetite ores could be overcome by blending the titanium-rich ore or concentrate with a titanium-free ore (Lander, 1959, p. 58), or by smelting the titanium-rich concentrate in an electric furnace (Armstrong, 1959). Whether either of these techniques would be economically feasible is not known, but the low grade and reserves of the Crowsnest deposits indicate that the question is largely academic.

Certainly, the results obtained from the mineral dressing tests of the Alberta deposits are predictable from the grain size and mineral composition of the rocks. That portion of the total titanium content of the rocks present in slightly magnetic or nonmagnetic minerals (anatase, leucoxene, discrete ilmenite grains) will be concentrated largely in the tailings resulting from magnetic concentration of a finely ground feed, whereas the titanium in titaniferous magnetite or in ilmenite intergrown with magnetite will end up in the iron-rich concentrate.

Another compositional factor that must be considered in assessing the the commercial prospects of the iron-rich sandstones is the amount of "nonmagnetic" iron in the rocks. The mineralogical distribution of the iron has been discussed in a previous section (p. 61 - 63), where the amount of iron occurring in minerals other than magnetite or ilmenite was determined to be about 12 per cent Fe_2O_3 or 8.5 per cent Fe, present largely in authigenic chlorite. If this amount is constant for rocks containing variable proportions of magnetite, then about 19 per cent of the total iron in magnetite-rich ore assaying 40 per cent Fe by weight (8:5/40 × 100 = 19 will be present in chlorite (or its weathered product, limonite), and will be lost in the nonmagnetic tailings of a crushed feed treated by some magnetic concentration process.

The results of the magnetic concentration tests in table 10 support this contention. There, the nonmagnetic tailings of initial feeds assaying 47.39 and 49.35 per cent Fe contain 22 and 21 per cent of the total Fe content of the samples, respectively. Thus, the grade of the deposits based on chemical analyses of the total Fe content must be scaled down by a factor ranging from 20 to 50 per cent, depending on the magnetite content of the rocks in question.

Description of the Deposits

Burmis

The Burmis magnetite deposits occur within a narrow zone of folded and faulted Belly River strata which crops out for a distance of 13 miles north of the village of Burmis along the eastern flank of the Livingstone Range. A map showing the location and outcrop distribution pattern of the deposits is illustrated in figure 18, accompanied by cross sections that indicate the topographic expression and structural relationships of the strata. All of the deposits are located within 1½ miles of a well travelled municipal road that runs north from Burmis to the Oldman River.

The most prominent geological feature of the Burmis area is the Livingstone Range, a south-plunging, tightly folded anticline bounded by a west-dipping fault plane along which Mississippian, Jurassic, and Lower Cretaceous rocks have been thrust over Upper Cretaceous strata to the east (Douglas, 1950). Upper Cretaceous rocks on the eastern flank of the Livingstone Range have been folded, generally speaking, into a broad,

north-plunging anticlinal structure broken by numerous closely spaced, north-striking, west-dipping thrust faults and minor folds, which have been omitted from the map in figure 18. Wapiabi strata crop out along the axis of the anticline and underlie a north-trending, cultivated valley, which is flanked on either side by steeply rising sandstone ridges composed largely of Belly River strata. Many of the structural details omitted from the map in figure 18 are shown on a map of the general Blairmore area (Norris, 1955), which includes the area containing the magnetite deposits described below.

The magnetite-bearing sandstones form part of a narrow zone of thrust-faulted, west-dipping Belly River strata that lies between the Livingstone Range on the west and the valley on the east underlain by Wapiabi shales. Within this zone the basal sandstones of the Belly River formation form a series of north-striking, subparallel ridges that rise to a maximum height of about 1000 feet above the adjacent valley, abutting rather abruptly against the steep eastern slope of the Livingstone Range. The topographic continuity of the ridges is broken by a series of U-shaped, gravel-filled valleys containing small streams, which cut across the strike of the strata as they flow from their headwaters in the Livingstone Range out into the valley to the east.

The most northerly occurrences of magnetite-bearing sandstones (north Burmis deposits) are situated between Connelly and Dupret Creeks (Fig. 18), about 8 miles north of the village of Burmis. Magnetite-bearing sandstones crop out at what appear to be successively higher stratigraphic horizons along the east-facing slopes of several gullied hills that rise in step-like fashion from the valley below to the base of the carbonate scarp face that forms the Livingstone Range on the west. The deposits were originally described by Allan (1931), who was uncertain about the stratigraphic and structural relationships of the beds, but it is now obvious from fresh exposures and borehole data that the deposits were originally part of a single lens-shaped unit that has been broken up by thrust-faulting, forming the sequence of stratigraphically superimposed outcrops shown in section W - W′, figure 18.

Section W - W′ is a cross section through the highest part of the north Burmis deposits, showing the general structure of the beds and the locations of the sampled sections listed in table 8. The basal Belly River sandstone crops out at four successively higher levels along the east-facing slope of a high hill due to repetition by low angle thrust-faulting. The fault planes are probably located near the base of the Wapiabi "transition beds" and dip to the west at about the same angle as the overlying beds (25 - 30 degrees).

The basal sandstone member crops out along the base of the hill for about 3000 feet north from a tributary of Connelly Creek, forming a massive cliff of white-weathering, cross-bedded sandstone up to 100 feet

thick. The sandstone loses its topographic expression south of the creek, although patchy outcrops can be followed south to Dupret Creek. Magnetite-bearing sandstones are absent along the length of this lower outcrop zone, although the upper 2 or 3 feet of the basal member is silty and slightly chloritic at locality B.

The basal sandstone member crops out again about 200 feet above the ridge at locality B, forming a prominent scarp that can be traced along the face of the hill for 4000 feet north of locality 307. The two outcrop zones are presumably separated by a west-dipping, low angle thrust fault, as shown in section W - W'. The upper 10 feet of the member is composed of dark brown weathering, fine-grained, greenish sandstone containing scattered magnetite-rich bands several inches thick, and was sampled near the southeast corner of the outcrop zone at localities 307 and 314. The iron-rich sandstones contain 8.5 and 9.1 per cent Fe at these localities (table 8), and the low magnetite content appears to persist along the northern extension of the outcrop zone.

The most northerly occurrence of iron-rich sandstones was observed at locality 329 and is separated from the main band of outcrops described above by a shallow wooded valley which forms a re-entrant in the east slope of the hill. The iron-rich zone is 6 to 7 feet thick, with an average Fe content of 8.9 per cent (table 8). Outcrops of the basal sandstones to the north of this occurrence are rare.

On the south face of the hill, which is flanked by a narrow V-shaped gully that cuts across the strike of the beds, the magnetite-bearing zone can be traced from locality 367 to locality 322. Near locality 322, the west-dipping strata are folded into a tight anticline and are faulted off, as shown in section W - W'. The magnetite content of the iron-rich zone progressively increases across strike to locality 322, where the beds are estimated to be 15 to 20 feet thick with an average Fe content of 16.9 per cent (table 8). However, the iron-rich sandstones are strongly fractured and sheared within the folded zone, and the feasibility of strip-mining the deposits here is doubtful.

The thickest and richest magnetite-bearing section was sampled just below the crest of the hill at locality 301, where the iron-rich sandstones are about 20 feet thick, with an average Fe content of 27.5 per cent (table 8). The outcrop has little lateral continuity and appears to be a local fault slice which has been overridden by a low angle thrust fault. Above this fault the basal sandstone outcrops again, forming a west-dipping scarp from 75 to 100 feet thick, which can be traced for 1200 feet along the crest of the hill north from locality 301. The iron-rich section forms a dark brown weathering zone at the top of the basal sandstone from 5 to 8 feet thick, composed largely of green chloritic sandstone with a low magnetite content. The iron-rich zone was sampled along the south face of the hill at localities 302 and 324, where the average Fe content of the rocks is 7.5 and 10.2 per cent, respectively (table 8).

Discontinuous outcrops of the basal sandstone member overlying the upper thrust fault can be traced to the south of localities 302 and 324 as far as Dupret Creek. At locality A the iron-rich zone is represented by 3 to 4 feet of pale green, chloritic sandstone, but magnetite-bearing sandstones are absent. Along the outcrop zone extending between the southern tributary of Connelly Creek and Dupret Creek, magnetite occurrences were neither observed in outcrops nor in a section cored at locality C.

A narrow V-shaped gully separates the magnetite deposits illustrated in section W - W′ from those to the south at localities 325 - 386 and 326 - 327. The latter form two north-trending outcrop zones separated from each other by the valley of a small stream, the intervening strata having been eroded away. In both places the magnetite-bearing sandstones crop out along the trough of a tightly folded, overturned syncline (section X - X′, Fig. 18) that appears to be a southward continuation of the structure observed just below locality 322. The iron-rich zone is absent in cored sections immediately to the west of the sampled outcrop localities, and it is obvious that the greater volume of magnetite-rich sandstone has been removed by erosion.

The more northerly of the two occurrences is exposed along the face of a steep, east-facing slope for approximately 300 feet, where the magnetite-bearing sandstones crop out along the axis of an overturned syncline. This has the effect of doubling the apparent thickness of the iron-rich zone along the face of the outcrop, as shown in the structure profile superimposed on section X - X′. The outcrop section was sampled in an old trench at locality 325, and a cored section was sampled at locality 386, the rocks averaging 22.2 and 27.3 per cent Fe across thicknesses of 15 and 18 feet, respectively (table 8).

The southern deposit crops out along the eastern margin of a grassy bench, which is flanked on the west by a series of gently sloping, gravel-covered terraces (section X - X′). The outcrop can be traced for about 1200 feet along the strike of the beds and is cut off by creek valleys to the north and south. The average width of the iron-rich zone along the length of the outcrop is no more than 50 feet, the magnetite-bearing sandstones having been truncated by erosion on both sides of the synclinal axis, as shown in section X - X.

The iron-rich zone was sampled in an old trench near the north end of the outcrop at locality 326, where the average Fe content of the rocks across an interval of 9 feet is 30.6 per cent (table 8). The magnetite content of the rocks decreases towards the southern end of the outcrop, where the average Fe content is 22.2 per cent over an interval of 10 feet at locality 327 (table 8).

The wide, glaciated valley of Dupret Creek separates the magnetite occurrences of north Burmis from those of the north-central Burmis area, the latter extending south to the valley of Rock Creek. In this area the

basal Belly River sandstone forms two outcrop zones separated by a thrust fault, which may have been continuous with the central and lower faulted outcrop zones to the north prior to the erosion of contiguous strata where the valley of Dupret Creek is now situated.

The more accessible of the two outcrop zones lies along the eastern margin of the hills that abut against the base of the Livingstone Range, forming a prominent scarp composed of the basal sandstone member, including the magnetite-bearing rocks at the top, overlain by a similar homogeneous, massive-weathering sandstone unit at least 50 feet thick. In general, the beds are part of a homoclinal structure that extends back into the hill for an unknown distance at dips that range from 30 to 45 degrees (section Y - Y′, Fig. 18). At locality 344 that part of the section including the magnetite-bearing sandstones is disrupted by minor folding, possibly as a consequence of transverse faulting.

The magnetite-bearing sandstones crop out sporadically along the scarp face from locality 341 to locality 345, a distance of about one-half mile, beyond which point the continuity of outcrop is broken by a grass-covered re-entrant between localities 342 and 345. Magnetite-bearing sandstones crop out again at locality 342, but the lateral extent of the deposits along strike is unknown. The thickness of the iron-rich zone ranges from 8 to 12 feet along the length of the outcrop belt, and the average Fe content of the sampled sections ranges from about 14.8 to 40.9 per cent (table 8), both the thickness and Fe content decreasing toward the valley of Rock Creek (Fig. 18). The highest magnetite content (40.8 per cent) was observed at locality 344, where only the upper 7 feet of the section is exposed near an inferred transverse fault zone.

Magnetite-bearing sandstones crop out again to the west of and about 500 feet higher than the main occurrence described above. Section Y - Y′ is a cross section through the area of greatest topographic relief in the north-central Burmis region, showing the inferred structure of the magnetite-bearing sandstones and related strata. The Wapiabi "transition beds" are well exposed along an access road cut below locality 334, and there is little doubt that the beds have been thrust-faulted over younger Belly River strata, as indicated in section Y - Y′. The upper magnetite-bearing section was sampled at locality 334, where the average Fe content of the rocks is 11.5 per cent across an interval of 9 feet (table 8), but the beds cannot be traced for more than 300 feet along strike.

The continuity of outcrops in the central Burmis area is broken by the valleys of several creeks and their tributaries, indicated on the map in figure 18, between which generally west-dipping Belly River strata form a series of north-striking, west-dipping ridges similar to those described above. Between Rock and George Creeks (south-central Burmis) the basal Belly River sandstone is repeated by faulting, forming as many as four north-striking, en echelon outcrop zones, analogous to those in the northern part of the area.

The iron-rich sandstones at the top of the basal member are either poorly developed or absent in the south-central Burmis area. They are absent in the western outcrop zone (Loc. D), but low grade magnetite-bearing sandstones, strongly sheared by local faulting, are present in the central outcrop zone at locality E. The central outcrop zone, in which the basal sandstone member is repeated by faulting, forming two closely spaced west-dipping sandstone ridges, extends from Milvain Creek to Rock Creek where the lower ridge is faulted out. The sheared magnetite-bearing sandstones in the upper ridge at locality E, which appears to be on strike with the beds at locality 334, disappear to the south at locality F, where the iron-rich zone is represented by a few feet of slightly chloritic sandstone. The lower ridge appears to be "barren" along the length of the outcrop zone.

The eastern extension of the basal sandstone member crops out sporadically along the western margin of the Wapiabi valley from Rock Creek to George Creek and appears to be on strike with the magnetite-bearing outcrop zone to the north at locality 341. The iron-rich zone is absent north of Milvain Creek (Loc. G) and is poorly developed south of Milvain Creek (Loc. H).

The south Burmis deposits are located between George Creek and Burmis village, where the outcrop belt of Belly River strata is overridden by Lower Cretaceous rocks of the Livingstone thrust sheet, which to the south of the Crowsnest River is in contact with the shaly beds of the Alberta group. In this area, the main magnetite occurrences are located along the eastern margin of the outcrop area, which, like the central outcrop zone in north-central Burmis, consists of two closely spaced, west-dipping basal sandstone ridges separated by a thrust fault (section Z - Z′, Fig. 18). The lower outcrop zone (Loc. I) is "barren", but magnetite-bearing sandstones crop out sporadically at the top of the upper zone (Loc. 348 to 354) from south of George Creek to the southern limit of the outcrop. Near George Creek magnetite-bearing sandstones are exposed along the south flank of an east-sloping spur (Loc. 348) for about 300 feet along the trace of the outcrop zone. The beds dip west at about 40 degrees, and the rocks have an average Fe content of 18.1 per cent across an interval of 9 feet (table 8).

About three-quarters of a mile to the south, magnetite-bearing sandstones are exposed along the continuation of the same outcrop trend observed at locality 348, cropping out sporadically along the west-dipping slope of a prominent sandstone ridge that abuts against the alluvial terraces of the Crowsnest River at the southern end. The estimated length of the outcrop is about 4500 feet, but only the lower 4 to 7 feet of the iron-rich zone is exposed at any one locality. A nearly complete section cored farther down the dip slope was sampled at locality 385, yielding an average Fe content of 24.1 per cent over a corrected interval of 10 to 11 feet (table 8).

To the west of the main outcrop zone scattered exposures of basal Belly River sandstone crop out on either side of a tributary of George Creek

below Lower Cretaceous rocks overlying the Livingstone fault. Magnetite-bearing sandstones crop out at locality 349, but the beds are highly jointed and folded, and the section is only partly exposed. The iron-rich zone was not observed in outcrops of the basal sandstone member immediately to the north or south of locality 349.

Dungarvan Creek

The Dungarvan Creek magnetite deposits are located near the northeast boundary of Waterton Lakes National Park, about 20 miles due south of Pincher Creek. Magnetite-bearing sandstones crop out sporadically in parts of Secs. 11, 12, 13, and 14, Tp. 3, R. 30, W. 4th Mer., within an area of approximately 1½ square miles. The deposits are from 2 to 3 miles west of Highway No. 6 and are easily accessible from a municipal road that runs west from the highway 4 miles south of Twin Butte.

The location and structure of the Dungarvan Creek deposits is illustrated in figure 19. The base map has been compiled from data collected by West Canadian Magnetic Ores Ltd., who conducted a detailed magnetometer and drilling survey of the deposits. The structural interpretation is based on examination of outcrops and cores from boreholes, the locations of which are shown on the map. The structure contours are drawn on the base of the iron-rich zone, which is commonly marked in the Dungarvan Creek area by a thin bed of dark grey shale locally containing fossil molluscs.

The Dungarvan Creek area is part of the faulted Foothills belt of southwestern Alberta and lies about 3 miles to the east of the front range of the Rocky Mountains, which in the Waterton Lakes region is composed of Precambrian sedimentary rocks thrust over Upper Cretaceous strata to the east. The latter are largely rocks of the Wapiabi and Belly River formations which have been deformed by thrust faulting, forming a series of closely spaced, west-dipping fault blocks, with a typical imbricate pattern in cross section (Douglas, 1950). The topography of the Foothills belt in this area is a function of the regional fault pattern and gross lithology of the rocks and is characterized by a series of northwest-trending, subparallel sandstone ridges separated by valleys underlain by predominantly shaly strata.

The main physiographic features of the Dungarvan Creek area are the wide, gravel-filled channel of Dungarvan Creek itself, and the valley of Baird Creek to the north, which has its source in a broad marshy depression in the southeast corner of section 14. The interstream areas are gently undulating, the general slope of the land rising more steeply to the west as the base of the front range is approached. Bedrock exposures are scarce, the basal Belly River member forming low grass-covered ridges in the western part of the area, along which sporadic outcrops of magnetite-bearing sandstones are found.

The rocks in the Dungarvan Creek area have been broken up into three blocks of strata separated by northwest-striking fault zones. On the eastern margin of the area magnetite-bearing sandstones crop out intermittently in section 12 on the north bank of Dungarvan Creek for a distance of 500 feet. The structure of the beds is shown in section A - A′ (Fig. 19), from which it appears that generally west-dipping strata have been broken up into a number of small blocks by a complex system of faults. Soft, white, kaolinitic sandstone crops out at the eastern end of the section; hard, buff, calcareous sandstones interbedded with magnetite-rich sandstones crop out in the central part; and magnetite-rich sandstones crop out at the western end. The magnetite-rich sandstones are about 10 feet thick at the western end of the outcrop and have been shattered by closely spaced, vertical joints and faults.

No complete stratigraphic section across the iron-rich zone is exposed, so that its thickness is unknown. The areal extent of the deposits, indicated by the borehole locations shown in figure 19, is limited, the more magnetite-rich beds having been eroded to the east of locality 308. A series of boreholes drilled between the outcrops on Dungarvan Creek and those in the vicinity of the Baird ranch house failed to reach the iron-rich zone, which presumably dips steeply to the west beyond locality 308 beneath the cover of younger rocks and alluvial deposits.

Magnetite-bearing sandstones crop out sporadically for a distance of 300 feet in the vicinity of the Baird ranch house (locality 310), and across the creek from the ranch house at the south end of a low grass-covered ridge (locality 368). The beds are nearly flat-lying, and the magnetite-bearing sandstones have been trenched at both localities, exposing a nearly complete stratigraphic section across the iron-rich zone. At locality 310 the rocks have an average Fe content of 20.9 per cent across an interval of 24 feet, and at locality 368 have an average Fe content of 25.7 per cent across an interval of 14 feet (table 8). The distribution of magnetite in both sections is shown in figure 4.

According to Douglas (1950), the magnetite-bearing sandstones crop out along the eastern margin of a fault zone that can be traced across the Waterton map-area to the International Boundary, those in the vicinity of the Baird ranch house having been thrust over younger strata to the east. The areal extent and structure of the deposits to the west of the fault zone is indicated by the location of outcrops and cored sections shown in figure 19. The magnetite-bearing sandstones appear to have been removed by erosion along the valley of Baird Creek and northwest of locality 368. The rocks are not exposed between locality 368 and a second fault zone to the west. Borehole data indicate that they have been folded into a basin-like structure near the margin of the western fault zone, the structural low coinciding with a shallow topographic depression in which Baird Creek has its source. The thickness of overburden is estimated to range up to 125 feet between the exposure at locality 368 and the margin of the western

fault zone. The southern extent of the deposits is uncertain, although magnetite-bearing sandstones are present in two cored sections about 2500 feet due south of the Baird ranch house, near Dungarvan Creek.

The most westerly outcrops of magnetite-bearing sandstones occur along two low, north-trending terraces separated by a marshy depression, which gradually rise to the crest of a prominent tree-covered ridge on the west. The rocks outcrop at the southern end of the northern terrace at locality 366, where magnetite-bearing sandstones are exposed across the crest of a small anticline for about 100 feet. The strata have been broken by numerous small faults and drag folds, so that it is impossible to obtain an accurate estimate of the thickness and magnetite content of the iron-rich zone at this locality. Less than 5 feet of magnetite-rich sandstone are present in any one part of the outcrop. The rocks are similarly faulted and folded at the north end of the southern ridge at locality 367.

It is apparent from borehole data that the two outcrop bands are exposed along the margin of a complex fault zone, shown in figure 19, and on the map of the Waterton area by Douglas (op. cit.). Structure contours drawn on the base of the iron-rich zone indicate that the rocks dip steeply to the west beyond the faulted and folded zone, disappearing beneath the thick overburden of the ridge to the west. The magnetite-bearing sandstones appear to have been removed by erosion by a few hundred feet north of locality 366, but their southern extent is uncertain. Unfortunately, the most accessible part of the deposits is within the faulted zone along the crest of the anticline margining the fault shown in figure 19.

Todd Creek

Scattered outcrops of magnetite-bearing sandstone occur in the general vicinity of Todd Creek (Locs. 10 to 15 inclusive, Fig. 1) several miles to the north and east of the main Burmis deposits. The occurrences are located in a zone of complexly faulted and folded Wapiabi and Belly River strata on the eastern margin of the broad valley underlain by Wapiabi shales, which runs north from Burmis along the eastern flank of the Livingstone Range[1]. The deposits have a limited areal extent and their magnetite content is low, indicating that they have little value at present as a potential source of iron ore.

The most northerly of these occurrences (Loc. 15, Fig. 1) crops out along the southwestern flank of a north-plunging syncline, about the margin of which the basal Belly River member forms a prominent sandstone scarp. The iron-rich zone at the top of the basal member crops out from 200 to 300 feet above the level of the valley on the west, the beds dipping 15 to 20 degrees north and east into the face of the hill. The rocks were sampled

[1] The detailed geological setting of the individual deposits is shown on maps of the following areas: locality 10—Burmis map-area (Norris, 1955); locality 11—Cowley map-area (Hage, 1945); locality 12—Callum Creek map-area (Douglas, 1950); localities 13, 14, and 15—Gap map-area (Douglas, 1950).

at localities 279 and 281 (table 8), the former in the northeast quarter of Sec. 10, Tp. 10, R. 3, W. 5th Mer., and the latter about half a mile to the south in the southeast quarter of Sec. 11, Tp. 10, R. 3, W. 5th Mer. The iron-rich zone is composed of dark brown weathering, green, chloritic sandstone from 5 to 7 feet thick, but the magnetite content of the rocks in both sampled sections is negligible.

Magnetite-bearing sandstones are exposed about 2 miles to the southeast of the occurrences described above in the southeast quarter of Sec. 1, Tp. 10, R. 3, W. 5th Mer. (Loc. 14, Fig. 1). The rocks crop out on the west limb of a faulted anticline, dipping 40 degrees west for a distance of approximately 1000 feet along the north slope of a shallow valley. The iron-rich section is from 10 to 12 feet thick and was sampled at localities 290 and 292, the former at the northeast end of the outcrop zone, and the latter about 600 feet downdip to the west. The magnetite content of both sampled sections is concentrated in a zone from 1 to 2 feet thick near the base of the chloritic sandstone interval (Fig. 4), and the average Fe content of the sections is 13.7 and 16.6 per cent, respectively (table 8).

Iron-rich sandstones crop out again about 1½ miles south of the occurrence described above in Secs. 25 and 36, Tp. 9, R. 3, W. 5th Mer. (Loc. 13, Fig. 1). The basal Belly River sandstone is exposed along the east limb of a small anticline, forming a low ridge that rises from road level in section 25 towards the complexly faulted and folded strata of the hills to the north. Magnetite-bearing sandstones crop out sporadically along the strike of the ridge for several hundred feet, dipping 50 to 60 degrees east between two thick, massive-weathering sandstone units. The rocks were sampled at three localities along the length of the outcrop zone, but the upper part of the section is faulted out at locality 275, and only patchy "grass roots" outcrops are exposed at locality 277. A completely exposed section across the iron-rich zone was sampled at locality 278, yielding an average Fe content of 16.4 per cent (table 8). Magnetite-rich beds appear to be thin and sporadically distributed, and the average iron content of the rocks is probably lower than that suggested by the data in table 8.

Magnetite-bearing sandstones are exposed in Secs. 21 and 28, Tp. 9, R. 2, W. 5th Mer. (Loc. 12, Fig. 1), near the eastern margin of Belly River outcrops in the Foothills. There, the basal Belly River member is preserved along the axis of a gently folded, south-plunging syncline, forming the cap rock of an elongated, butte-like prominence (locally called Antelope Butte) that stands several hundred feet above the surrounding terrain. The basal Belly River sandstone crops out about the rim of the butte, which is cut off to the south by the valley of Todd Creek. Loose blocks of magnetite-rich sandstone are present among the grass-covered rubble on the gently sloping upper surface of the butte, from which it would seem that most of the magnetite-rich rocks and younger Belly River strata have been removed by erosion. This interpretation is supported by cored sections recovered from two boreholes drilled by West Canadian Magnetic Ores

Ltd., near the north and south ends of the butte: about 2 feet of magnetite-rich sandstone underlie a thin veneer of weathered rubble at the one locality, but the magnetite-bearing sandstones have apparently been eroded at the other.

Magnetite-bearing sandstones crop out a short distance to the south of Todd Creek in Sec. 16, Tp. 9, R. 2, W. 5th Mer. (Loc. 11, Fig. 1). There, the basal Belly River member is exposed along the west limb of the syncline observed to the north on Antelope Butte, forming a thick sandstone ledge at the top of the steep western slope of a cuesta that rises 200 to 300 feet above a narrow valley on the west. The iron-rich zone crops out for about 600 feet along the strike of the beds near the top of the ridge, disappearing to the east under the cover of younger beds. The magnetite-bearing beds dip about 30 degrees east and are displaced along strike by several minor transverse faults. The section was sampled at locality 295 (table 9), where the iron-rich sandstones are from 8 to 9 feet thick, although most of the magnetite is concentrated in a bed about 1 foot thick near the base of the section. The average Fe content of the section at locality 295 is 12.0 per cent (table 8). The relatively low magnetite content of the rocks appears to be nearly constant along the outcrop zone and in sections cored at various distances downdip from the outcrop face.

The remaining occurrence of magnetite-bearing sandstones examined in the Todd Creek area is located in Sec. 18, Tp. 9, R. 2, W. 5th Mer. (Loc. 10, Fig. 1). The rocks crop out along a low, grass-covered ridge south of the valley of Wildcat Creek, and about 1 mile north of a prominent, sandstone-capped hill called Chapel Butte. The outcrops are situated on the west limb of a narrow, north-striking anticline, the beds dipping about 50 degrees west. The outcrop is about 200 feet in length, and the iron-rich zone, which is poorly exposed and severely oxidized, is about 7 feet thick. The section was sampled at locality 297, where the average Fe content of 11 samples is 10.9 per cent (table 8).

Southern Localities

Magnetite-bearing sandstones crop out at several localities within the zone of folded and faulted Belly River strata that underlies a large area of the Foothills belt between the Crowsnest Pass and the International Boundary. The Dungarvan Creek deposits, which contain the largest potential reserves of any of the occurrences examined, have been described separately. Other occurrences south of Burmis, the locations of which are indicated on the map in figure 1,[1] are of low grade and limited areal extent and appear to have little value as potential iron ore. However, for completeness, the geology and extent of these low grade deposits are briefly de-

[1] The detailed geological setting of the individual deposits is shown on maps of the following areas: localities 1, 3, 4, 5, 7(Dungarvan Creek)—Waterton map-area, (Douglas, 1951); locality 6—Pincher Creek map-area (Douglas, 1950); locality 8—Beaver Mines map-area (Hage, 1943). The geology of the area in which locality 2 is situated has not been mapped in detail.

scribed below, and analyses of the magnetite and iron content of several representative sets of samples are summarized in table 8.

The most northerly of these occurrences is located in Sec. 12, Tp. 5, R. 2, W. 5th Mer., about 2 miles to the northeast of the trace of the Lewis fault (Loc. 8, Fig. 1). There, magnetite-bearing sandstones crop out on Mill Creek, which has cut a deep narrow valley that runs nearly parallel to the strike of the beds for several hundred yards before crossing the Belly River-Wapiabi contact. Upstream from the contact, the creek has cut back into vertically dipping basal Belly River strata, forming a steep slope along which large fractured blocks of sandstone are exposed for a distance of 200 to 300 feet along the strike of the beds. The magnetite-bearing sandstones crop out near the top of the exposure, which is from 75 to 125 feet high, and are cut by a large number of minor bedding plane faults and closely spaced joints, many of which are filled with calcite. The iron-rich zone is estimated to be from 10 to 12 feet thick and is composed of dark green, chloritic sandstone containing scattered thin magnetite laminae. The rocks were sampled at locality 364 and have an average Fe content of 11.4 per cent (table 8).

Magnetite-bearing sandstones crop out about 2 miles east of the British American Oil Company's sulfur extraction plant in Sec. 19, Tp. 4, R. 28, W. 4th Mer. (Loc. 6, Fig. 1). The rocks are poorly exposed, forming a narrow "grass roots" outcrop zone which extends diagonally across a cultivated field for approximately 1000 feet. The rocks strike north 40 degrees west and dip 40 degrees west, and, according to Douglas (1950), are part of a narrow block of west-dipping strata bounded on both sides by west-dipping thrust faults. The iron-rich zone is about 10 feet thick but is composed largely of brown-weathering, green, chloritic sandstone. Scattered magnetite-rich beds, 1 or 2 inches thick, were observed in the lower part of the section, but even these appear to lense out towards the northern end of the outcrop zone. The obviously low magnetite content of the rocks and the relatively poor exposures did not warrant the collection of samples for analysis.

Low-grade, iron-rich sandstones crop out about 6 miles to the southeast of the occurrence described above, in Secs. 26 and 35, Tp. 3, R. 28, W. 4th Mer. (Loc. 5, Fig. 1). At this locality, the basal Belly River sandstone strikes north 40 degrees west and dips 30 degrees west, forming a narrow, grass-covered ridge more than 1 mile in length along the western margin of the Harland Lakes fault zone (Douglas, 1951). The crest of the ridge rises more than 100 feet above the surrounding plains on the east, but descends more gradually to the west along the dip slope of the rocks. The iron-rich phase of the basal sandstone member is exposed near the top of the dip slope for about 2000 feet along the strike of the beds, but the rocks are composed largely of brown weathering, green, chloritic sandstone containing rare magnetite-rich lenses a few inches thick. A relatively complete section across the iron-rich zone was sampled near the centre

of the ridge at locality 378, where the rocks have an average Fe content of 9.2 per cent over an interval estimated to be 15 feet thick (table 8).

Magnetite-bearing sandstones crop out in the hilly terrain several miles west of Mountain View in Sec. 33, Tp. 2, R. 27, W. 4th Mer. (Loc. 4, Fig. 1). The rocks are exposed on the west slope of a long grass-covered ridge, where patchy outcrops of brown weathering, iron-rich sandstone underlain by pale grey, calcareous sandstone striking north 30 degrees west and dipping 40 degrees west can be traced for a distance of 700 feet. The exposed thickness of the iron-rich zone does not exceed 5 or 6 feet, and the magnetite content of the rocks appears to be concentrated in thin lenses interbedded with thicker beds of green, chloritic sandstone. The rocks were sampled at locality 376, but the analyses in table 8 are not necessarily representative of the entire iron-rich zone.

A small, low-grade deposit of magnetite-bearing sandstone is located 4 miles south of Beazer in Sec. 33, Tp. 2, R. 27, W. 4th Mer., a short distance north of Goose Lake (Loc. 3, Fig. 1). The rocks crop out along the southwestern margin of a series of low rolling hills for a distance of 900 feet in an area where basal Belly River strata are repeated several times by a sequence of closely spaced, imbricate thrust faults (Douglas, 1951). The beds strike north 20 degrees west and dip 40 to 65 degrees west but are disrupted by minor transverse faults and drag folds towards the northern end of the outcrop zone. Only the lower part of the iron-rich zone is exposed. The rocks are composed of green chloritic sandstone interbedded with magnetite-rich beds up to two feet thick. Intervals from 4 to 6 feet thick were sampled at three localities (371, 372, 373) along the outcrop zone, and the average Fe content of the samples from all three sections is 24.5 per cent (table 8).

Iron-rich sandstones are exposed along the trend of a narrow sandstone ridge 3 miles southwest of Beazer in Secs. 28 and 33, Tp. 1, R. 26, W. 4th Mer. (Loc. 2, Fig. 1). The beds strike north 30 degrees west and dip 55 degrees west, and are probably bounded on the east by a fault zone. Green chloritic sandstones are exposed sporadically along the crest and western slope of the ridge for about half a mile, but the magnetite content of the beds is practically negligible. The iron-rich zone is about 7 feet thick towards the southern end of the ridge, where the section was sampled at locality 374, yielding an average Fe content of 8.6 per cent.

The most southerly magnetite-bearing sandstone occurrence is located near the International Boundary in Sec. 3, Tp. 1, R. 27, W. 4th Mer. (Loc. 1, Fig. 1). The rocks are exposed along the crests of two low, en echelon ridges separated by a shallow, wooded gully. Patchy "grass roots" outcrops of laminated, magnetite-bearing sandstone dipping 25 degrees west can be traced along the strike of the northern ridge for about 600 feet. Only a few feet of magnetite-bearing beds are exposed at any one locality along the outcrop zone, and no complete section of the iron-rich zone was observed. Blocks of magnetite-bearing sandstone are present also in

Table 11. Estimated Iron Ore Reserves, Burmis

Locality	Block	Sampled section (Fig. 18)	Thickness of sampled section (feet)	% Fe (Table 8)	Average thickness of iron-rich zone (feet)	Area (thousands of square feet)	Estimated reserves[1] (thousands of long tons)	Over-burden thickness (feet)
North Burmis	1	301	20	27.5	20	30	55	uncertain
	2	325	15	22.2	16	15	22	nil
		386	17	27.3				
	3	326	12	30.6	11	60	60	nil
		327	10	22.2				
North-central Burmis	4	342	11	21.1	11	45	45	0-200
	5	345	8	24.1	10[2]	375	341	0-200
		344	7	40.9				
		338	12	18.5				
		341	7	14.8				
South Burmis	6	348[3]	9	18.1	10[2]	1,500	1,363	0-200
		350	4	30.8				
		354	9	8.8				
		385	15	24.1				
Total estimated reserves							1,886	

(1) Assuming that 11 cubic feet of ore, averaging 25 per cent Fe, weigh 1 long ton.
(2) Thickness assumed.
(3) North of but on strike with the beds in block 6.

loose rubble along the crest of the southern ridge, which is bisected by the International Boundary, but the rocks were not observed in place.

Reserves

Burmis

Estimated reserves of potential iron ore in the Burmis area are shown in table 11. The reserves have been calculated separately for each of six blocks, the general locations of which are indicated by the locations of the sampled sections in figure 18. The estimated reserves have been calculated from the formula (area×average thickness) /no. of cu. ft. of ore per ton, where it is assumed that 11 cubic feet of ore weigh approximately 1 long ton. This assumption is based on an average ore grade of 25 per cent Fe (approximately 35 per cent Fe_2O_3), in which case the bulk density of the ore can be calculated from the equation on p. 66 as approximately 3.2.

A better indication of the actual grade of the deposits is given by the average iron content of the sampled sections in each block, also shown in table 11. The corresponding magnetite and titania percentages are given in table 8. However, the data are not sufficient to give an accurate weighted estimate of the average iron content of the potential ore in each block, because of the thin, lensing nature of the deposits and the numerous structural complexities. Undoubtedly, much of the volume of rock included in the estimated reserves in tables 11 and 12 has an average iron content well below the minimum economic limit, but whether the complexly interbedded magnetite-rich and magnetite-poor beds (Fig. 4) could be separated by some selective mining process is problematical. In this light, the estimates of reserves in the Burmis and Dungarvan Creek areas are, on the whole, probably too high.

The tonnages of potential ore in north Burmis are particularly difficult to predict because of the complex structure of the rocks (sections W - W′, X - X′; Fig. 25). Reserves have been calculated for three separate magnetite-rich occurrences, indicated as blocks 1, 2, and 3 in table 11. Block 1 contains the magnetite-rich sandstones that crop out at locality 301. The lateral extent of these beds is uncertain, and borehole data indicate that the rocks are complexly folded and faulted a short distance back from the outcrop face. Estimated reserves have been caluculated for a block of ore 150 feet long and extending 250 feet back into the hill. The reserves are 55,000 tons, which may be conservative. The reserves of potential ore in the zone of folded strata near locality 322 (section W - W′, Fig. 18) have not been estimated, as the overburden appears too thick there for strip-mining.

The estimated reserves of the two isolated deposits (blocks 2 and 3) south of the main body of outcrops in north Burmis (Fig. 18) are low but easily accessible. The reserves contained by block 2 have been calculated for an ore body 300 feet long extending along the outcrop face, and 25 feet wide extending back into the hill. The volume of reserves has been calculated by multiplying the area so obtained by twice the thickness of the iron-rich zone, as the rocks have been isoclinally folded and overturned along the axis of the syncline shown in figure 18. Estimated reserves are 22,000 tons.

The reserves contained by block 3 have been calculated for an ore body 1200 feet long paralleling the strike of the beds and 50 feet wide paralleling the dip of the beds. Estimated reserves are 60,000 tons, although the grade of the deposit tapers off towards the southern end (Loc. 327, Fig. 18). Total reserves in North Burmis are about 140,000 tons of potential iron ore.

The reserves in north-central Burmis are located within the eastern zone of outcrops near the base of the hills that flank the Livingstone Range (Fig. 18). The once-continuous outcrop zone has been broken by a low grass-covered re-entrant between localities 342 and 345, from which the

iron-rich deposits have been removed by erosion. The dip of the beds (30 to 65 degrees west) and the steep slope of the scarp face (section Y - Y′, Fig. 25) indicates that the deposits would be difficult to strip, because of the thick massive sandstone overlying the magnetite-bearing sandstones.

Reserves have been calculated for the northern extension of the deposit (block 4) on the assumption that it extends for 300 feet along strike and can be stripped back into the hill for a distance of 150 feet across the dip of the beds. Reserves have been calculated for the main southern extension of the deposit (block 5), assuming that it is continuous for 2500 feet along strike, and can also be stripped back into the hill for a distance of 150 feet across the dip of the beds. The estimated reserves contained in block 4 are 45,000 tons, and in block 5 are 341,000 tons, giving total estimated reserves of potential iron ore in north-central Burmis of 386,000 tons.

Magnetite-bearing sandstones which crop out sporadically along the eastern margin of the hills below the Livingstone fault from north of Burmis village to George Creek (Fig. 18) constitute the only potential source of iron ore in south Burmis. The main, southern part of the west-dipping outcrop zone can be traced for about 5000 feet north of locality 354, although exposures are poor and borehole data are scarce. Much of the overburden on the dip slope has been removed by erosion, but it is also possible that a large proportion of the magnetite-bearing beds have been eroded away. If, however, the average thickness of the iron-rich zone is 10 feet, and the beds can be stripped across the dip for a distance of 300 feet, then the reserves of the resultant block of ore (block 6) are 1,363,000 tons.

The volume of ore contained by the iron-rich occurrence north of but on strike with the beds in block 6 (Loc. 348, Fig. 18) is uncertain. However, the thickness of overburden is high (section Z - Z′, Fig. 18), and the outcrops cannot be traced for more than a few hundred feet up the south flank of the hill. The reserves of the deposit have not been estimated.

Total estimated reserves of potential iron ore in the Burmis region are 1,886,000 tons.

Dungarvan Creek

The accuracy of the estimated reserves of potential iron ore in the Dungarvan Creek area is subjected to the same qualifications as that of those in the Burmis region; the rocks have been complexly folded and faulted; the magnetite-bearing beds are thin and lensing; and exposures are scarce. Reserves have been calculated for each of four blocks of ore, as shown in table 12. The average thickness of the iron-rich zone in each block has been determined from various cored sections, the locations of which are shown in figure 19.

Table 12. Estimated Iron Ore Reserves, Dungarvan Creek

Block	Sampled section (Fig. 19)	Thickness of sampled section (feet)	% Fe (Table 8)	Average thickness of iron-rich zone(1) (feet)	Area (thousands of square feet)	Estimated reserves(2) (thousands of long tons)	Overburden thickness (feet)
1	308	10(?)	39.9	13.6	280	346	nil
	309	10	18.2				
2	310	15 (3)	27.4	13.3	960	1,160	0-50
3	368	14	25.7	12.3	2,560	2,863	0-100
4	366	5½	18.4	8.6	1,750	1,368	0-200
	367	5(?)	26.8				
Total estimated reserves						5,737	

(1) Determined from cored sections (Fig. 19).

(2) Assuming that 11 cubic feet of ore, averaging 25 per cent Fe, weighs 1 long ton.

(3) Upper 15 feet of the section (Fig. 4).

The grade of the deposits is uncertain. Samples from six outcrop sections were analysed for their iron and titania content (tables 8, 12), but only two of the sections are undisturbed by faulting or folding (Locs. 310, 368; Fig. 19). The average thicknesses of the iron-rich zone used for calculation of the reserves in the four blocks in table 12 include much low-grade chloritic sandstone, similar to the sampled outcrop sections at localities 310 and 368 (Fig. 4). The average iron content of these two sections is 20.9 and 25.7 per cent Fe, respectively, although the upper 15 feet of the section at locality 310 contains 27.4 per cent Fe. The distribution and amounts of magnetite in the cored sections are similar to those of the sampled sections, and an average grade of 25 per cent Fe seems reasonable for the reserves in table 12 as a first approximation.

Block 1 is an area about 400 x 700 feet containing the magnetite-bearing sandstones outlined by the boreholes and outcrops on the north bank of Dungarvan Creek (Fig. 19). The iron-rich rocks are covered by a thin veneer of soil and alluvium, but the rocks have been broken up by numerous small faults and folds (section A - A′, Fig. 19). Estimated reserves are 346,000 tons.

Block 2 is an area about 800 x 1200 feet in the vicinity of the Baird ranch house, bounded on the east by a fault, and to the north and west by the valley of Baird Creek (Fig. 19). The rocks appear to be relatively flat-lying, and the thickness of overburden is low. Estimated reserves are 1,160,000 tons.

Block 3 is a wedge-shaped area bounded by the valley of Baird Creek on the east and a fault zone to the west and south (Fig. 19). The northern boundary is defined by the line of boreholes west of locality 368, beyond which point the iron-rich zone appears to have been eroded. The rocks are folded at depth, and the thickness of overburden increases towards the fault zone. Estimated reserves are 2,863,000 tons.

Block 4 is an area about 700 x 2500 feet on the west flank of the western fault zone Fig. 19). The iron-rich rocks are broken up along the crest of the anticline margining the fault zone, and the thickness of overburden increases rapidly to the west. This block of potential ore appears to be the least favorable of the four blocks for stripping. Estimated reserves are 1,368,000 tons.

Total estimated reserves of potential iron ore in the Dungarvan Creek area are 5,737,000 tons.

Discussion

The total reserves of potential iron ore in the Burmis and Dungarvan Creek areas are estimated at less than 8,000,000 tons, grading between 20 and 30 per cent Fe. The reserves contained in the other widely scattered deposits near Todd Creek and south of the Crowsnest Pass are of too low a grade to warrant consideration.

The accuracy of these estimates is uncertain because of the complex geology of the individual deposits, but there can be little doubt that the reserves shown in tables 11 and 12 are of the correct order of magnitude. Thus, to illustrate the point, if it is assumed that three tons of ore grading 25 per cent Fe will yield one long ton of metallic iron, and that the minimum ingot capacity for an economic blast furnace operation is 280,000 tons of pig iron per annum (Janes, 1959), then the estimated reserves of iron ore in the Burmis and Dungarvan Creek areas would be sufficient to operate such a smelter for only nine to ten years. This assumes that all of the iron in the rocks would be recovered in beneficiating and smelting the ore, which, as previously shown, would not hold true in practice.

In the light of these observations alone, there can be little doubt that the Crowsnest magnetite deposits do not constitute a major source of potential iron ore under current economic conditions using conventional beneficiation and smelting techniques. This is especially true in view of the recent discovery of large reserves of easily accessible oolitic iron ore in the Clear Hills district of northwestern Alberta (Kidd, 1959). These deposits, if developed, could easily supply all of the foreseeable requirements for pig iron in Alberta for many years to come.

Summary and Conclusions

The economic potential of the Crowsnest magnetite deposits as a source of iron ore is low. The only factor that favors the development of

the deposits is their general location with respect to the large coal reserves and transportation facilities of the Crowsnest Pass region. However, those geological and compositional factors which govern the ultimate availability of the raw ore and the ease with which it can be beneficiated and smelted are overwhelmingly unfavorable to the development of the deposits under current economic conditions.

In the first place, the rocks themselves are unsuitable for treatment by conventional mineral dressing and smelting techniques because of their fine grain size, high titanium content, and high chlorite content. Even if the problems posed by the petrographic and chemical properties of the rocks were overcome by the development of some new smelting technique, the complex structure and low reserves of the deposits would still be strongly detrimental to their exploitation.

Other geological factors affecting the economic potential of the deposits are the structure and topographic setting of the deposits. The Burmis deposits are in an area of relatively high relief and would require the building of a network of access roads. Moreover, the beds have been complexly folded and faulted in such a way that the thickness and nature of the overburden drastically limits the volume of ore that could be profitably strip-mined at most localities in the area. The Dungarvan Creek deposits are in an area of low relief and easy access, but some of the occurrences have been so broken up by local faulting that it would be almost impossible to separate the magnetite-rich rocks from the "barren" or low-grade sandstones by strip-mining.

The low tonnages and the grade of the potential ore reserves are the most important factors that argue against the development of the Crowsnest deposits. The Burmis and Dungarvan Creek areas, which contain the only sizeable deposits among the various occurrences examined in the course of the investigation, have combined reserves estimated at less than 8,000,000 tons, averaging between 20 and 30 per cent Fe.

The estimated reserves of the other widely scattered deposits from Todd Creek to the International Boundary are small or of too low a grade in comparison with those at Burmis and Dungarvan Creek. In respect to these occurrences, it should be noted that numerous similar lenses of magnetite-bearing sandstone are undoubtedly present throughout the Foothills belt of southwestern Alberta. Most of the deposits are buried beneath the thick overburden of younger rocks, but a few are undoubtedly either exposed at or buried just beneath the surface in unprospected areas. There is little reason to suppose that these yet undiscovered deposits would contain reserves of sufficient size to warrant their development, if it is assumed that the composition, grade, and size of such deposits would be similar to those of the deposits in the Crowsnest Pass - Waterton Lakes region.

REFERENCES CITED

Allan, J. A. (1931): Report of the Geological Survey Division; Res. Coun. Alberta Rept. 27, 12th Ann. Rept., p. 19-23.

Armstrong, W. M. (1959): Electric smelting processes - reducing materials; Proceedings of Symposium on Iron and Steel in Western Canada; Res. Coun. Alberta Inform. Ser. No. 30, p. 157-164.

Basta, E. Z. (1957): Accurate determination of the cell dimensions of magnetite; Mineral. Mag., Vol. 31, No. 237, p. 431-442.

Bennett, C. A. and Franklin, N. L. (1954): Statistical Analysis in Chemistry and the Chemical Industry; John Wiley & Sons, Inc., New York, 724 pages.

Biederman, E. W. (1958): Shoreline sedimentation in New Jersey; unpublished Ph.D. thesis, Penn. State Univ., State College, Penn., 270 pages.

Chayes, F. (1952): Notes on the staining of potash feldspar; Am. Mineral. Vol. 37, No. 4, p. 337-340.

---------- (1956): Petrographic Modal Analysis; John Wiley & Sons, Inc., New York, 113 pages.

Claisse, Fernand (1960): Sample preparation techniques for X-ray fluorescence analysis; Quebec Dept. Mines Prelim. Rept. 402, 14 pages.

Cobban, W. A. (1955): Cretaceous rocks of northwestern Montana; Billings Geol. Soc. Guide Book, 6th Ann. Field Conf., p. 107-119.

De Munk, Victor C. (1956): Iron deposits in Montana; Montana Bur. Mines and Geol. Inform. Circ. 26, 55 pages.

Douglas, R. J. W. (1950): Callum Creek, Langford Creek, and Gap map-areas, Alberta; Geol. Surv. Can. Mem. 255, 124 pages.

---------- (1951): Pincher Creek, Alberta; Geol. Surv. Can. Paper 51-22, map with marginal notes.

---------- (1952): Waterton, Alberta; Geol. Can. Paper 52-10, map with marginal notes.

Friedman, G. M. (1959): Identification of carbonate minerals by staining methods; Jour. Sedimentary Petrology, Vol. 29, No. 1, p. 87-97.

Gardner, D. E. (1955): Beach and heavy-mineral deposits of eastern Australia; Australia Dept. National Development, Bur. Min. Res., Geol., and Geophys., 103 pages.

Government of Canada:

(1941): Magnetic concentration and microscopic examination of iron-bearing material from the Burmis titaniferous iron deposit, Crowsnest Pass, Alberta; Bur. Mines Rept. MD-995, mimeo., 6 pages.

(1951) Microscopic examination and magnetic concentration of a sample of magnetic iron ore from the International Coal and Coke Company, Coleman, Alberta; Mines Br. Mineral Dressing and Process Metallurgy Div. Rept. MD-507-OD, mimeo., 3 pages.

(1954) Magnetic and gravity concentration test on a sample of iron ore form the West Canadian Collieries Limited, Blairmore, Alberta; Mines Br. Mineral Dressing and Process Metallurgy Div. Rept. MD-3034, mimeo., 26 pages.

(1957a) Concentration and magnetic roasting tests on three samples of iron ore from West Canadian Collieries Limited, Blairmore, Alberta; Mines Br. Mineral Dressing and Process Metallurgy Div. Rept. MD-3187, mimeo., 26 pages.

(1957b) Heavy-media separation tests of a sample of iron ore from West Canadian Collieries Limited, Blairmore, Alberta; Mines Br. Mineral Dressing and Process Metallurgy Div. Rept. MD-913-OD, mimeo., 6 pages.

Griffiths, J. C. (1959): Statistical methods in sedimentary petrography, Chapter 16 in Milner, H. B., Sedimentary Petrography; Thomas Murby & Co., London, 4th ed. (2 vols., in press).

---------- (1960a): Frequency distributions in accessory mineral analysis; Jour. Geol., Vol. 68, No. 4, p. 353-365.

---------- (1960b): Modal analysis of sediments; Révue de géographie physique et de géologie dynamique (2), Vol. 3, Fasc. 1, p. 29-48.

Hague, C. O. (1943): Beaver Mines, Alberta; Geol. Surv. Can. Map 739A, with marginal notes.

---------- (1945):Cowley, Alberta; Geol. Surv. Can Map 816A, with marginal notes.

Janes, T. H. (1959): Markets for iron and steel products in Western Canada; Proceedings of Symposium on Iron and Steel in Western Canada, Res. Coun. Alberta Inform. Ser. No. 30, p. 13-37.

Kidd, D. J. (1959): Iron occurrences in the Peace River region, Alberta; Res. Coun. Alberta Prelim. Rept. 59-3, 38 pages.

Krumbein, W. C. (1934): Size frequency distributions of sediments; Jour. Sedimentary Petrology, Vol. 4, p. 65-77.

---------- and Pettijohn, F. J. (1938): Manual of Sedimentary Petrography; Appleton-Century-Crofts, Inc., New York, 549 pages.

Krynine, P. D. (1948): The megascopic study and field classification of sedimentary rocks; Jour. Geol., Vol. 56, No. 2, p. 130-165.

---------- (1951): Reservoir petrography of sandstones; U.S. Geol. Surv. Map 126 (Geology of the Arctic slope of Alaska), with marginal notes.

Lander, H. N. (1959): in Proceedings of Symposium on Iron and Steel in Western Canada; Res. Coun. Alberta Inform. Ser. No. 30, p. 58.

Leach, W. W. (1912): Geology of the Blairmore map-area, Alberta; Geol. Surv. Can. Summ. Rept. 1911, p. 192-200.

Mellon, G. B. (1959): The petrology of the Blairmore group, Alberta, Canada; unpublished Ph.D. thesis, Penn. State Univ., State College, Penn., 279 pages.

Meyboom, P. (1960): Geology and groundwater resources of the Milk River sandstone in southern Alberta; Res. Coun. Alberta Mem. 2, 89 pages.

Norris, D. K. (1955): Blairmore, Alberta; Geol. Surv. Can. Paper 55-18, map with marginal notes.

Rittenhouse, Gordon (1943): The transportation and deposition of heavy minerals; Bull. Geol. Soc. Am., Vol. 54, No. 12, p. 1725-1780.

Roe, Lawrence A. (1957): Iron Ore Beneficiation; Minerals Publishing Company, Lake Bluff, Illinois, 305 pages.

Russell, L. S. and Landes, R. W. (1940): Geology of the southern Alberta Plains; Geol. Surv. Can. Mem. 221, 219 pages.

Slipper, S. E. and Hunter, H. M. (1931): Stratigraphy of Foremost, Pakowki, and Milk River formations of the southern Plains of Alberta; Bull. Am. Assoc. Petroleum Geol., Vol. 15, No. 10, p. 53-68.

Snedecor, G. W. (1956); Statistical Methods; Iowa State College Press, Ames, Iowa, 2nd ed., 534 pages.

Stebinger, Eugene (1912): Titaniferous magnetite beds on the Blackfeet Indian reservation, Montana; U.S. Geol. Surv. Bull. 540, p. 329-337.

Vincent, E. A. *et al.* (1957): Heating experiments on some natural titaniferous magnetites; Mineral. Mag., Vol. 31, No. 239, p. 624-655.

Webb, J. B. and Hertlein, L. G. (1934): Zones in Alberta shale ("Benton" group) in Foothills of southwestern Alberta; Bull. Am. Assoc. Petroleum Geol., Vol. 18, No. 11, p. 1387-1416.

Wimmler, N. L. (1946): Exploration of Choteau titaniferous magnetite deposit, Teton County; Montana; U.S. Bur. Mines Rept. Investig. 3981, 12 pages.

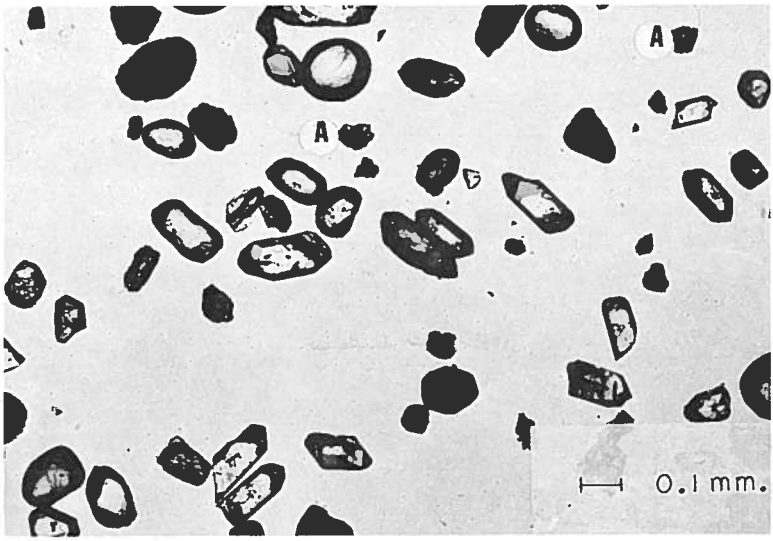

FIGURE 20. Nonmagnetic heavy minerals from sample 308-01. The grains are largely euhedral and rounded zircon, with a few small anatase (A) grains

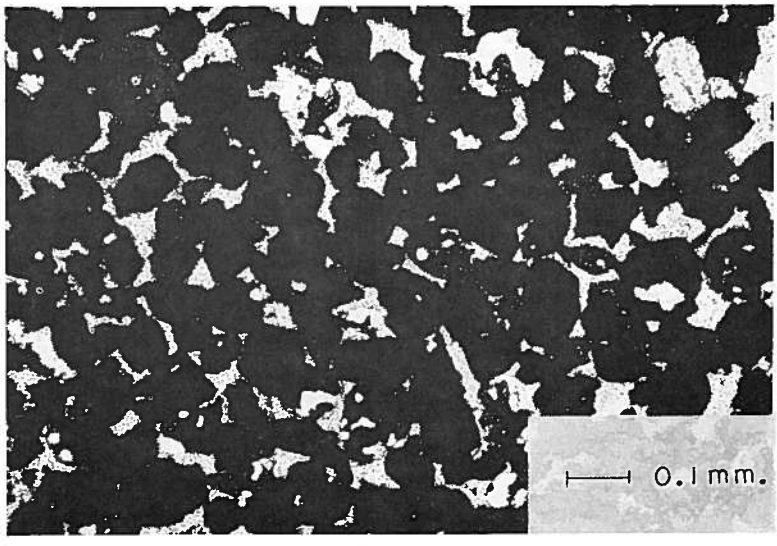

FIGURE 21. Magnetite-rich sandstone, sample 310-36. The magnetite grains (black) are cemented by yellowish-green authigenic chlorite (stippled)

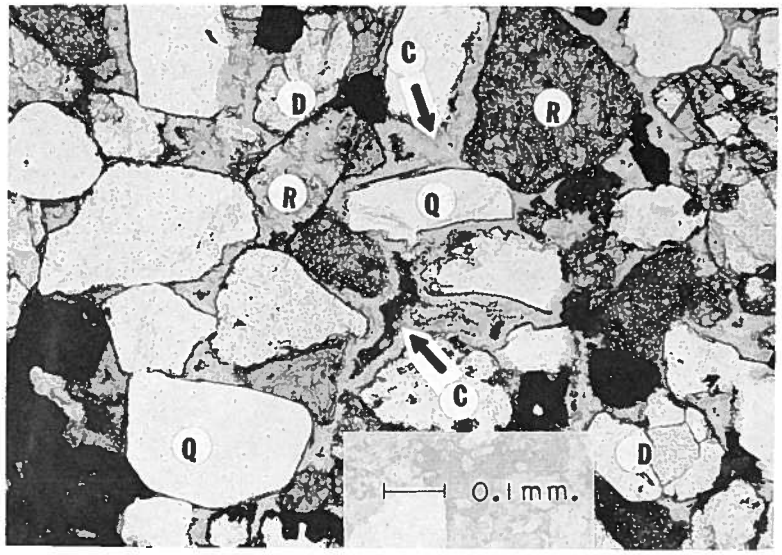

FIGURE 22. Chlorite-cemented iron-rich sandstone, sample 372-03. The clastic grains are quartz (Q), dolomite (D), finely crystalline rock fragments (R), and magnetite (black), and are cemented by green vermicular chlorite (C) which has filled nearly all of the pore spaces in the rock

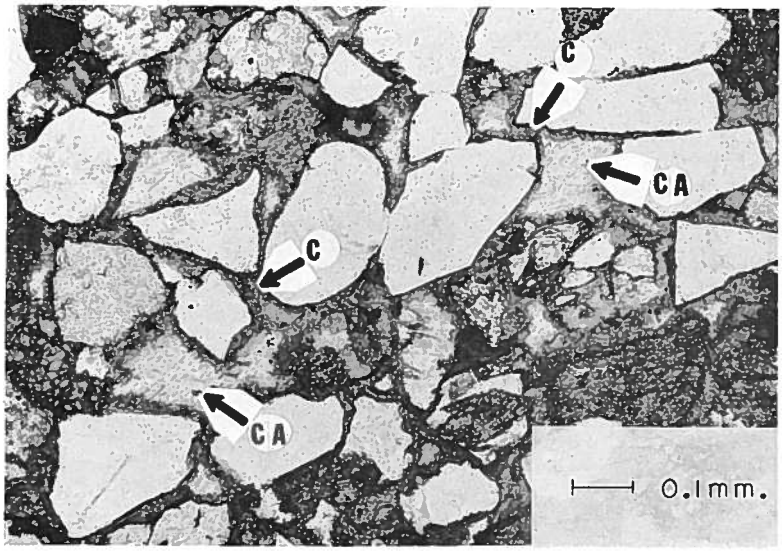

FIGURE 23. Chlorite- and calcite-cemented iron-rich sandstone, sample 278-05. The clastic grains are similar to those in sample 372-03, above. Authigenic chlorite (C) has crystallized as a thin coating about the walls of the grains. The remaining pore space has been filled by authigenic calcite (CA), emplaced after chlorite and distributed as optically continuous units which fill clusters of adjacent pores throughout areas of several square millimeters (cf. Fig. 11)

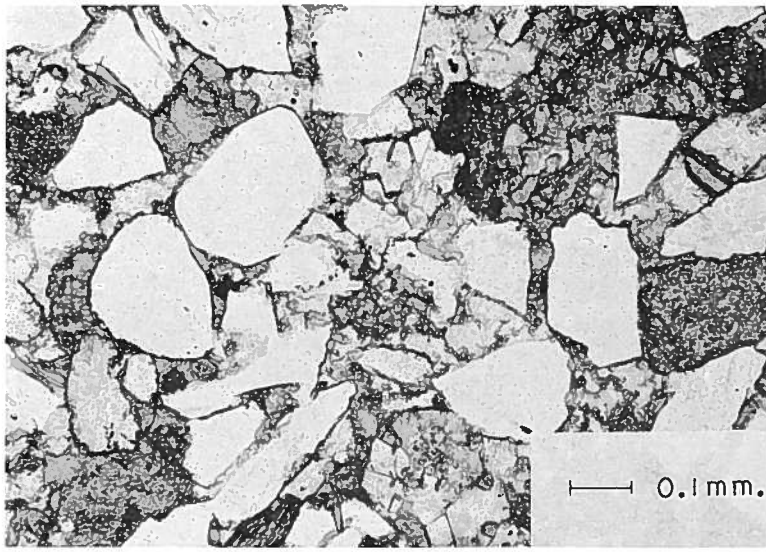

FIGURE 24. Carbonate-rich sandstone, sample 309-04. The clastic grains are largely angular or subhedral quartz, feldspar, and finely crystalline rock fragments in a carbonate "matrix." The "matrix" is composed of clastic dolomite grains, and equigranular, anhedral carbonate (probably calcite) of inferred authigenic origin

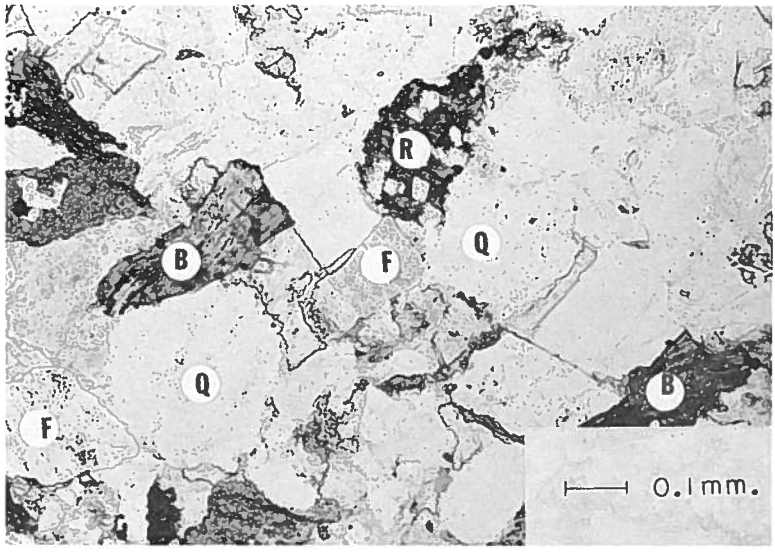

FIGURE 25. "Barren" basal Belly River sandstone underlying the iron-rich zone, south Burmis; sample 387. The main clastic constituents are quartz (Q), feldspar (F), finely crystalline, largely volcanic rock fragments (R), and brown biotite (B). The grains are cemented by authigenic quartz, kaolinite, and calcite (cf. Fig. 11)

FIGURE 26. North Burmis magnetite deposits, looking north. The Livingstone Range is on the left, and some of the Todd Creek deposits are located in the hills in the distance on the right

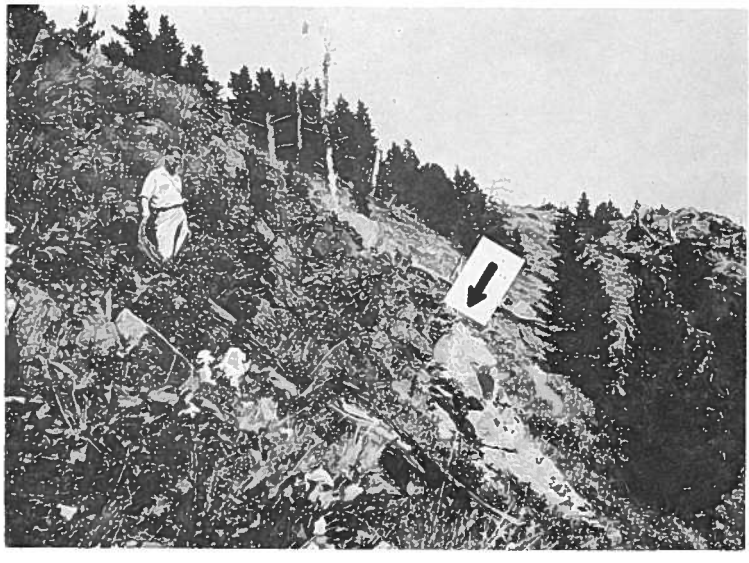

FIGURE 27. Low-grade, iron-rich sandstones at locality 290, north of Todd Creek. Assistant is standing at the top of the dark brown weathering, iron-rich zone, which grades below into pale grey weathering "barren" sandstone (arrow)

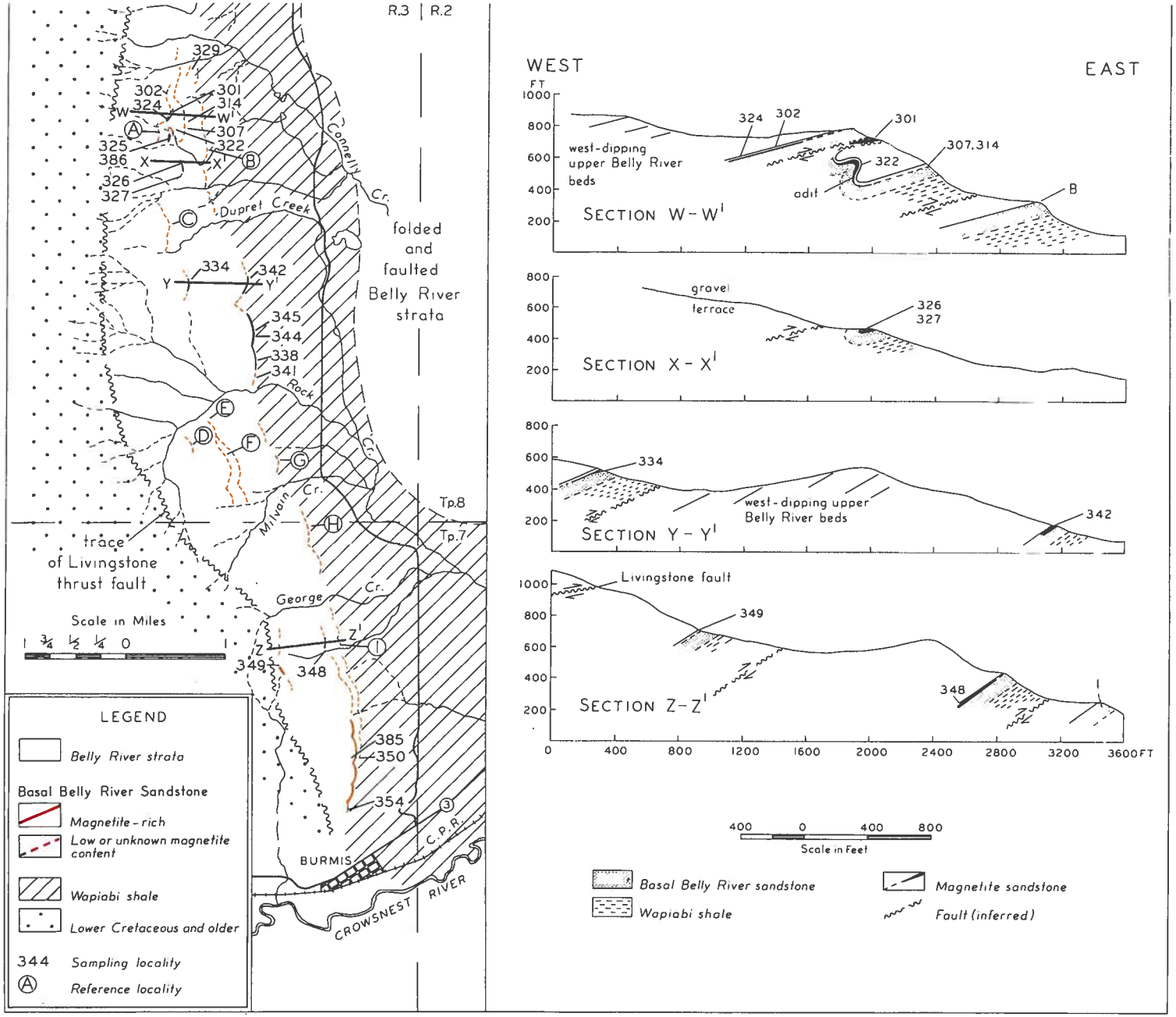

FIGURE 18. Map and structure cross sections of the Burmis magnetite deposits,

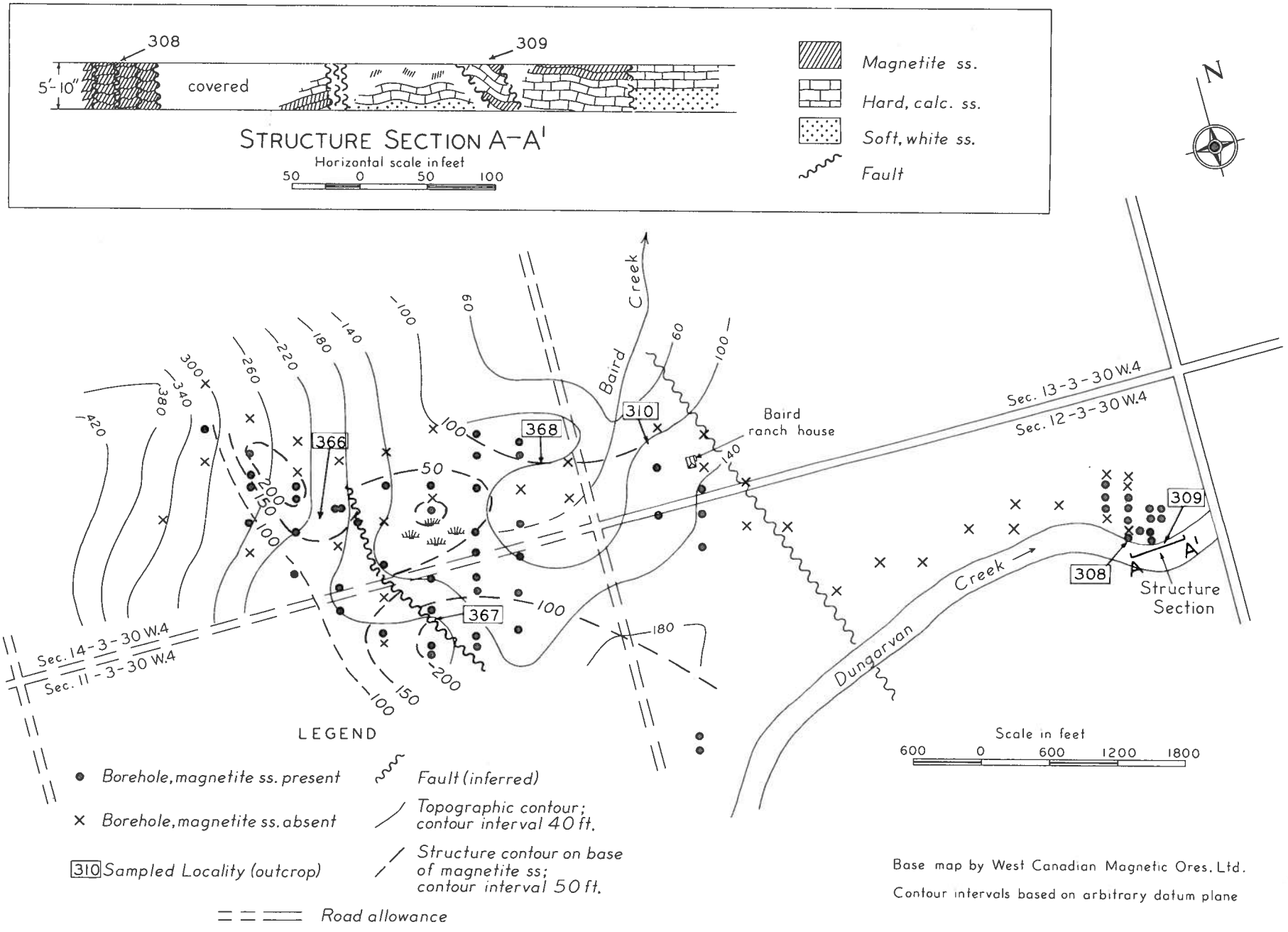

FIGURE 19. Map and structure cross section of the Dungarvan Creek magnetite deposits, southwestern Alberta

Table 8. Locations, Thicknesses, Bulk Densities, and Grade of Sampled Outcrop and Borehole Sections

Sampled section No.	Locality	Locality (Fig. 1)	Comments	Part of section sampled	Sampled interval thickness (ft.)	Number of samples	Mean bulk density (gm./cc.)	% Magnetite by vol.(1) mean	% Magnetite by vol.(1) standard deviation	% Fe_2O_3(2)	% TiO_2(3)
275	Sec. 25- 9- 3 W.5 Todd Creek	13	faulted	lower part	5	5	3.182	19.1	7.4	33.5	4.0
277	Sec. 36- 9- 3 W.5 Todd Creek	13	poorly exposed	talus	?	6	3.198	19.8	18.6	34.3	4.1
278	Sec. 25- 9- 3 W.5 Todd Creek	13		complete	10	5	2.984	10.3	11.3	23.4	2.9
279	Sec. 10-10- 3 W.5 Todd Creek	15		complete	7	7	2.774	1.0	3.6	12.7	1.7
281	Sec. 11-10- 3 W.5 Todd Creek	15		complete	6½	5	2.650	1.0	1.1	6.4	1.0
290	Sec. 1-10- 3 W.5 Todd Creek	14		complete	12	14	2.907	6.9	6.9	19.5	2.4
292	Sec. 1-10- 3 W.5 Todd Creek	14		complete	10½	12	2.989	10.5	19.9	23.7	2.9
295	Sec. 16- 9- 2 W.5 Todd Creek	11		complete	8½	15	2.860	4.8	12.3	17.1	2.2
297	Sec. 18- 9- 2 W.5 Todd Creek	10	poorly exposed	complete	7	11	2.830	3.5	10.2	15.6	2.0
329	Sec. 27- 8- 3 W.5 North Burmis	9		complete	6	6	2.773	1.0	1.3	12.7	1.7
302	Sec. 27- 8- 3 W.5 North Burmis	9	faulted	lower part	5	5	2.810	2.6	3.5	14.6	1.9
324	Sec. 22- 8- 3 W.5 North Burmis	9		complete	8	6	2.735	1.0	6.4	10.7	1.5
301	Sec. 27- 8- 3 W.5 North Burmis	9		complete	20	18	3.296	24.1	17.9	39.3	4.7
307	Sec. 22- 8- 3 W.5 North Burmis	9	composite section	complete	11	11	2.798	2.0	4.5	13.0	1.7
314	Sec. 22- 8- 3 W.5 North Burmis	9		complete	11	10	2.762	1.0	3.0	12.1	1.6
322	Sec. 22- 8- 3 W.5 North Burmis	9	folded	complete ?	17	21	2.999	10.9	12.1	24.2	3.0
325	Sec. 22- 8- 3 W.5 North Burmis	9	folded	upper part missing	15	15	3.146	17.5	20.6	31.7	3.8
326	Sec. 22- 8- 3 W.5 North Burmis	9	trenched	middle part	12	13	3.362	27.0	18.3	43.7	5.2
327	Sec. 22- 8- 3 W.5 North Burmis	9		complete	10	10	3.148	17.5	16.9	31.8	3.8
386	Sec. 22- 8- 3 W.5 North Burmis	9	borehole	complete	17	18	3.292	23.9	21.5	39.1	4.7
334	Sec. 15- 8- 3 W.5 N.-central Burmis	9		complete	9	10	2.846	4.2	5.8	16.4	2.1
338	Sec. 11- 8- 3 W.5 N.-central Burmis	9		complete	12	23	3.045	13.0	12.3	26.5	3.2
341	Sec. 11- 8- 3 W.5 N.-central Burmis	9		complete	7	8	2.941	8.4	7.7	21.2	2.6
342	Sec. 14- 8- 3 W.5 N.-central Burmis	9		complete	11	11	3.118	16.2	16.3	30.2	3.7
344	Sec. 11- 8- 3 W.5 N.-central Burmis	9	faulted	upper part	7	8	3.673	40.8	24.8	58.5	6.9
345	Sec. 14- 8- 3 W.5 N.-central Burmis	9	trenched	lower part	8	9	3.200	19.9	27.9	34.4	4.1
348	Sec. 26- 7- 3 W.5 South Burmis	9	trenched	upper part missing	9	8	3.032	12.0	26.8	25.9	3.2
350	Sec. 24- 7- 3 W.5 South Burmis	9	trenched	middle part	4	5	3.388	28.2	24.3	44.0	5.2
354	Sec. 13- 7- 3 W.5 South Burmis	9	poorly exposed	lower part	9	4	2.771	1.0	3.7	12.6	1.7
385	Sec. 24- 7- 3 W.5 South Burmis	9	borehole	complete	15	16	3.201	19.9	24.6	34.5	4.1
349	Sec. 26- 7- 3 W.5 South Burmis	9	faulted	talus	?	5	3.111	15.9	16.1	29.9	3.6
308	Sec. 12- 3-30 W.4 Dungarvan Cr.	7	faulted	upper part ?	10 ?	10	3.643	39.5	15.9	57.0	6.7
309	Sec. 12- 3-30 W.4 Dungarvan Cr.	7	faulted	lower part	10	11	3.035	12.5	15.9	26.0	3.2
310	Sec. 13- 3-30 W.4 Dungarvan Cr.	7	trenched	complete ?	24	48	3.111	15.9	16.5	29.9	3.6
368	Sec. 14- 3-30 W.4 Dungarvan Cr.	7	trenched	complete ?	14	15	3.244	21.8	28.1	36.7	4.4
366	Sec. 14- 3-30 W.4 Dungarvan Cr.	7	faulted	upper part	5½	6	3.040	12.7	15.7	26.3	3.2
367	Sec. 11- 3-30 W.4 Dungarvan Cr.	7	folded and faulted	lower part ?	5 ?	8	3.277	23.3	18.8	38.3	4.6
364	Sec. 12- 5- 2 W.5 Mill Creek	8	faulted	complete ?	10 ?	11	2.845	4.1	5.0	16.3	2.1
371-2-3	Sec. 26- 1-27 W.4 Goose Lake	3	composite section	lower part	5½	13	3.214	20.5	23.4	35.1	4.2
374	Secs.28, 33- 1-26 W.4 Beazer	2		complete	7	8	2.765	1.0	5.9	12.3	1.6
376	Sec. 33- 2-27 W.4 Mountain View	4	poorly exposed	complete	5	5	2.893	6.2	15.4	18.8	2.4
278	Secs. 26, 35- 3-28 W.4 Hillspring	5		complete	15 ?	14	2.782	1.3	5.1	13.1	1.7

(1) Calculated from the mean bulk density using the regression equation on p. 66.

(2) Calculated from the mean bulk density using the regression equation on p. 66.

(3) Calculated from % Fe_2O_3 using the regression equation on p. 60.

(4) Calculated from % Fe_2O_3.